# Energy Analysis of the New Dual Pressure Low-Temperature Distillation Process for Natural Gas Purification Integrated with NGLs Recovery.

*Stefano Langé*[a*], *Laura A. Pellegrini*[a]

[a]Politecnico di Milano, Department of Chemistry, Materials and Chemical Engineering "G. Natta", piazza L. da Vinci 32, I-20133, Milano, Italy.

The increase of the global energy demand, a scenario in which natural gas plays a key-role, together with the availability of natural gas reserves with high $CO_2$ and/or $H_2S$ contents have been two important drivers for the recent studies and developments of new low-temperature processes for natural gas purification, in order to allow the profitable exploitation of low-quality gas reserves that up to some years ago were not considered suitable for their commercialization. When dealing with natural gas, not only acidic gases are present in the main stream, but also hydrocarbons heavier than methane (ethane, propane, n-butane, etc…). These substances have to be removed from the produced gas for the dew point control of the sales gas. Moreover, they are widely used for petrochemical productions and their recovery can be profitable for natural gas producers.

In this work, an energy analysis is carried out in order to assess the energy requirements for the recovery of Natural Gas Liquids (NGLs) during natural gas purification at low-temperatures. The

results are compared with the ones obtained when traditional processes are used for the same purpose, in order to define the trade-off between the two technologies, extended to the overall production chain, under different possible feed stream compositions. Results prove the feasibility of low-temperature purification processes when dealing with gases having high amounts of acidic compounds and different concentrations of NGLs.

## 1. Introduction

Forecasts on the global energy demand show a rapid increase worldwide over the next twenty years. Natural gas is the fossil fuel which shows the highest growth trend[1]. Reports and studies made in the open literature on the distribution of currently known gas reserves establish that about 40% of the remaining ones are sour[2] and about 30% present high $CO_2$ contents[3], typically between 15% and 80%[4]. $H_2S$ concentrations may reach the 15%[5]. These kinds of low-quality gas reserves are located in different geographic areas, such as South-East Asia, North Africa, Middle East, USA and Australia[3]. Examples of these gas fields with high concentrations of $CO_2$ and/or $H_2S$ contents are shown in Table 1.

**Table 1.** Acidic gases contents in some natural gas reserves.

| Gas Field | Location | Acidic gases | Reference |
|---|---|---|---|
| **Natuna** | Indonesia | >70% $CO_2$ | 3 |
| **Kapuni** | New Zeland | 43.8% $CO_2$ | 5 |
| **Uch** | Pakistan | 46.2% $CO_2$ | 5 |
| **LaBarge** | USA | 65% $CO_2$ | 6 |
| **Harweel Cluster** | Oman | 20% $CO_2$ | 7 |
| **Lacq** | France | 15% $H_2S$ | 5 |

| | | | |
|---|---|---|---|
| **Bearberry** | Canada | 90% $H_2S$ | 7 |
| **Bujang** | Malaysia | 66% $CO_2$ | 8 |
| **Sepat, Noring, Inas** | Malaysia | 60% $CO_2$ | 8 |
| **Tangga Barat** | Malaysia | 32% of $CO_2$ | 8 |
| **Ular, Gajah** | Malaysia | 50% of $CO_2$ | 8 |
| **Beranang** | Malasyia | 28% of $CO_2$ | 8 |
| **Bergading** | Malaysia | 40% of $CO_2$ | 8 |
| **Palas NAG** | Malaysia | 46% of $CO_2$ | 8 |
| **K5** | Malaysia | 70% of $CO_2$ | 8 |
| **J5** | Malaysia | 87% of $CO_2$ | 8 |
| **J1** | Malasyia | 59% of $CO_2$ | 8 |
| **T3** | Malaysia | 62% of $CO_2$ | 8 |
| **Tenggiri Mrn.** | Malaysia | 47% of $CO_2$ | 8 |
| **Shah** | United Arab Emirates | 23 % $H_2S$, 10% $CO_2$ | 9 |
| **El Tapial** | Argentina | 72.24% of $CO_2$ | 10 |
| **Molve** | Croatia | 23% of $CO_2$ | 11 |
| **Kalinovac** | Croatia | 12.5 % of $CO_2$ | 11 |

Traditional natural gas sweetening processes (chemical or physical absorption), in particular chemical scrubbing by means of aqueous alkanolamine solutions, can be too energy intensive when the acidic gases content in the feed stream is high[12-14]. In this scenario, attention has been devoted in the last decades to study and develop new natural gas purification processes, particularly low-temperature ones, in order to decrease the overall production costs[13] and allow the profitable exploitation of sub-quality gas reserves that up to some years ago were not considered suitable for the market. Low-temperature processes for natural gas purification operate at temperatures and pressures where a $CO_2$ rich solid phase can form inside process equipment. Several solutions have been proposed in literature to handle carbon dioxide freezing. These processes can be designed to allow the formation of a solid phase in a dedicated zone or to completely avoid $CO_2$ freezing. Low-temperature purification processes that allow the formation of a $CO_2$-rich solid phase are: the CFZ$^{TM}$ process[15-20], the Cryocell® process[21-22], the Cryopur® process[23-24], the integrated cryogenic $CO_2$ removal coupled with pressurized natural gas liquefaction[25]. Processes which avoid the freezing of carbon dioxide are: the Ryan-Holmes process[26-28] where an entrainer (normally a hydrocarbon heavier than methane, such as n-butane) is used to shift $CO_2$ freezing conditions at lower temperatures and pressures; the Sprex® process[29-30] where a bulk removal of $CO_2$ is performed in a pressurized low-temperature distillation column, operated away from freezing conditions, while the final purification of the gas is made with a traditional MDEA unit and, recently, a new patented dual pressure low-temperature distillation process[31, 14] designed to bypass the freezing point of $CO_2$ in mixtures with methane by means of a specific thermodynamic cycle.

In this work, the dual pressure low-temperature distillation process[31] has been taken into account, since it allows to perform the purification by means of a distillation unit made by common equipment of the process industry. The process allows to reach commercial purity avoiding solid phase formation, without the need of *ad-hoc* designed units to handle dry ice formation or the addition of a third component, the entrainer, that must be regenerated.

Moreover, from low-temperature distillation processes, $CO_2$ can be obtained in liquid phase under pressure, suitable conditions for EOR or CCS purposes.

When performing the purification by means of low-temperature process distillation, the compounds with lower volatility than $CO_2$ are collected in the bottom product, hence suitable purification technologies are needed to recover $C_{2+}$. On the contrary, when natural gas sweetening is performed by means of classical chemical scrubbing, ethane and heavier hydrocarbons are recovered in the sweet gas, since they are less soluble in the aqueous phase.

NGLs have their own market and they can be used for energy production or as raw materials for petrochemical productions[32]; therefore their recovery can be of interest, depending on the overall process economics. The increasing production of NGLs is mostly related to the exploitation of associated natural gas[32-33] and to the reduction of gas flaring practices. The content of $C_{2+}$ in gas streams may vary greatly depending on the kind of the considered gas reserve; examples are listed in Table 2.

**Table 2.** $C_{2+}$ contents in some gas reserves.

| **Gas Field** | **Location** | **$C_{2+}$ [%]** | **Kind of gas** | **Reference** |
|---|---|---|---|---|
| **Parentis** | France | 26.4 | Associated | 5 |
| **Ekofisk** | Norway | 14.4 | Associated | 5 |
| **Maracaibo** | Venezuela | 16.3 | Associated | 5 |
| **Uthmaniyah** | Saudi Arabia | 33.9 | Associated | 5 |
| **Burgan** | Kwait | 22.7 | Associated | 5 |
| **Kirkuk** | Iraq | 32.5 | Associated | 5 |
| **Ardjuna** | Indonesia | 28.9 | Associated | 5 |
| **El Tapial** | Argentina | 12.78 | Associated | 10 |
| **Bakken Lean** | USA | 27 | Shale | 34 |
| **Bakken Rich** | USA | 36.2 | Shale | 35 |
| **Rockies Lean** | USA | 23.5 | Shale | 34 |
| **Rockies Rich** | USA | 39 | Shale | 34 |

| | | | | |
|---|---|---|---|---|
| **Permian/Delaware Lean** | USA | 25.1 | Shale | 34 |
| **Permian/Delaware Rich** | USA | 35.2 | Shale | 34 |
| **Haynesville Lean** | USA | 8.6 | Shale | 34 |
| **Haynesville Rich** | USA | 18.6 | Shale | 34 |
| **Molve** | Croatia | 6.7 | Conventional | 11 |
| **Kalinovac** | Croatia | 12.2 | Conventional | 11 |

When dealing with classical natural gas production processes, specific technologies, well known in the open literature[35], are available. These technologies operate mostly the separation between $C_{2+}$ and methane, without incurring in non-ideal VLE behaviors that occur when also acidic gases ($CO_2$ and $H_2S$) are present in the mixture. For low-temperature natural gas purification processes, non-ideal VLE behaviors, regarding basically $CO_2$-$C_2H_6$ and hydrocarbons-$H_2S$ systems[35], should be taken into account during process design for the efficient recovery of $C_{2+}$. On the GPSA Handbook[35] some possible process schemes have been proposed. Finn and O'Brien[33] considered possible pathways for the purification of $CO_2$-rich gas streams and the recovery of NGLs; in particular they discussed the feasibility of the application of the CFZ™ technology to a demethanizer unit inside the four-column Ryan-Holmes process[35] and considered the recovery of heavy hydrocarbons before the separation between methane and carbon dioxide. To break the azeotrope that occurs in the $CO_2$-$C_2H_6$ system, an entrainer should be used to enhance the relative volatility between the two components[35]. Some authors[36-39] considered the performances of the extractive distillation to separate ethane and carbon dioxide, studying the controllability, different configurations for energy savings and the effect of the selected entrainer on the separation process. In all these works, only a two-column configuration has been investigated.

In the present work, several possibilities have been taken into account to perform the NGLs recovery. In particular two different configurations have been adopted and compared to break the $CO_2$-$C_2H_6$ azeotrope: the standard two-columns extractive distillation has been compared with a three-columns scheme, where a preliminary distillation unit performs the bulk removal of $CO_2$ or ethane from the main stream, depending on the global composition of the mixture respect to the azeotrope composition. Then, the analysis has been devoted to define whether it is energetically profitable to recover NGLs before or after the methane purification unit, depending on the inlet content of $C_{2+}$ in the gas stream.

Hence, energy requirements of the low-temperature distillation plant for natural gas production have been estimated adopting the net equivalent methane concept, as described by Pellegrini et al.[40]. Results have been compared with the overall energy requirements of a traditional natural gas production plant, where purification is performed by means of chemical scrubbing with MDEA. The trade-off between the two solutions has been defined, depending on the acidic gases content and on the NGLs content of the feed stream. The comparison has been carried out considering also the case when $CO_2$ has to be compressed for EOR or CCS in order to better estimate the weight of $CO_2$ recompression on the trade-off between the two processes.

Process configurations have been studied by means of rules of thumb, when possible, and by means of process simulations with Aspen Hysys® V7.3[41]. The energy expenses in terms of net equivalent methane useful to supply energy to the overall production plant have been converted in terms of percentage of the produced gas that needs to be burned to drive the entire process forward. The study has been performed considering several possible compositions of the feed gas in terms of acidic gases ($CO_2$ and $H_2S$) and $C_{2+}$, trying to cover the widest range of natural gas compositions.

## 2. Thermodynamic considerations

To perform an accurate process design and simulation, it is of paramount importance to set-up a proper and reliable thermodynamic framework that accurately describes phase equilibria. In low-temperature natural gas purification by means of distillation, not only VLE should be taken into account, since, at temperatures below 216.59 K[42], the triple point of $CO_2$, carbon dioxide can form a solid phase; hence SLVE must be calculated in order to define suitable operating conditions to avoid solid formation inside process equipment. In this work the SRK EoS[43] and the $CO_2$ Freeze out utility available in Aspen Hysys® V7.3 have been considered. The reliability of the selected thermodynamic framework has been tested by comparison with literature-available experimental data and results obtained by means of an in-house Fortran routine based on a classical approach for solid-fluid phase equilibria already used and tested in previous works[44, 14]. This routine calculates fluid phase fugacities with the SRK[43] and PR[45] EoSs and the solid phase fugacity from the Gibbs free energy of $CO_2$ melting. The reliability of the thermodynamic framework has been already discussed in a previous work[14] for the VLE and SLVE of $CH_4$-$CO_2$, $CO_2$-$H_2S$ and $CH_4$-$H_2S$ systems. In this work, the validation is presented for different binary systems of interest when dealing with multicomponent mixtures of natural gas. Prediction of solubility of solid $CO_2$ in mixtures with hydrocarbon is discussed; $CO_2$-$C_2H_6$, $CO_2$-$C_3H_8$ and $CO_2$-n-$C_4H_{10}$ systems are taken into account (Figure 1). Regarding VLE, the validation is made considering binary mixtures of $CO_2$ and $H_2S$ with ethane, propane and n-butane (Figures 2-3). Experimental data for the solubility of solid $CO_2$ in mixtures with hydrocarbons are taken from the work by Kurata[46], while binary VLE data are taken from the NIST TDE database[47].

a)

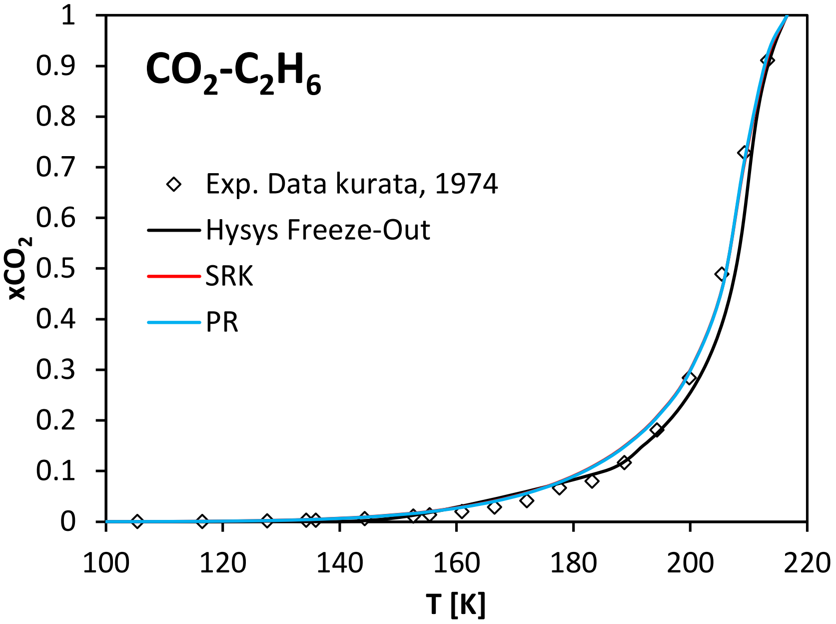
$CO_2$-$C_2H_6$
◇ Exp. Data kurata, 1974
Hysys Freeze-Out
SRK
PR
$xCO_2$
1
0.9
0.8
0.7
0.6
0.5
0.4
0.3
0.2
0.1
0
100
120
140
160
180
200
220
T [K]

b)

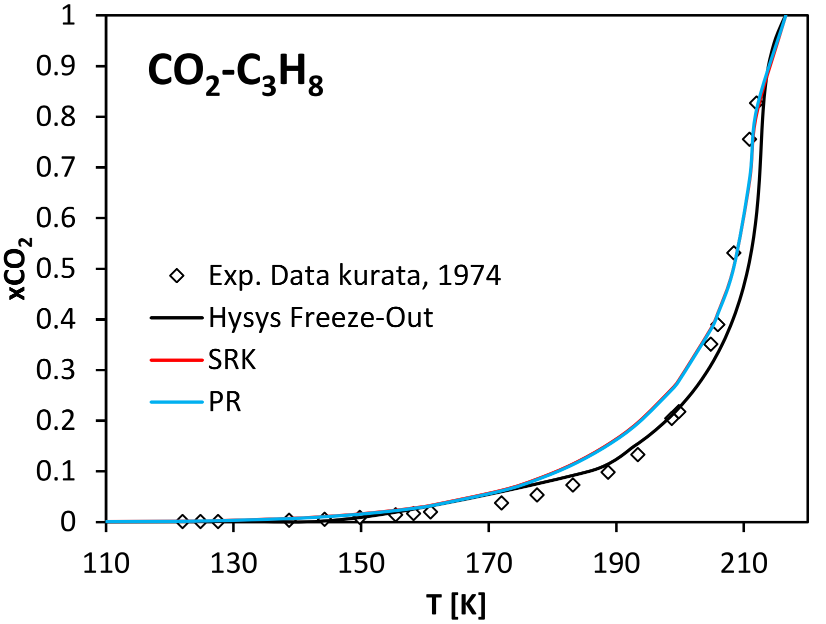
$CO_2$-$C_3H_8$
◇ Exp. Data kurata, 1974
Hysys Freeze-Out
SRK
PR
$xCO_2$
1
0.9
0.8
0.7
0.6
0.5
0.4
0.3
0.2
0.1
0
110
130
150
170
190
210
T [K]

c)

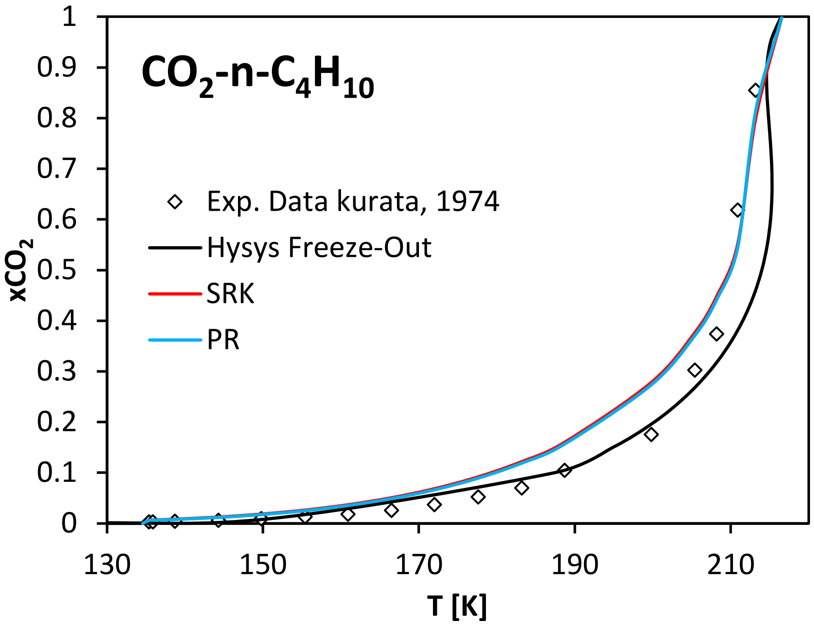

**Figure 1.** Comparison among results obtained with the Hysys $CO_2$ Freeze-Out utility, results obtained using a classical approach[44] and experimental data[46] for the Tx solubility diagrams of: a) $CO_2$-$C_2H_6$, b) $CO_2$-$C_3H_8$ and c) $CO_2$-n-$C_4H_{10}$ systems.

The results obtained using the classic approach with the two cubic EoSs match very well and are in good agreement with the experimental data by Kurata[46] at high and low concentrations (close to 0) of $CO_2$ in the liquid phase, while larger discrepancies are present for molar fractions of $CO_2$ in the liquid phase below 0.4. The results obtained with the $CO_2$ Freeze-out utility available in Aspen Hysys® are in good agreement with the ones obtained with the Fortran routine for the $CO_2$-$C_2H_6$ system (Fig. 1a), while the difference increases for the $CO_2$-$C_3H_8$ and $CO_2$-n-$C_4H_{10}$ systems. The results obtained with the $CO_2$ Freeze-out utility are closer to the experimental points for values of the $CO_2$ molar fractions in the liquid phase between about 0.1-0.5, where the classic approach shows higher deviations. For each value of the $CO_2$ concentration in the liquid phase, the $CO_2$ Freeze-Out utility overestimates the freezing temperature, remaining more conservative.

The presence of heavier hydrocarbons in the natural gas stream, when performing low-temperature distillation for natural gas purification, enhances the solubility of dry ice in the liquid phase; hence, freezing points of $CO_2$ are shifted at lower temperatures and pressures, as highlighted also by Ryan and Holmes[28], GPSA[35] and by Pellegrini et al.[48].

a)

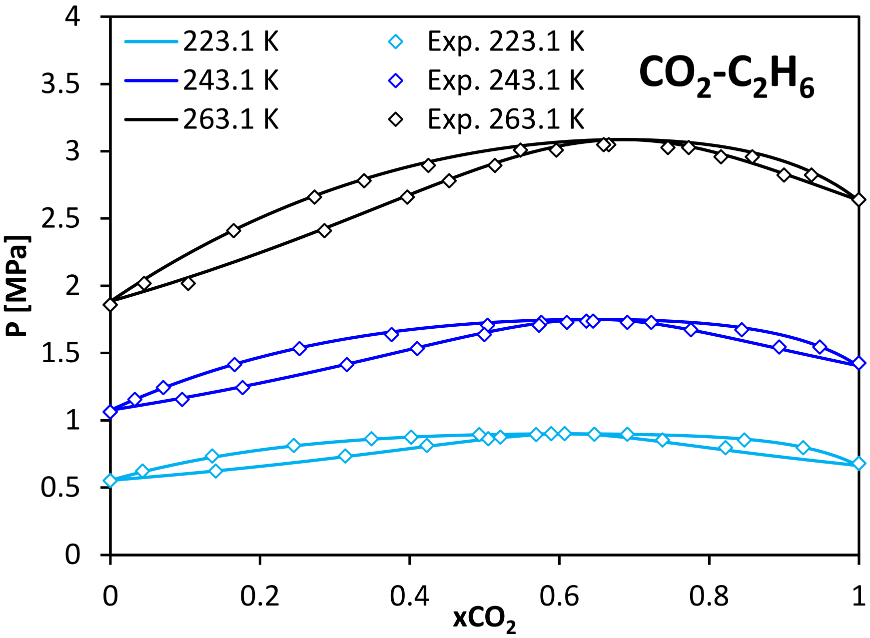

b)

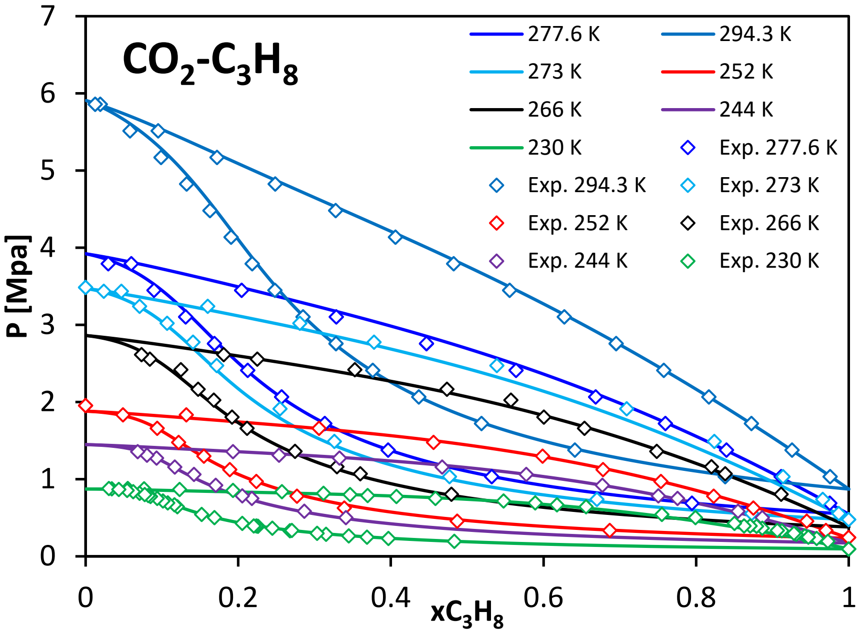

c)

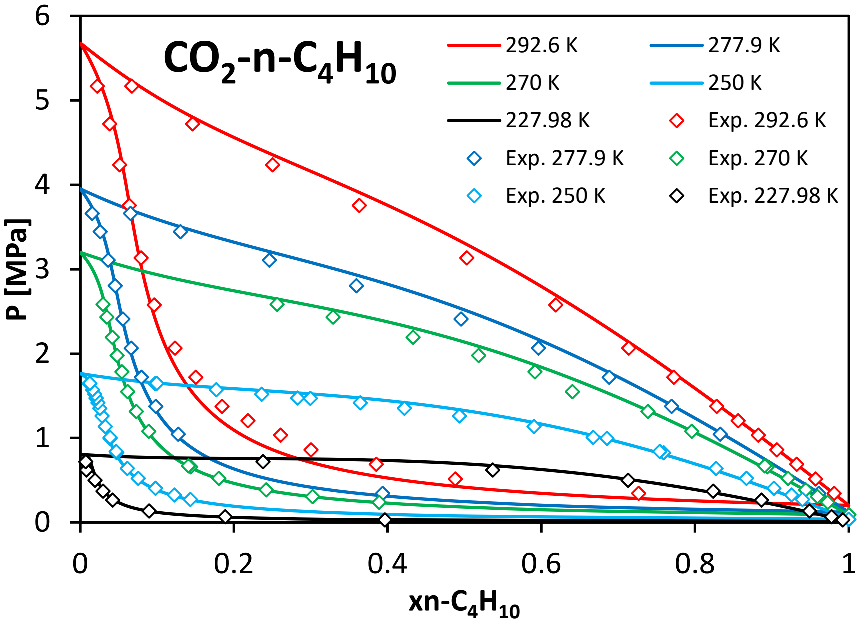

**Figure 2.** Comparison between results obtained with the SRK EoS[43] and experimental data taken from the NIST TDE database[47] for the VLE of binary $CO_2$-hydrocarbons systems at different temperatures. Pxy diagrams of: a) $CO_2$-$C_2H_6$[48], b) $CO_2$-$C_3H_8$ and c) $CO_2$-n-$C_4H_{10}$ systems.

The representation of the VLE of binary $CO_2$-hydrocarbons systems is satisfactory: model results are in good agreement with experimental data, also for the azeotropic behavior of the $CO_2$-$C_2H_6$ system. The mixture presents a minimum azeotrope, the composition of which does not vary significantly with pressure. This is the reason why extractive distillation is needed to break the azeotrope and separate $CO_2$ and ethane.

a)

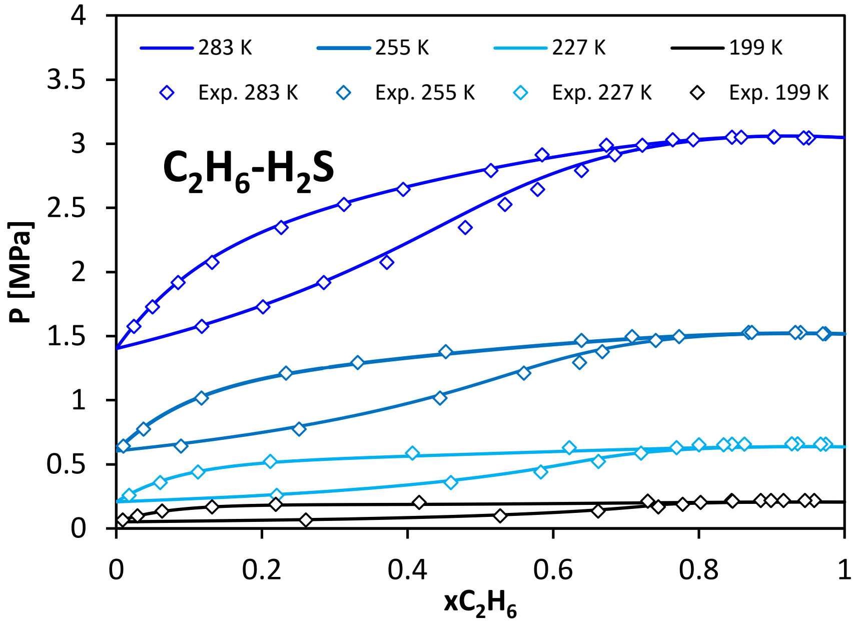

b)

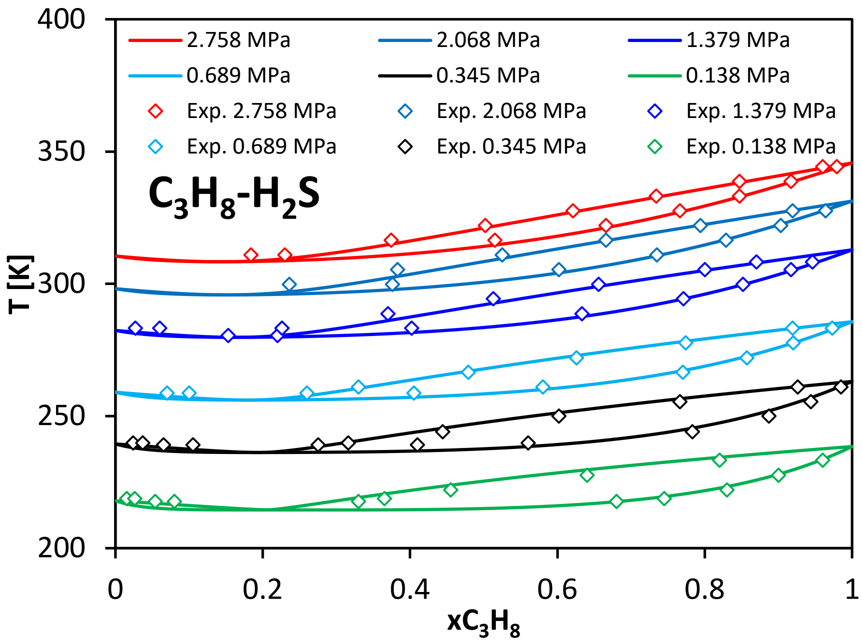

c)

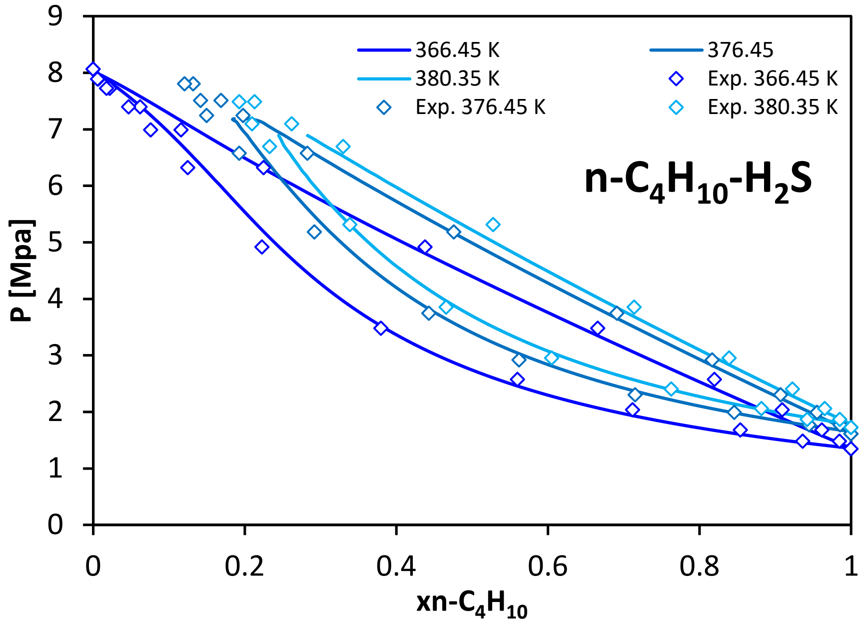

**Figure 3.** Comparison between results obtained with the SRK EoS[43] and experimental data taken from the NIST TDE database[47] for the VLE of binary $H_2S$-hydrocarbons systems: a) Txy diagram for $H_2S$-$C_2H_6$[48], b) Pxy diagram for $H_2S$ -$C_3H_8$ (Pellegrini et al., 2015b) and c) Pxy diagram for $H_2S$ -n-$C_4H_{10}$.

The VLE of binary $H_2S$-hydrocarbons mixtures is well reproduced by the thermodynamic model, except for the $H_2S$-n-$C_4H_{10}$ system close to the critical conditions, where deviations between calculation results and experimental data are significant. Hydrogen sulfide and ethane does not form an azeotrope, but, at high concentrations of ethane, the relative volatility is greatly reduced. The $H_2S$-$C_3H_8$ system presents a minimum azeotrope at low molar fractions of propane. Also for this system, the composition of the azeotrope does not change significantly with pressure. So, the separation of hydrogen sulfide from the main hydrocarbon stream is difficult. Finn and O'Brien[33], according to the GPSA handbook[35], suggested a preliminary removal of $H_2S$ and $C_{2+}$ from the main natural gas stream by means of extractive distillation.

The thermodynamic framework has proven to be reliable and has been used for process simulations.

## 3. Description of process layouts and calculation methods

The global natural gas purification process has been considered. Each unit of the main process has been studied in order to determine the overall energy requirements. In this work the following main assumptions have been considered:

- $H_2S$ is removed before the low-temperature processes for natural gas purification;
- the final product is pipeline-quality gas: $CO_2 < 2$mol%; $H_2S < 4$ ppm[49-50];
- maximum hydrocarbons recovery is required;
- $C_{2+}$ are considered as ethane during process simulations;
- produced ethane has a molar purity > 99%;
- $CO_2$ quality is for pipeline transmission[51].

$H_2S$ removal before the low-temperature purification has been chosen because of its toxicity, according to the suggestion of Turton et al.[52], its VLE behavior in mixtures with hydrocarbons and its SLVE behavior in mixtures with $CO_2$ and $CH_4$, as discussed by Pellegrini et al.[48] and Langé et al.[53].

Heavier hydrocarbons have been lumped as ethane for the sake of semplicty. It has to be pointed out that, usually, the recovery of the $C_{2+}$ fraction is not mandatory and can be considered on the basis of economic considerations and of transportability of the final product (dew point control). In this work, the $C_{2+}$ fraction has been assumed to be always recoverable in order to extend the generality of the study.

The inlet raw natural gas stream has been considered to be available at 50 bar, with a composition varying for $H_2S$ from 0 to 15 mol%, for $CO_2$ from 5 to 65 mol% and for $C_{2+}$ from 0 to 25 mol%, while the methane content results from the balance.

The energy requirements of each process unit have been calculated in terms of equivalent methane[40]. The different quality of the energy has been considered, assuming to produce electric energy to drive compressors by means of a methane-fired combined cycle, to produce steam by means of a methane-fired boiler and to produce cooling duties by means of vapor-compression refrigeration cycles. Internal energy that can be recovered (such as heat at high temperature) has been considered as a methane saving. The overall energy performance of the plant has been calculated, in this way, as the percentage of the produced gas that has to be burned to supply energy to the overall purification plant.

Useful parameters to perform equivalent methane calculations are reported in Table 3, while the relevant procedure is described below.

| **Table 3.** Parameters for the calculation of the equivalent methane[40]. | | |
|---|---|---|
| **Parameter** | **Symbol** | **Value** |
| **Methane Lower Heating Value** | $LHV_{CH_4}$ | 50 MJ kg$^{-1}$ |
| **Boiler Efficiency** | $\eta_B$ | 0.80 |
| **Combined Cycle Efficiency** | $\eta_{CC}$ | 0.55 |
| **Second Law Efficiency** | $\eta_{II}$ | 0.60 |
| **Ambient Temperature** | $T_0$ | 298.15 K |

- Useful heat $\dot{Q}$, needed to heat a process stream above the ambient temperature, is supplied by means of LP steam produced by a methane-fired boiler, that burns a methane mass flow equal to $\dot{m}_{CH_4}$ with an efficiency equal to $\eta_B$:

$$\dot{m}_{CH_4} = \frac{\dot{Q}}{\eta_B LHV_{CH_4}} \tag{1}$$

- Cooling duty $\dot{Q}_{COLD}$, needed to cool a process stream below the ambient temperature, is produced by means of a vapor compression refrigeration cycle, having a coefficient of performance $COP_f$, that burns a methane mass flow equal to $\dot{m}_{CH_4}$ to drive cycle compressors that require a mechanical power $\dot{W}_{el}$. The mechanical power can be calculated according to Eq. (2), where the actual value of the $COP_f$ can be calculated starting from the ideal one of a Carnot cycle (Eq.(3)) and the Second Law efficiency $\eta_{II}$ (Eq.(4)).

$$COP_f = \frac{\dot{Q}_{COLD}}{\dot{W}_{el}} \tag{2}$$

$$COP_{f,id} = \frac{1}{\left(\frac{T_0}{T} - 1\right)} \tag{3}$$

$$\eta_{II} = \frac{COP_f}{COP_{f,id}} \tag{4}$$

- The mechanical power is produced by means of a methane-fired combined cycle, having an efficiency equal to $\eta_{CC}$:

$$\eta_{CC} = \frac{\dot{W}_{el}}{\dot{m}_{CH_4} LHV_{CH_4}} \tag{5}$$

- The equivalent methane for the production of cooling duties is:

$$\dot{m}_{CH_4} = \frac{\dot{Q}_{COLD}}{COP_f \eta_{CC} LHV_{CH_4}} \tag{6}$$

- Mechanical power $\dot{W}_{el}$, needed to drive process machineries, is supplied by means of a methane-fired combined cycle with an efficiency equal to $\eta_{CC}$, that burns a methane mass flow equal to $\dot{m}_{CH_4}$:

$$\dot{m}_{CH_4} = \frac{\dot{W}_{el}}{\eta_{CC} LHV_{CH_4}} \tag{7}$$

Methane saving terms are represented by heat flows that can be recovered inside the process and mechanical powers produced by process streams expansion in turbines.

For each block of the Block Flow Diagrams (BFDs) shown in Figs. 4-5, the net equivalent methane has been calculated in terms of kg s$^{-1}$ per kmol h$^{-1}$ of feed stream to the process unit.

In the following sub-sections, each process unit is described and the energy terms accounted for the analysis are discussed.

### *3.1 Global BFDs of the considered natural gas production plants*

In this work, two complete natural gas production plants have been considered: a classic scheme (Fig. 4), composed of an acid gas removal unit, a dehydration unit and a demethanizer, and a low-temperature scheme (Fig. 5) that can be organized according to two different ways. In both these ways, $H_2S$ is selectively removed at the beginning and the desulfurized stream is then dehydrated before entering the cold part of the process. In the first pathway (Fig. 5a), the $C_{2+}$ fraction is removed before the low-temperature dual pressure distillation process for the $CH_4/CO_2$ split, while in the second one (Fig. 5b) the $C_{2+}$ fraction is separated after the low-temperature dual pressure distillation unit.

In this work the different processes have been compared considering also the $CO_2$ recompression unit, that differs between the classic scheme (Fig. 4b) and the low-temperature one (Figs. 5c–5d) according to the operating conditions at which the $CO_2$ stream is obtained. This part will be discussed more in detail in the next sections.

The BFDs of the two considered natural gas production plants are presented in Figs. 4-5.

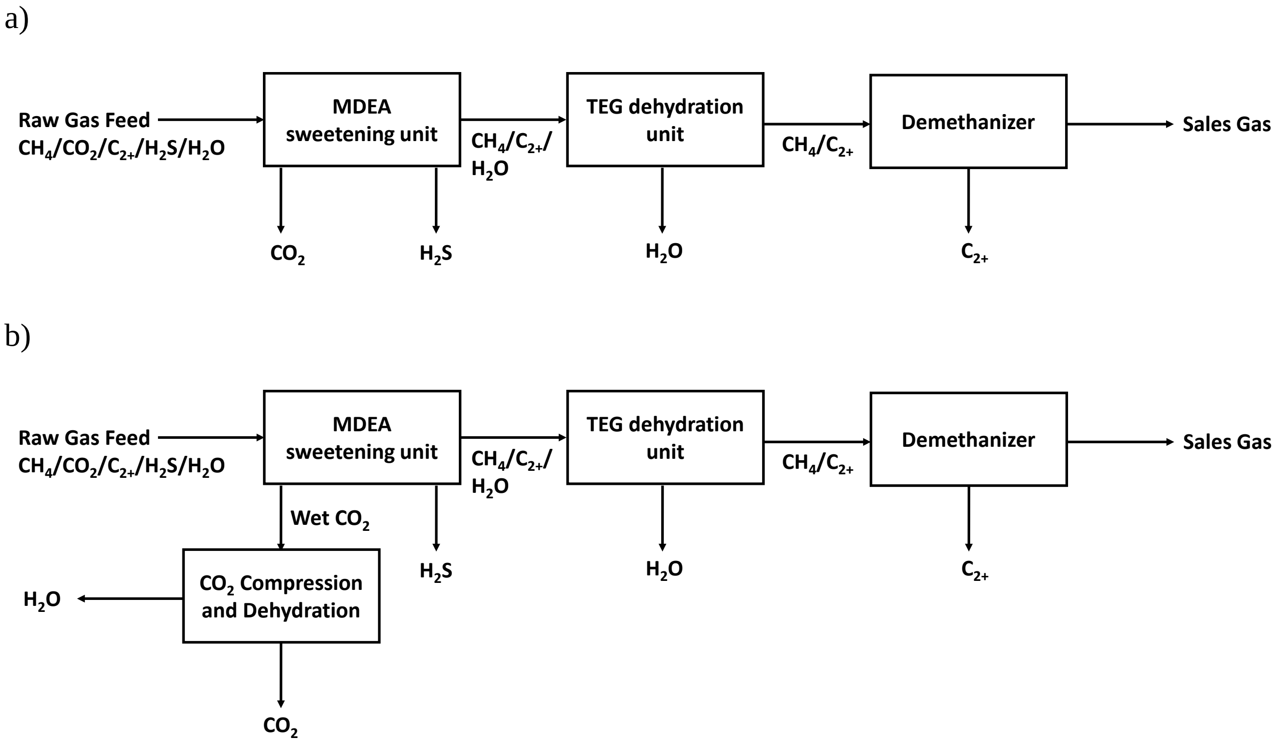

**Figure 4.** Classic scheme for the overall natural gas purification chain: a) without $CO_2$ recompression and b) with $CO_2$ recompression.

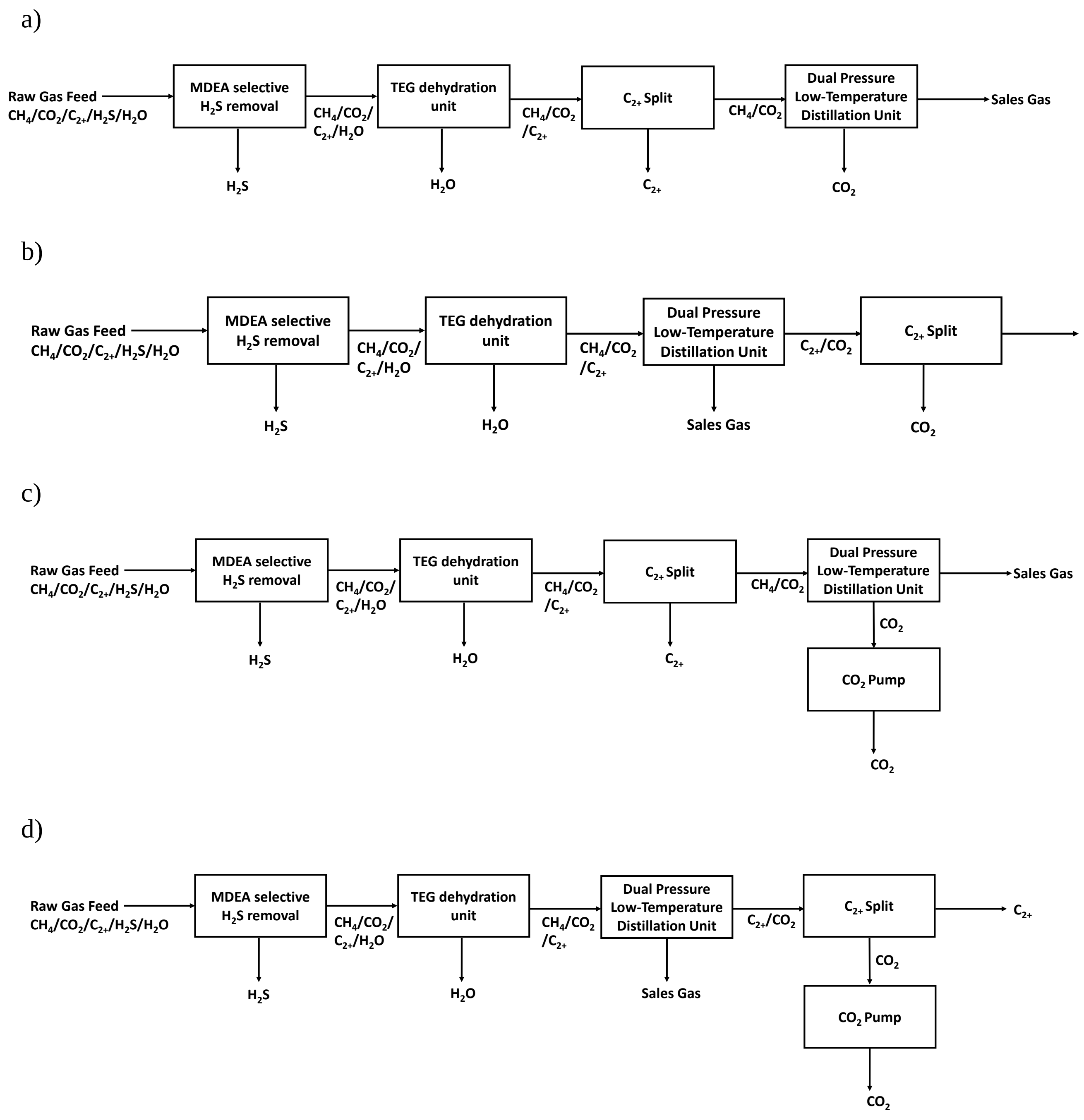

**Figure 5.** Low-temperature scheme for the overall natural gas purification chain: a) with $C_{2+}$ recovery before the $CH_4$ / $CO_2$ separation by means of the dual pressure low-temperature process and without $CO_2$ recompression; b) with $C_{2+}$ recovery after the $CH_4$ / $CO_2$ separation by means of the dual pressure low-temperature process and without $CO_2$ recompression; c) with $C_{2+}$ recovery before the $CH_4$ / $CO_2$ separation by means of the dual pressure low-temperature process

and with $CO_2$ recompression and d) with $C_{2+}$ recovery after the $CH_4$ / $CO_2$ separation by means of the dual pressure low-temperature process and with $CO_2$ recompression.

The overall energy consumptions of each block of the BFDs and the relevant specific net equivalent methane (kg $s^{-1}$ per kmol $h^{-1}$ of feed stream) can be calculated starting from material balances. The net specific equivalent methane per each block has been parametrized as mathematic functions of simulations results when rules of thumb cannot be used. Rules of thumb are available for the MDEA unit[14] and for the TEG dehydration unit[54, 49]. The energy performances of each process scheme have been evaluated as percentage of the produced gas to be burned in order to provide energy to the overall purification chain, according to:

$$\%BurnedGas = \frac{\left(\sum_{i=1}^{Nproc} FEED_i CH_{4,EQ}^{i}\right)}{CH_4^{PROD}} \times 100 \qquad (8)$$

Furthermore, the detail of the process units corresponding to the block in Figs. 4-5, the modeling and the methodologies adopted to calculate their relative energy expenses are discussed.

### *3.2 MDEA sweetening unit*

Chemical absorption by means of aqueous solutions of MDEA is the classic scheme (Fig. 4) considered for the removal of acidic gases ($CO_2$ and $H_2S$) from the main gas stream. Due to the selectivity of the solvent, this unit has been adopted also for the removal of $H_2S$ in the low-temperature process (Fig. 5). This choice has been already discussed (see Section 3). Moreover, since $H_2S$ is fed to Sulfur Recovery Units (SRUs) at atmospheric pressure, the choice of a preliminary removal by means of selective chemical absorption allows to obtain $H_2S$ for the SRU unit at the desired pressure, without complicated separations from the main stream (strong non-idealities in the VLE behavior of mixtures of $H_2S$ with hydrocarbons and $CO_2$).

The main energy consumption of the absorption unit is the heat required by the reboiler of the regeneration column[55]. The amount of heat necessary for the regeneration of the solvent is mainly due to the high heat of vaporization of water (that is the compound of the solvent mixture present in largest amounts) and to the heat required to break chemical bonds formed during acidic gases absorption.

A Process Flow Diagram (PFD) for the MDEA unit is reported in Fig. 6. The calculation of energy consumptions related to this process unit has been performed according to a rule of thumb[14] which considers an overall LP steam consumption at the reboiler of the regeneration column equal to 0.14 kg per L of lean circulating solvent. The validity of this assumption has been discussed in a previous work[14]. Once calculated the volumetric flowrate $\dot{V}$ of the circulating lean solvent, the amount of heat required by the regeneration column is:

$$\dot{Q} = 0.14\dot{V}\Delta H_{ev}^{H2O} \tag{9}$$

where $\Delta H_{ev}^{H2O}$ is the heat of vaporization of water at about 3.5 bar[14].

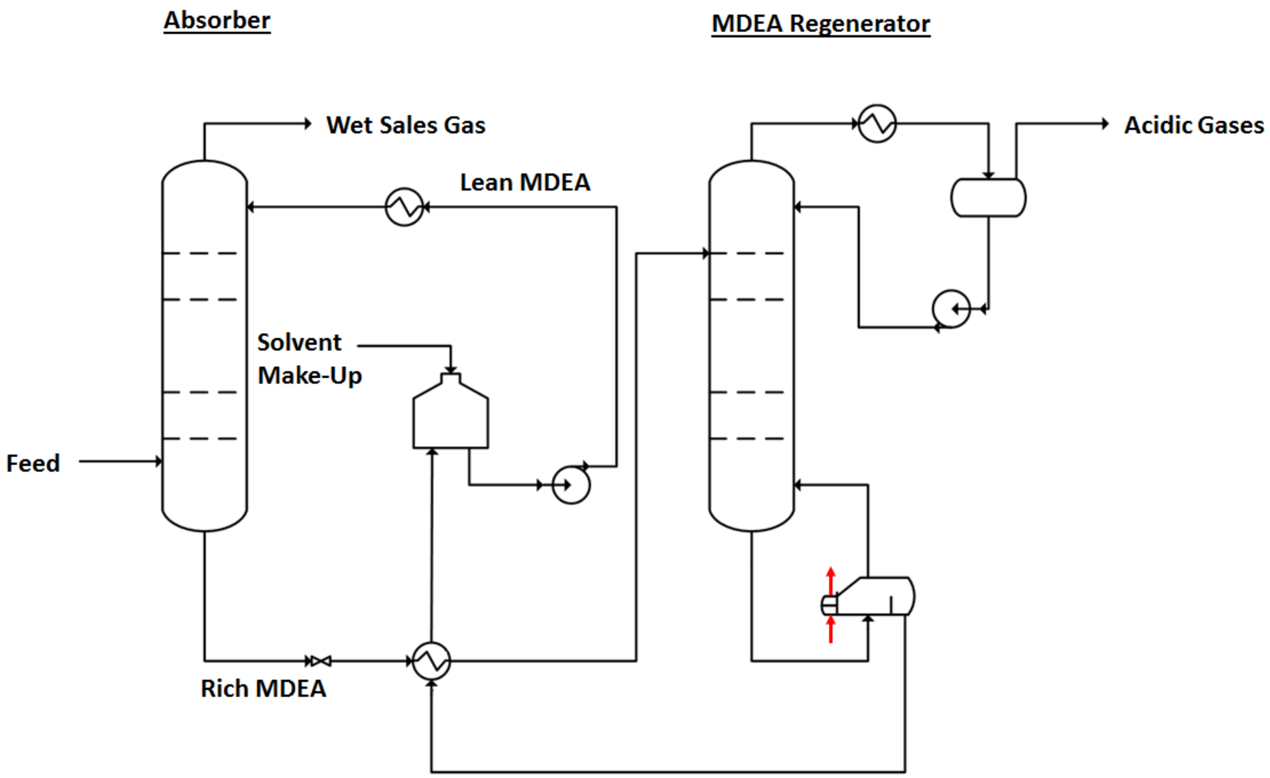

**Figure 6.** PFD of a classic MDEA unit. → Heat required by the reboiler, accounted as key parameter for the net equivalent methane calculations (Eq. (1)).

The unit consists of an absorption column, where the gas feed is sweetened by contacting in counter-current the lean solvent, and of a regeneration column, where acidic gases are rejected at the top of the column and the lean regenerated solvent is recycled to the process. A proper make-up of the solvent is needed. In order to save energy, the sensible heat of the hot lean solvent, coming from the reboiler of the regeneration column, is recovered by means of a cross heat exchanger, heating the rich amine stream (loaded with the acidic compounds) to be fed to the regeneration column. The absorption is operated under pressure, while, in order to favor the recovery of acidic gases, the regeneration is operated at low-pressures, typically about 1-2 bar.

For the removal of $CO_2$ and $H_2S$ (Fig. 4) two units in series are used, while, when only $H_2S$ removal is needed (Fig. 5), only one unit is required.

The sweet gas from the top of the absorber is saturated with water. The water content in this gas stream is affected by the presence of $CO_2$ and $H_2S$, which allow a larger amount of water at saturation conditions as discussed in the GPSA Handbook[35]. The amount of water in the produced sweet gas has been calculated by means of process simulations with Aspen Hysys® V7.3, using the DBR Amine Package. Calculations have been performed considering, for the absorption column, the same configuration reported in the work by Langé et al.[14]. For the classic scheme (Fig. 4), the inlet content of $CO_2$ has been varied from 5 to 65 mol%, while the one of $H_2S$ from 0 to 15 mol%. The absorber pressure has been set at 50 bar, the same of the natural gas feed. For this process layout, acidic gases should be removed as indicated in Section 3, thus, since their content in the sweetened gas is much lower than the one of hydrocarbons, the water content is not affected by their presence and it results to be constant and equal to 0.0018 mol/mol, according to the operating conditions of the top tray of the absorber (50 bar and 40 – 41 °C).

When considering the selective removal of $H_2S$ for the second process scheme (Fig. 5), the presence of $CO_2$ in the remaining gas is not negligible and affects the content of water in the produced gas[35] from the top of the absorber. For this reason, process simulations have been performed in order to define the variation of the molar fraction of water with the inlet content of acidic gases ($CO_2$ and $H_2S$). Conversely, the number of absorber trays has been varied in order to meet the specification on the final $H_2S$ content.

Since $H_2S$ is removed to the level of ppms, the molar fraction of water in the produced gas is affected only by the presence of $CO_2$.

The obtained results from absorber simulations have been correlated. The final water content in the desulfurized gas has been expressed as a function of the $CO_2$ mol% of the feed gas (Eq. (10)).

$$y_{H2O}^{Gas} = 6.267 \times 10^{-6} \ \%CO_2^{FEED} + 1.759 \times 10^{-3} \quad (10)$$

The graphic representation of the reliability of Eq. (10) is shown in Fig. 7.

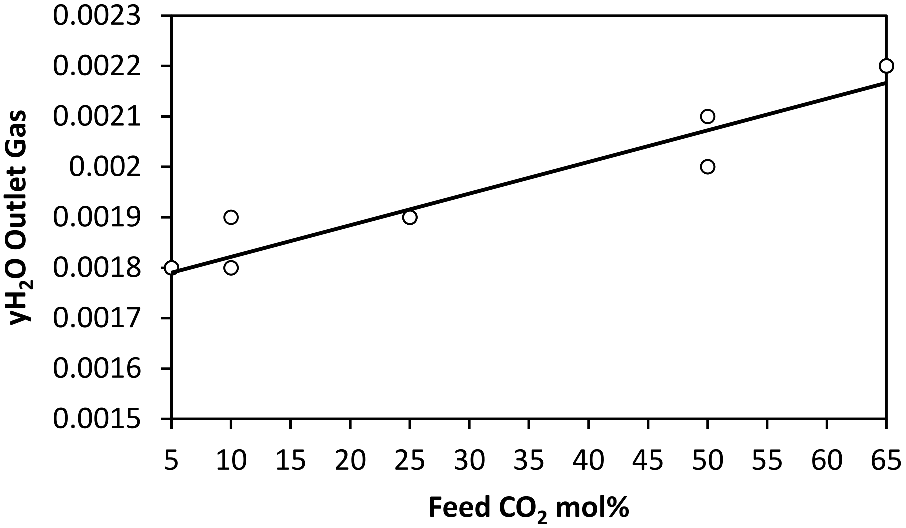

**Figure 7.** Correlation (Eq. (10)) of the absorber simulation results (Aspen Hysys V.7.3, DBR Amine Package) for the desulfurization of the inlet feed gas by means of chemical absorption of $H_2S$ in a 40 wt% MDEA aqueous solution at 50 bar.

The obtained correlation allows a good representation of the water content of the desulfurized gas.

It has to be pointed out that, for the second process layout (Fig. 5), where no $H_2S$ is present in the gas feed, Eq. (10) has been still adopted to calculate the amount of water in the raw gas feed.

This is correct because, after desulfurization, the gas is saturated with water according to the operating conditions of the top absorber tray.

### *3.3 TEG dehydration unit*

For the removal of water before the demethanizer unit (Fig. 4) and the low-temperature purification (Fig. 5), Triethylene Glycol (TEG) has been considered as solvent for gas dehydration. The configuration of the TEG dehydration process is similar to the one of the MDEA sweetening unit (Fig. 8).

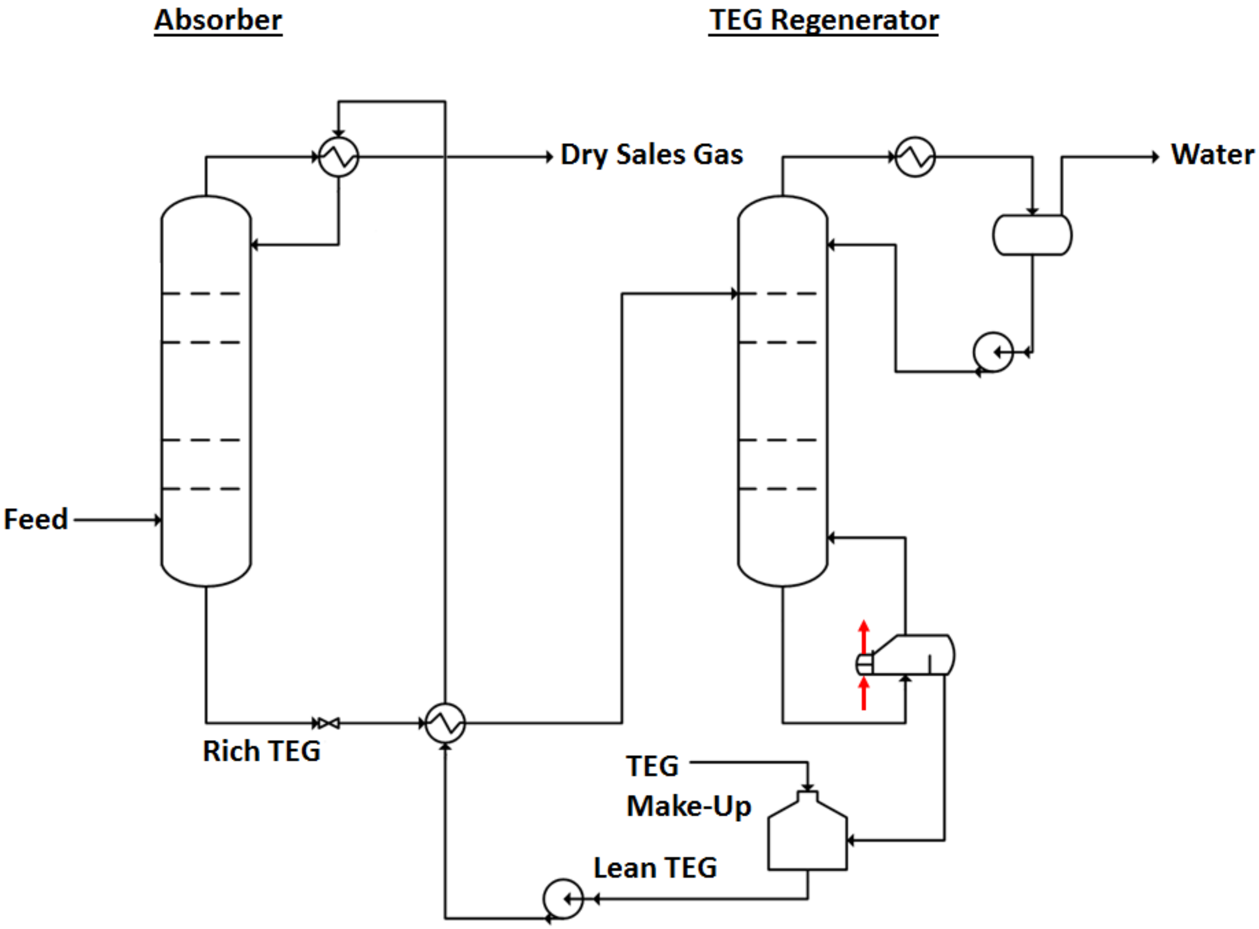

**Figure 8.** PFD of a classic TEG Dehydration unit. → Heat required by the reboiler, accounted as key parameter for the net equivalent methane calculations (Eq. (1)).

The wet natural gas is contacted counter-currently with the lean regenerated TEG in an absorption column. The produced gas is dry, while the solvent, loaded with water, is sent to a regeneration unit. The regenerator separates water at the top and TEG at the bottom. Hot TEG is then pumped (lower viscosity), cooled in a cross heat exchanger, furthermore cooled by heat exchange with the produced dry gas and recycled to the top of the absorption column. Absorption occurs under pressure, while regeneration is operated at low pressure, close to the atmospheric one. The limit for the temperature at the reboiler of the regeneration section is given by the maximum allowable temperature at which the solvent is stable. TEG is chosen because of its high decomposition temperature[54, 49], its high boiling point and because it is easier to be efficiently regenerated at atmospheric pressure than other glycols[49]. Heat required for TEG regeneration is the most important term of energy requirement in the dehydration unit. The calculations of the heat duty required by the reboiler of the TEG regeneration column have been made adopting rules of thumb, as suggested by Maddox[54] and Mokhatab et al.[49]. Maddox[54] suggested to adopt as energy consumption at the reboiler a duty equal to 560 kJ per L of circulating TEG. Mokhatab et al.[49] suggested to calculate the circulating TEG in the range 2–6 US gal of TEG per lb of removed water and to increase this value with a safety margin of 10–30%. In this work, 3 US gal of TEG per lb of water and a safety factor of 30% have been considered to calculate the circulating solvent.

### *3.4 Demethanizer*

The demethanizer unit is used in the classic purification scheme (Fig. 4) to remove the $C_{2+}$ fraction from a sweetened and dehydrated natural gas stream. The unit performs the separation between methane and heavier hydrocarbons in order to avoid possible retrograde condensation of the mixture during transportation. The PFD of this process unit is shown in Fig. 9.

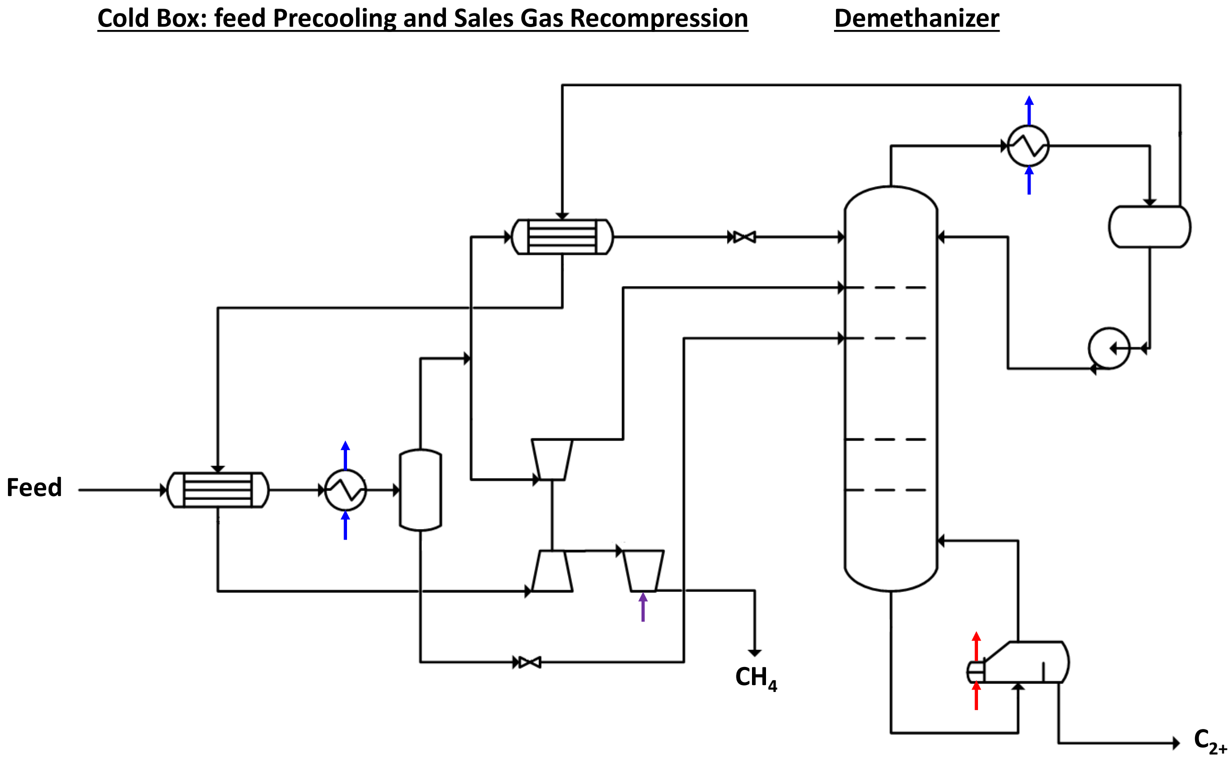

**Figure 9.** PFD of the demethanizer unit. → cooling duty required by low-temperature heat exchangers; → mechanical power required by compressors and → heat required by the reboiler. Only cooling duties and mechanical power are accounted as key parameter for equivalent methane calculations (Eqs. (6-7)).

The unit consists of two sections: a cold box and a distillation column. In the cold box, cold recovery between the produced gas and the feed stream is realized. An external cooling duty is required to furthermore cool the feed stream down to the desired temperature level, obtaining a mixed vapor–liquid stream. The vapor fraction of the cold feed is separated into two streams: one gas stream is furthermore cooled by the distillation column product stream, expanded and fed to the top of the distillation unit to provide totally or part of the liquid reflux. The other stream is expanded in a turboexpander and fed on the fifth tray from the top of the column. The liquid portion of the main feed stream after the first cooler is expanded and sent to the eighteenth tray from the top. The gas feed has been considered at 25 °C, 50 bar. The feed has been considered as a binary $CH_4$-$C_2H_6$ mixture and its composition has been varied from 5 to 75 mol% of $C_2H_6$. The cold box operates at 50 bar. The distillation column has 30 theoretical trays and is operated at 25 bar, as suggested by Luyben[56]. A condenser is placed at the top of the distillation unit in order to guarantee a final methane content in the produced gas higher than 99 mol%, while the bottom product has 100 ppm of $CH_4$, in order to enhance the methane recovery. The final produced gas is re-compressed to 50 bar. The minimum approach in the heat exchangers has been set to 5 °C. The process unit has been simulated with Aspen Hysys® V7.3, using the SRK EoS[43]. Since the reboiler does not require heat at high temperatures, its contribution to the net equivalent methane has been neglected, while cooling duties at low-temperatures and mechanical power for compressors have been accounted as key-parameters for the energy analysis. Per each inlet composition, the process operating conditions have been optimized in order to find the minimum energy required to perform the separation according to the purity specifications. The vapor fraction of the cooled feed stream after the cold box (that determines the precooling temperature of the feed stream) and the split factor of the vapor portion of the feed stream have been considered as degrees of freedom for the optimization. It has to be pointed out that, for high amounts of ethane (above 15 mol%) in the inlet feed, it is not possible to guarantee the final methane purity in the produced gas providing the reflux only by means of the expanded portion of the gas feed. The results of process simulations have been used to parametrize the specific net equivalent methane of this process unit as function of the inlet molar fraction of ethane:

$$CH_{4,EQ}^{Demeth} = 7.419 \times 10^{-5} z_{C2H6} + 3.104 \times 10^{-5} \quad (11)$$

The reliability of the proposed correlation is shown in Fig. 10.

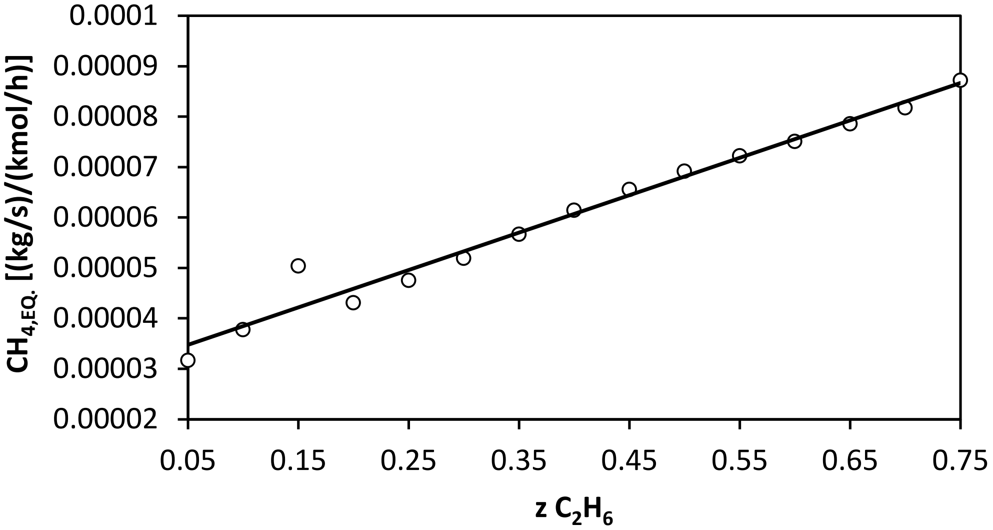

**Figure 10.** Reliability of the correlation (Eq. (11)) to represent the specific net equivalent methane as function of the molar fraction of ethane in the feed stream to the demethanizer.

The agreement is good, except for the point at 15 mol% of ethane in the inlet feed stream. For feed compositions below this value, the reflux ratio of the distillation column provided by the external condenser is zero and the reflux is produced only by using the portion of the expanded feed stream, which enters the column at the first tray from the top. In these conditions, the optimization has been constrained (purity equal to 99 mol%) in order to find the set of the degrees of freedom that allow to obtain the minimum energy consumptions together with the required purity of the final produced gas.

### 3.5 $CO_2$ recompression and dehydration

Carbon dioxide rejected from the MDEA unit is obtained at the top of the regeneration column at a temperature of about 30 °C[14] and is typically available at atmospheric pressure and saturated with water. To transport $CO_2$ for EOR or CCS, the stream should be dehydrated and compressed to a pressure of about 130 bar[57]. The water content of the produced $CO_2$ has been estimated through process simulations for the MDEA unit performed with Aspen Hysys® V7.3, using the DBR Amine Package. At 2 bar and 30 °C this value is 0.0216 mol/mol. The recompression and dehydration process has been simulated using Aspen Hysys® V7.3 and the SRK EoS[43]. The PFD of the compression and dehydration train adopted for the classic scheme (Fig. 4) is shown in Fig. 11.

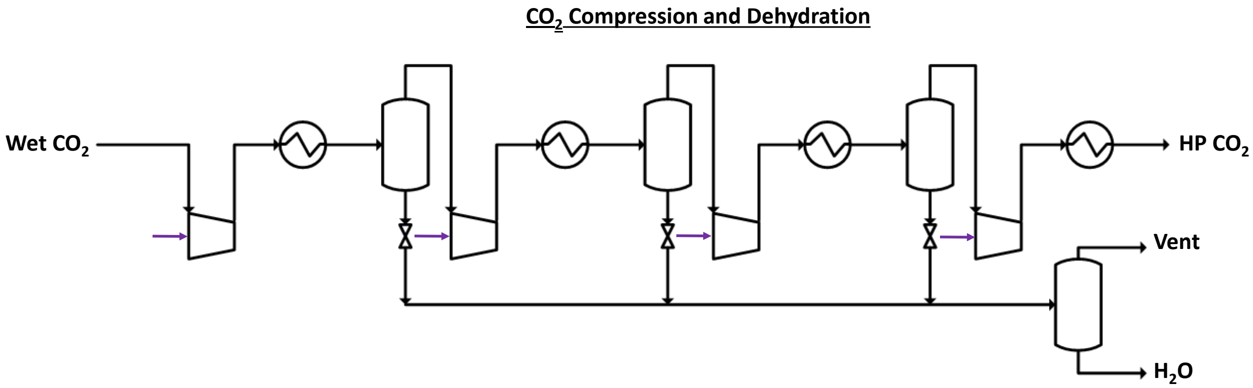

**Figure 11.** PFD of the $CO_2$ compression and dehydration unit. → mechanical power required by compressors, accounted as key parameter for equivalent methane calculations (Eq. (7)).

The inlet wet $CO_2$ stream is fed at 30 °C and 2 bar to a four-stage intercooled compression train. The temperature at the outlet of intercoolers has been set at 30 °C and pressure drops have been neglected. The outlet pressure, $P_n$, from the $n$-th compression stage has been calculated according to:

$$P_n = P_{n-1} \left(\frac{P_{out}}{P_{in}}\right)^{\frac{1}{n}} \tag{12}$$

where $\frac{P_{out}}{P_{in}}$ is the compression ratio between the inlet and outlet pressure of the fluid in the total compression train. The condensed water (with traces of $CO_2$) is separated after each intercooler and expanded to the atmospheric pressure. The specific work required by the unit is 3.95 kW per kmol $h^{-1}$ of inlet wet $CO_2$ feed stream. For the calculation of the net equivalent methane, only mechanical power has been considered for this unit (Eq. (7)).

### *3.6 Dual pressure low-temperature distillation process*

The dual pressure low-temperature distillation process proposed by Pellegrini[31] has been considered for the separation of methane from $CO_2$ and $CO_2$+$C_2H_6$. In this work, only the optimized layout has been taken into account for the energy evaluation while the detailed description of the process can be found elsewhere[31, 14]. The PFD of the process unit is shown in Fig. 12.

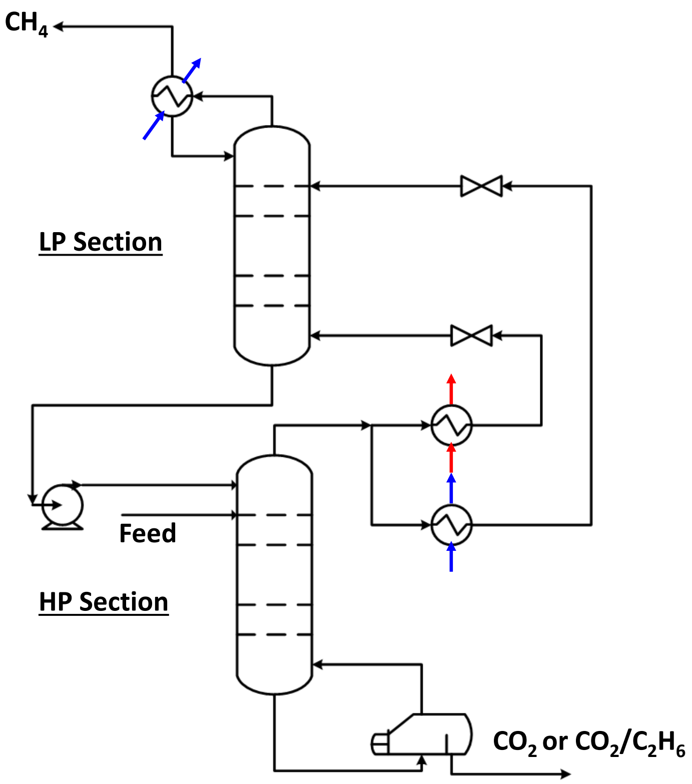

**Figure 12.** PFD of the Dual Pressure Low-Temperature Distillation process[31]. → cooling duty required by low-temperature condensers; → heat flow at low temperature required by the intermediate heater. Only cooling duties are accounted as key parameters for equivalent methane calculations (Eq. (6)). The value of $COP_f$ for the refrigeration cycle is 0.67[14].

The process involves two sections of a distillation unit, operated at 50 and 40 bar respectively. The produced gas is methane at high purity, while heavier compounds are collected in the bottom product. Simulations have been performed in Aspen Hysys® V7.3 with the SRK EoS[43] in order to define mathematical functions that relate the specific net equivalent methane to the inlet gas feed composition. The inlet gas is available at 50 bar at its dew point. Binary mixtures of $CH_4$-$CO_2$ and ternary mixtures of $CH_4$-$CO_2$-$C_2H_6$ have been considered in order to cover all the possible cases. When the $C_{2+}$ fraction is removed upstream of this process unit, the specific net equivalent methane is function only of the $CO_2$ content of the inlet gas stream. (Eq. (13)), while, when the $C_{2+}$ separation is performed downstream of the methane removal, the function depends also on the $C_2H_6$ content of the feed stream (Eq. (14)). For the first case, simulations have been performed changing the $CO_2$ molar fraction in the feed stream from 5 up to 90 mol%, while, for the second case, the $C_2H_6$ content has been varied from 0 up to 25 mol% and the $CO_2$ content from 5 to 65 mol%. For the calculation of the net equivalent methane only cooling duties have been considered, since the amount of heat required by the intermediate heater is at low-temperatures and the process feed stream can be used to provide it. Since the reboiler temperatures are close to the ambient one, no LP steam or other expensive heat sources are required.

$$CH_{4,EQ}^{DPLTD} = -6.955 \times 10^{-3} z_{CO2}^6 + 2.299 \times 10^{-2} z_{CO2}^5 - 3.0 \times 10^{-2} z_{CO2}^4 + 1.933 \times 10^{-2} z_{CO2}^3 - 6.251 \times 10^{-3} z_{CO2}^2 + 1.038 \times 10^{-3} z_{CO2} + 4.1 \times 10^{-5} \quad (13)$$

$$CH_{4,EQ}^{DPLTD} = a(z_{C2H6}) z_{CO2}^6 + b(z_{C2H6}) z_{CO2}^5 + c(z_{C2H6}) z_{CO2}^4 + d(z_{C2H6}) z_{CO2}^3 + e(z_{C2H6}) z_{CO2}^2 + f(z_{C2H6}) z_{CO2} + g(z_{C2H6}) \quad (14)$$

The parameters $a$, $b$, $c$, $d$, $e$, $f$, $g$ of Eq. (14) have been defined as functions of the inlet molar fraction of ethane according to:

$$\theta = K_1 z_{C2H6}^5 + K_2 z_{C2H6}^4 + K_3 z_{C2H6}^3 + K_4 z_{C2H6}^2 + K_5 z_{C2H6} + K_6 \quad \theta = a, b, c, d, e, f, g \quad (15)$$

The values for the parameters $K_1 - K_6$ are reported in Table 4 together with their accuracy $R^2$.

**Table 4.** Parameters used for the correlation adopted in Eq. (15) and their accuracy R2.

| **θ** | **$K_1$** | **$K_2$** | **$K_3$** | **$K_4$** | **$K_5$** | **$K_6$** | **$R^2$** |
|---|---|---|---|---|---|---|---|
| **a** | 2700.773 | -1505.447 | 306.608 | -20.926 | 0.562 | 6.701E-03 | 1 |
| **b** | -5959.493 | 3330.620 | -689.066 | 49.108 | -1.592 | -4.539E-03 | 1 |
| **c** | 5110.347 | -2867.227 | 606.635 | -45.760 | 1.804 | -8.748E-03 | 1 |

| | | | | | | | |
|---|---|---|---|---|---|---|---|
| **d** | -2141.973 | 1208.280 | -263.909 | 21.402 | -1.031 | 1.145E-02 | 1 |
| **e** | 449.733 | -254.900 | 58.102 | -5.117 | 0.303 | -4.815E-03 | 1 |
| **f** | -41.867 | 23.400 | -5.563 | 0.513 | -0.039 | 9.200E-04 | 1 |
| **g** | 0.427 | -5.333E-02 | -2.667E-03 | 7.333E-03 | 1.164E-03 | 4.400E-05 | 1 |

The reliability of the proposed correlations is shown in Fig. 13 for Eq. (13) and in Fig. 14 for Eq. (14).

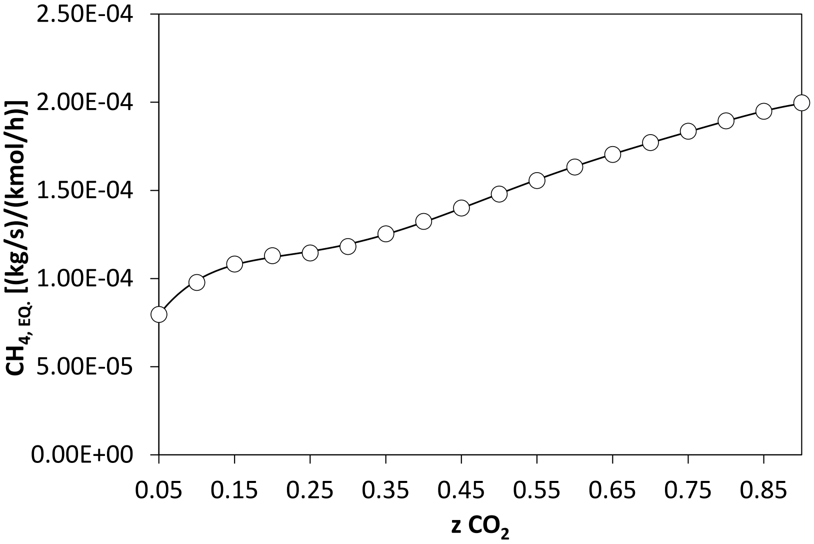

**Figure 13.** Reliability of the correlation (Eq. (13)) to represent the specific net equivalent methane as function of the molar fraction of carbon dioxide in the feed stream when ethane is removed upstream of the dual pressure low-temperature distillation process.

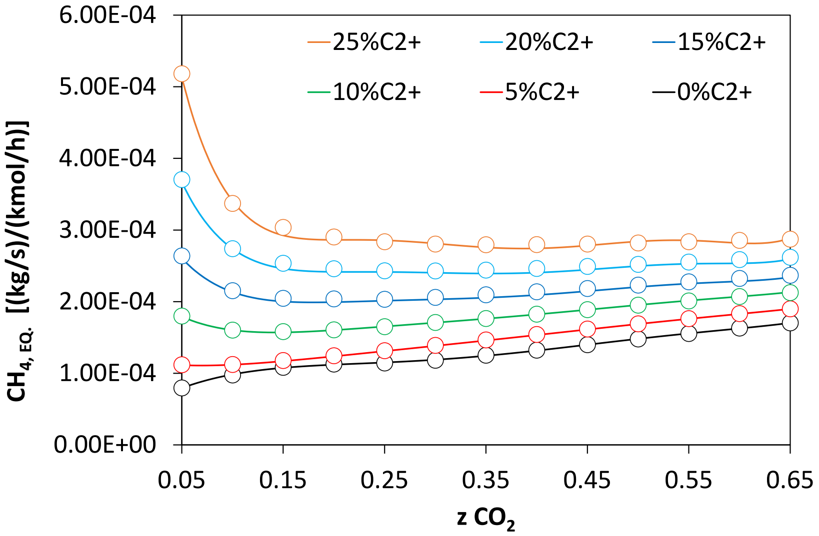

**Figure 14.** Reliability of the correlation (Eq. (14)) to represent the specific net equivalent methane as function of the molar fraction of carbon dioxide and ethane in the feed stream when ethane is removed downstream of the dual pressure low-temperature distillation process.

The agreement of the proposed correlations with simulation results is quite satisfactory.

### *3.7 Two-column extractive distillation for the removal of NGLs before Dual Pressure Low-Temperature Distillation for methane purification*

To perform the removal of the $C_{2+}$ fraction from the natural gas stream, a first analysis regards a two-column extractive distillation unit to break the $CO_2$-$C_2H_6$ azeotrope and extract NGLs before the $CH_4$-$CO_2$ separation. The PFD of the proposed solution is shown in Fig. 15.

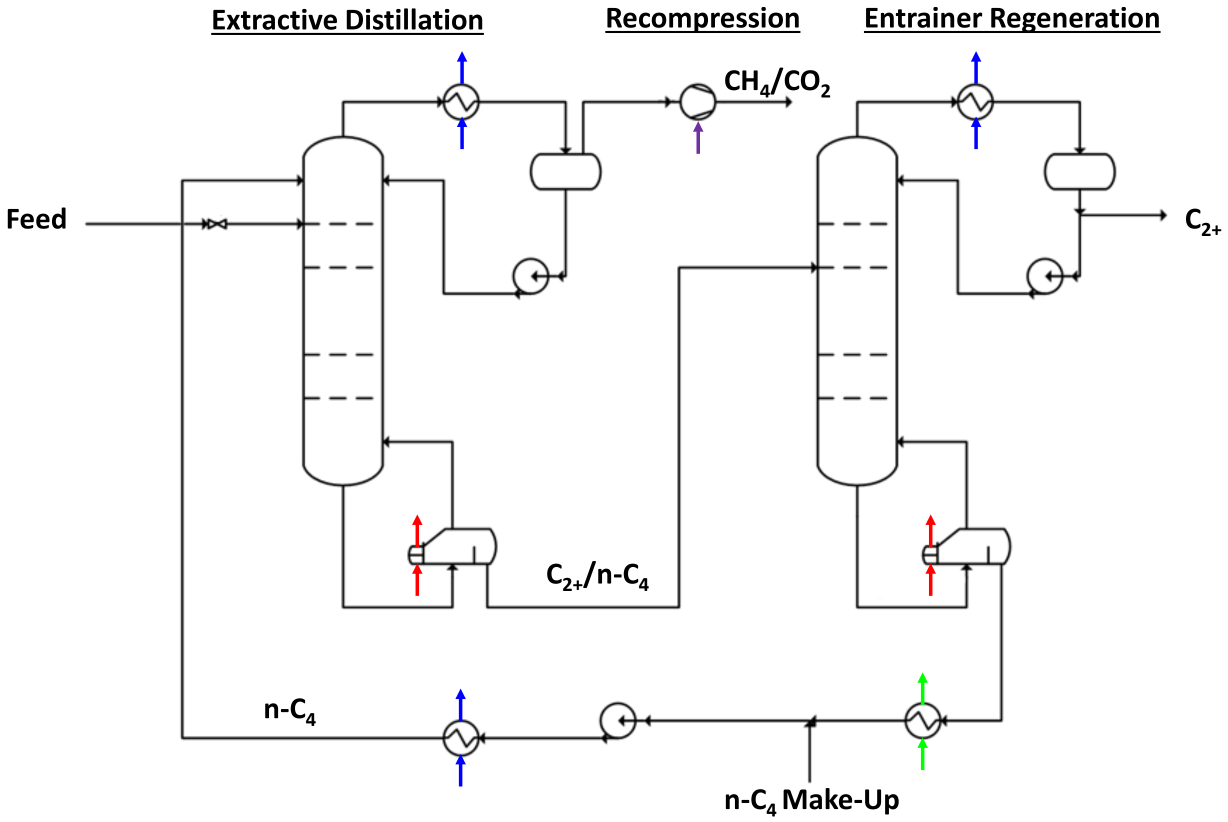

**Figure 15.** PFD of the two-column extractive distillation unit for the separation of the $C_{2+}$ fraction upstream of the Dual Pressure Low-Temperature Distillation process. → cooling duty required by low-temperature condensers; → heat flow required by reboilers; → mechanical power required by the compressor; → amount of useful heat at high temperature that can be recovered inside the process (net equivalent methane savings). For the specific net equivalent methane calculation, cooling duties have been calculated according to Eq. (6), heat flows have been calculated according to Eq. (1) and mechanical power has been calculated according to Eq. (7).

The inlet gas feed is available at 50 bar and at 25 °C. Due to the presence of a minimum azeotrope in the $CO_2$-$C_2H_6$ system, an entrainer (n-$C_4H_{10}$) has been adopted in order to break the azeotrope and separate the $C_{2+}$ fraction of the feed stream. Normal butane has a critical pressure of about 38 bar[58], hence, to perform the separation, the operating pressure should be lower than such a value. So, the feed stream is expanded to 35 bar. The level of pressure is chosen in order to remain below 38 bar and, at the same time, to keep the pressure sufficiently high to avoid excessively low temperatures at column condensers and higher pumping expenses for $CO_2$ recompression.

The process has been studied with Aspen Hysys V7.3®, using the SRK EoS[43]. The two distillation columns have 30 theoretical trays. The entrainer is fed at 10 °C on the fourth tray from the top of the first distillation column. Methane and carbon dioxide are recovered in gas phase as top product stream from the first distillation column, while ethane and n-butane at the bottom in liquid phase. The produced gas stream is compressed back to 50 bar and is sent to the Dual Pressure Low-Temperature Distillation process, while the entrainer is regenerated in a second distillation column. The entrainer flow-rate is chosen as the minimum value that allows to minimize the content of carbon dioxide in the bottom stream of the first distillation column and to maximize the recovery of $CO_2$ in the produced gas. Due to the high boiling point of n-butane under pressure, the temperatures at the reboilers of the two distillation units are higher than 100 °C, and so LP steam is needed. The sensible heat of the regenerated solvent can be recycled to the process.

The inlet composition of the feed stream has been varied in order to cover the range of interest: 5–25 mol% of ethane and 0-65 mol% of carbon dioxide, while methane is the balance.

Results of process simulations in terms of specific net equivalent methane have been correlated by means of the following expressions as function of the feed composition of ethane and carbon dioxide:

$$CH_{4,EQ}^{EDU} = A(z_{C2H6})exp(B(z_{C2H6})z_{CO2}) \qquad (16)$$

$$\vartheta(z_{C2H6}) = C_1 z_{C2H6}^3 + C_2 z_{C2H6}^2 + C_3 z_{C2H6} + C_4 \qquad \vartheta = A, B \qquad (17)$$

The values of $C_1$-$C_6$ parameters of Eq. (17) are reported in Table 5 together with their accuracy $R^2$.

**Table 5.** Parameters used for the correlation adopted in Eq. (17) and their accuracy R2.

| **ϑ** | **$C_1$** | **$C_2$** | **$C_3$** | **$C_4$** | **$R^2$** |
|---|---|---|---|---|---|
| **A** | 1.333E-02 | -5.143E-03 | 9.095E-04 | 9.600E-05 | 0.998 |
| **B** | 105.360 | -44.015 | -0.888 | 3.032 | 1 |

The reliability of the proposed correlation is shown in Fig. 16.

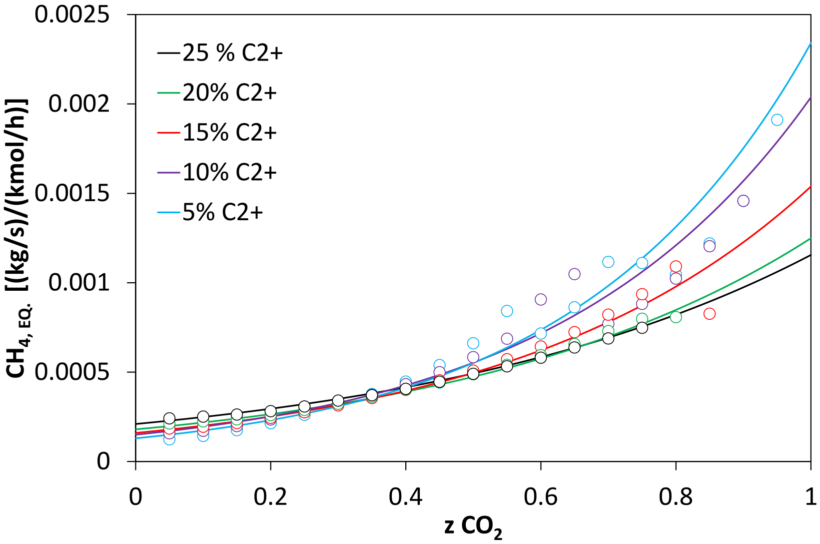

**Figure 16.** Reliability of the correlation (Eq. (16)) to represent the specific net equivalent methane as function of the molar fraction of carbon dioxide and ethane in the feed stream when ethane is removed upstream of the dual pressure low-temperature distillation process by extractive distillation.

Though some discrepancies between the results from the proposed correlation and from simulation can be noticed for z $CO_2 > 0.5$ and ~~high~~low $C_{2+}$ contents, the proposed correlation has been considered valid and it has been used for the overall energy analysis.

### *3.8 Two-column extractive distillation for the removal of NGLs after Dual Pressure Low-Temperature Distillation for methane purification*

In case of $C_{2+}$ fraction removal downstream of the dual pressure low-temperature distillation process, a two-column layout has been considered to perform an extractive distillation and break the $CO_2$-$C_2H_6$ azeotrope. This solution has been widely adopted in the open literature (see the Introduction section) and has been considered also in this work as state-of-the-art technology. The PFD of the process is shown in Fig. 17.

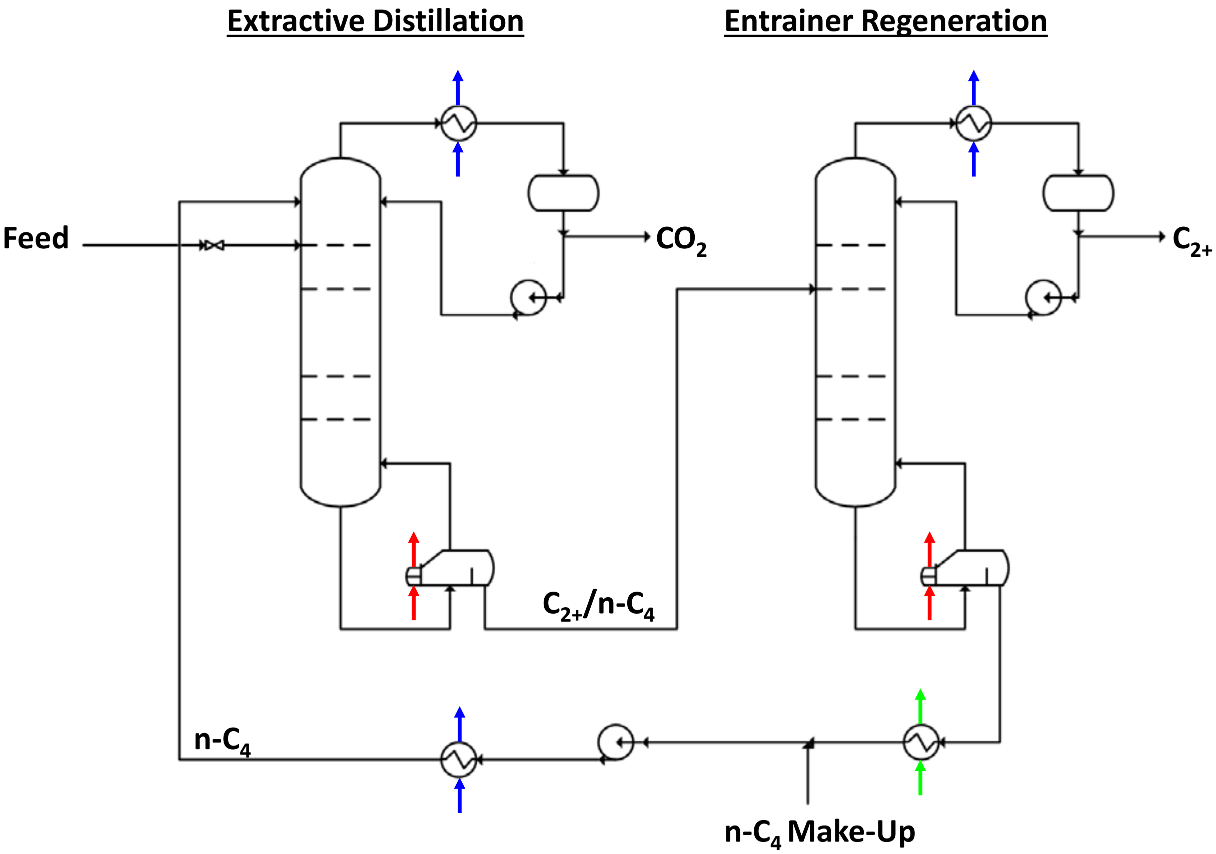

**Figure 17.** PFD of the two-columns extractive distillation unit for the separation of the $C_{2+}$ fraction downstream of the Dual Pressure Low-Temperature Distillation process. → cooling duty required by low-temperature condensers; → heat flow required by reboilers; → amount of useful heat at high temperature that can be recovered inside the process (net equivalent methane savings). For the specific net equivalent methane analysis, cooling duties have been calculated according to Eq. (6) and heat flows have been calculated according to Eq. (1).

The process has been studied with Aspen Hysys V7.3® and the SRK EoS[43]. The feed stream has been considered at 50 bar and at its bubble point, as the bottom stream of the dual pressure low-temperature distillation process. The ~~flow rate~~stream is a binary mixture of $CO_2$ and $C_2H_6$. The molar fraction of $CO_2$ has been varied from 20 to 95 mol%. Under 20 mol% convergence problems occurred. The two distillation columns have 30 theoretical trays and the entrainer (n-butane) is fed on the fourth tray from the top of the first distillation column. The pressure of the two distillation units has been set at 35 bar, to remain below the critical pressure of the entrainer as considered for the previous case (see Section 3.7). The flow rate of n-butane has been chosen as the minimum value that allows to break the $CO_2$-$C_2H_6$ azeotrope assuring high purity of the produced streams, minimizing the leakages of the entrainer. $CO_2$ and $C_2H_6$ are produced in liquid phase at the top respectively of the first distillation unit and of the entrainer regeneration column. The goal is to keep carbon dioxide in liquid phase, in order to use a pump for its further compression. LP steam is used to provide heat at temperatures above 100 °C at the reboilers of the distillation columns. Sensible heat of the hot regenerated n-butane can be recovered inside the process.

The results of process simulations for the specific net equivalent methane analysis have been correlated by means of the following expression, function of the molar fraction of $CO_2$ in the feed stream:

$$CH_{4,EQ}^{2EDD} = exp\left(0.0135\left(\frac{1}{z_{CO2}}\right)^2 + 0.2308\left(\frac{1}{z_{CO2}}\right) - 7.5564\right) \tag{18}$$

The reliability of the proposed correlation is shown in Fig. 18.

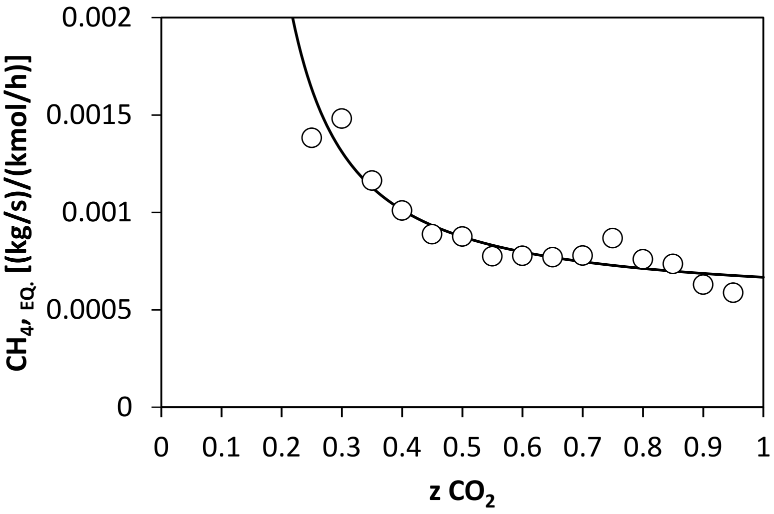

**Figure 18.** Reliability of the correlation (Eq. (18)) to represent the specific net equivalent methane as function of the molar fraction of carbon dioxide and ethane in the feed stream when ethane is removed downstream of the dual pressure low-temperature distillation process by means of a two-columns extractive distillation unit.

The agreement between simulation results and the correlation has been considered satisfactory for the purposes of the analysis object of this work.

### *3.9 Three-column extractive distillation for the removal of NGLs after Dual Pressure Low-Temperature Distillation for methane purification*

Alternatively, in order to split the $CO_2$-$C_2H_6$ minimum azeotrope, a three-column process has been considered. This process preliminarily removes $CO_2$ or $C_2H_6$ (depending on the feed composition) from the azeotrope, reducing the overall energy requirements for the considered separation. According to the isobaric phase diagram of this binary system (Fig. 19) at 35 bar, the minimum azeotrope occurs for a $CO_2$ molar fraction of about 0.7. $CO_2$ is the light compound of the mixture.

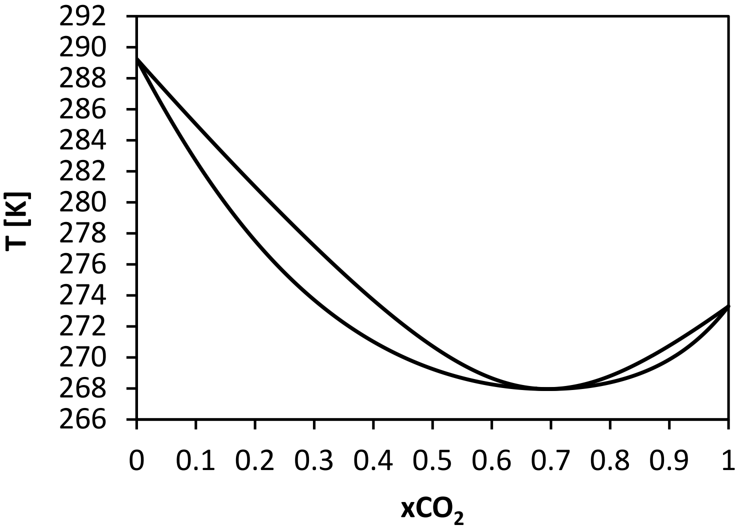

**Figure 19.** Isobaric phase diagram of the $CO_2$-$C_2H_6$ mixture at 35 bar. Calculations have been made using the SRK EoS[43].

When its composition is below 0.7, the first distillation column can be used to separate ethane at the bottom and the azeotrope at the top, while for compositions higher than 0.7, the first distillation unit is used to separate $CO_2$ in liquid phase as bottom product stream and the azeotrope at the top. Then, the azeotrope can be separated by means of an extractive distillation unit with n-butane (as for the previous scheme, see Section 3.8). In this way, the energy requirements to separate the azeotrope are reduced since the overall feed stream that enters the extractive distillation unit is lowered by the first distillation unit, which performs a bulk separation.

The PFD of the considered solution is shown in Fig. 20.

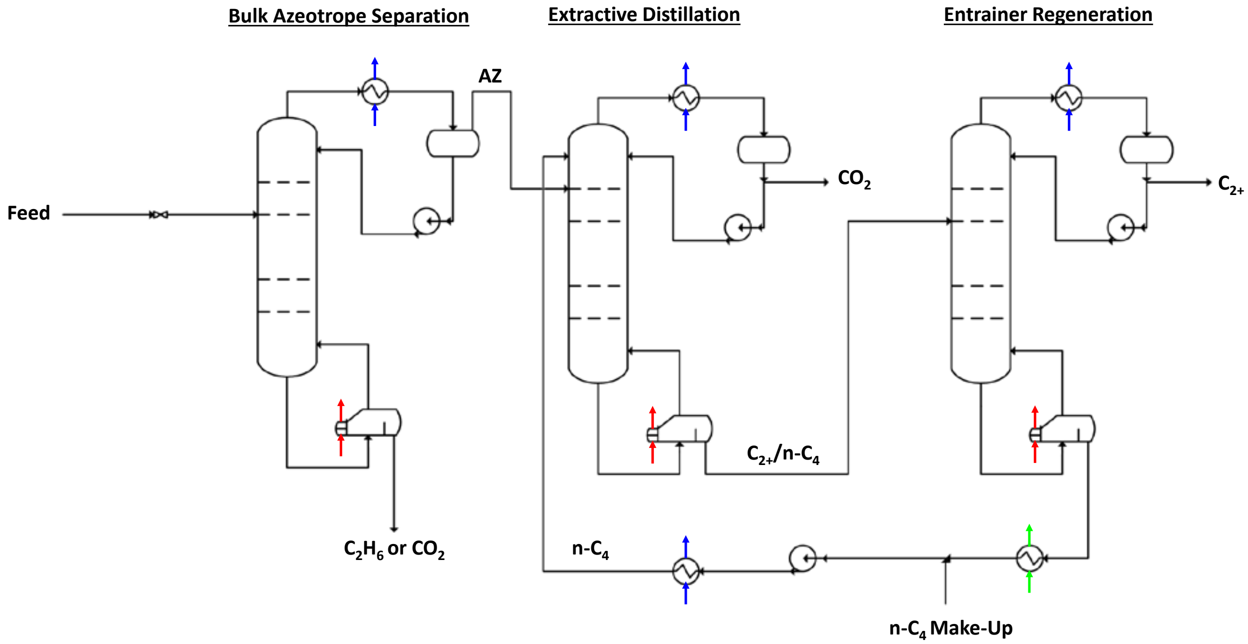

**Figure 20.** PFD of the three-columns extractive distillation unit for the separation of the $C_{2+}$ fraction downstream of the Dual Pressure Low-Temperature Distillation process. → cooling duty required by low-temperature condensers; → heat flow required by reboilers; → amount of useful heat at high temperature that can be recovered inside the process (net equivalent methane savings). For the specific net equivalent methane analysis, cooling duties have been calculated according to Eq. (6) and heat flows have been calculated according to Eq. (1).

The process has been studied with Aspen Hysys V7.3® and the SRK EoS[43]. The feed stream at its bubble point at 50 bar (as the bottom product from the dual pressure low-temperature distillation process) is a binary $CO_2$-$C_2H_6$ mixture. The $CO_2$ content has been varied from 5 up to 95 mol%. The three distillation columns have 30 theoretical trays and are operated at 35 bar. From the top of the first distillation column, the azeotrope is recovered in gas phase and sent to the extractive distillation unit, while the bottom stream contains ethane or carbon dioxide (depending on the feed composition) in liquid phase under pressure. The entrainer is n-butane and is fed on the fourth tray from the top of the second distillation column. Considerations made for the extractive distillation unit of the two-column scheme (see Section 3.8) are still valid. For energy calculations, since the reboiler of the first distillation column requires heat at low temperature (ambient or lower), its contribution has been neglected, while the two reboilers of the extractive distillation section require heat at temperatures higher than 100 °C, hence LP steam is used. The sensible heat of the hot regenerated entrainer is recycled to the process.

The results of process simulations, in terms of specific net equivalent methane, have been correlated as function of the inlet $CO_2$ molar fraction of the feed stream, according to:

$$CH_{4,EQ}^{3EDD} = \begin{cases} 1.116 \times 10^{-4} exp(4.2603 z_{CO2}) & z_{CO2} < 0.7 \\ -2.1 \times 10^{-4} z_{CO2}^2 - 2.43 \times 10^{-3} z_{CO2} + 2.68 \times 10^{-3} & z_{CO2} > 0.7 \end{cases} \quad (19)$$

The accuracy of the presented correlation is shown in Fig. 21.

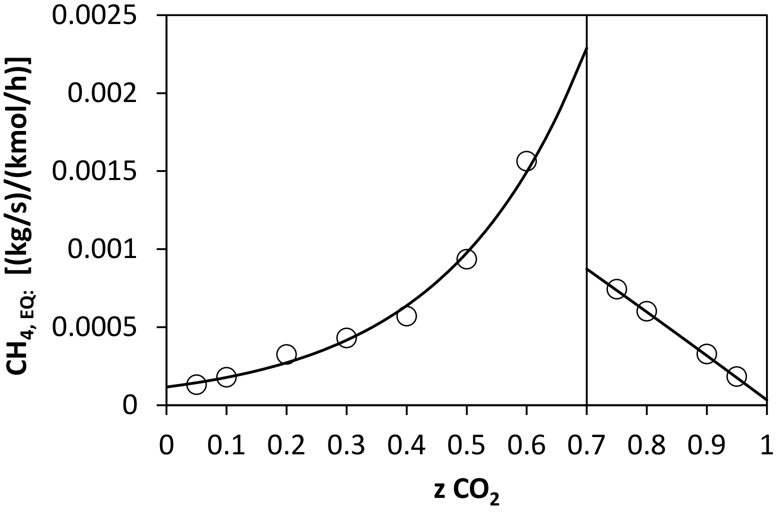

**Figure 21.** Reliability of the correlation (Eq. (19)) to represent the specific net equivalent methane as function of the molar fraction of carbon dioxide and ethane in the feed stream when ethane is removed downstream of the dual pressure low-temperature distillation process by means of a three-columns extractive distillation unit.

The agreement between simulations results and the correlation is good.

### *3.10 $CO_2$ pumping after low-temperature processes*

When $CO_2$ recompression for EOR or CCS is considered for the low-temperature purification scheme (Fig. 5), a pump (Fig. 22) can be used since carbon dioxide for this process solution is obtained in liquid phase under pressure.

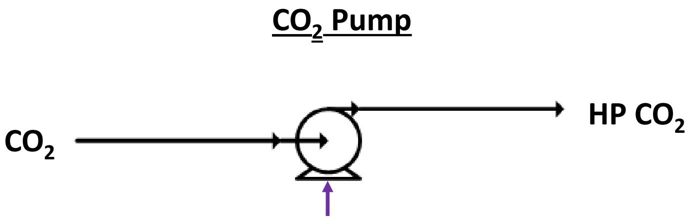

**Figure 22.** PFD of the $CO_2$ pump for carbon dioxide recompression in the low-temperature purification chain (Fig. 5). → mechanical power required by the pump, accounted as key parameter for energy analysis (Eq. (7)).

The specific power required by the pump has been calculated using Aspen Hysys V7.3® and the SRK EoS[43]. Carbon dioxide is available at 50 bar or 35 bar, according to the solution adopted for the $C_{2+}$ split in the process shown in Fig. (5). When $C_{2+}$ are removed upstream of the dual pressure low-temperature distillation process, $CO_2$ is produced in liquid phase at 50 bar and the specific pumping power required for its compression to 130 bar is 0.1561 kW per kmol $h^{-1}$ of $CO_2$. When $C_{2+}$ are removed downstream of the dual pressure low-temperature distillation process, $CO_2$ is produced in liquid phase at 35 bar and the specific pumping power required for its compression to 130 bar is 0.167 kW per kmol $h^{-1}$ of $CO_2$.

## 4. Results and discussion

The relative profitability of different process solutions has been discussed on the basis of the methane consumption for energy production. The net equivalent methane of each process has been converted in terms of percentage of produced gas that has to be burned to provide the energy for the process: in this way, the profitability is established on the basis of how much product can be effectively sold to the market, allowing to study also the feasibility of each stand-alone process according to the $CO_2$ and $C_{2+}$ content in the feed gas.

### *4.1 $CO_2$-$C_2H_6$ azeotrope separation by means of two vs three distillation columns*

As first step, two solutions for the separation of the $CO_2$-$C_2H_6$ minimum azeotrope have been compared: a classic two-column extractive distillation and a three-column process, which includes a bulk removal of the azeotrope and, subsequently, an extractive distillation.

The results of the comparison are shown in Fig. 23.

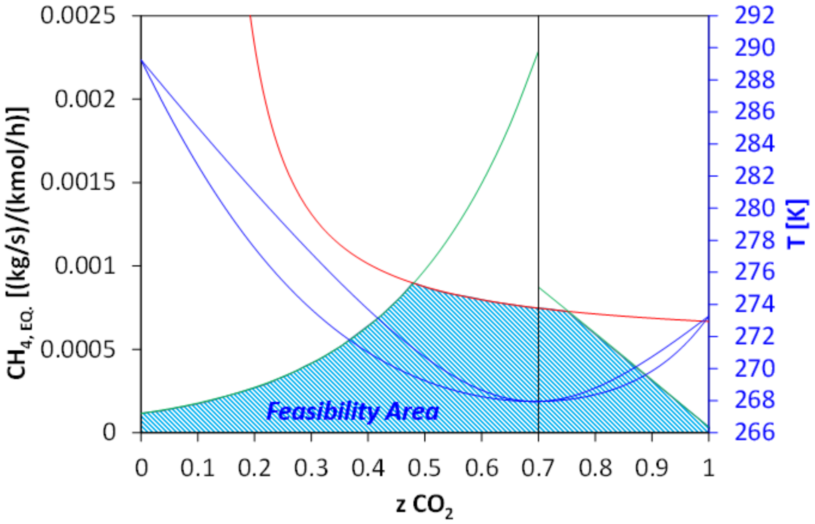

**Figure 23.** Energy comparison between (—) a two-column extractive distillation unit and (—) a three-column extractive distillation process for the split of the $CO_2$-$C_2H_6$ minimum azeotrope (—: isobaric phase diagram of the $CO_2$-$C_2H_6$ mixture at 35 bar, calculated with the SRK EoS[43].

There is a trade-off between the two proposed process solutions: for values of the inlet $CO_2$ molar fraction below 0.48 and above 0.75, the three-column process results to be less energy intensive than the classical two-column process, while for values around the azeotrope composition (about 0.7), the classic two-column process is less energy intensive. It is possible to notice, moreover, that, for values of the $CO_2$ molar fraction greater than 0.5, the energy consumptions of the two-column extractive distillation process is not very sensitive to the inlet content of carbon dioxide.

The feasibility area of Fig. 23 has been considered to account for the specific net equivalent methane of the $CO_2$-$C_2H_6$ separation unit downstream of the dual pressure low-temperature distillation process. Eq. (18) is considered for $z\ CO_2$ between 0.48 and 0.75, while Eq. (19) is used below 0.48 and above 0.75.

### *4.2 Downstream vs upstream $C_{2+}$ removal in the low-temperature purification plant*

A second step of the present work has been the energy comparison between the removal of the $C_{2+}$ fraction of natural gas upstream or downstream of the low-temperature purification process (Fig. 5). In literature, as discussed in the Introduction Section, different works have been proposed on process solutions for the integration between low-temperature natural gas purification processes and NGLs recovery, but no work has been found discussing the relative profitability of different schemes on the basis of a model-based approach and process simulations results. In this work, a numeric comparison is shown. For this analysis, only the energy costs of the dual pressure low-temperature distillation process and the ones of the $C_{2+}$ recovery units (upstream or downstream) have been considered, since desulfurization and dehydration steps are the same for both the cases. For this study, the inlet composition of $CO_2$ has been varied from 5 to 65 mol% and the $C_2H_6$ one from 5 to 25 mol%.

Results are shown in Fig. 24.

a)

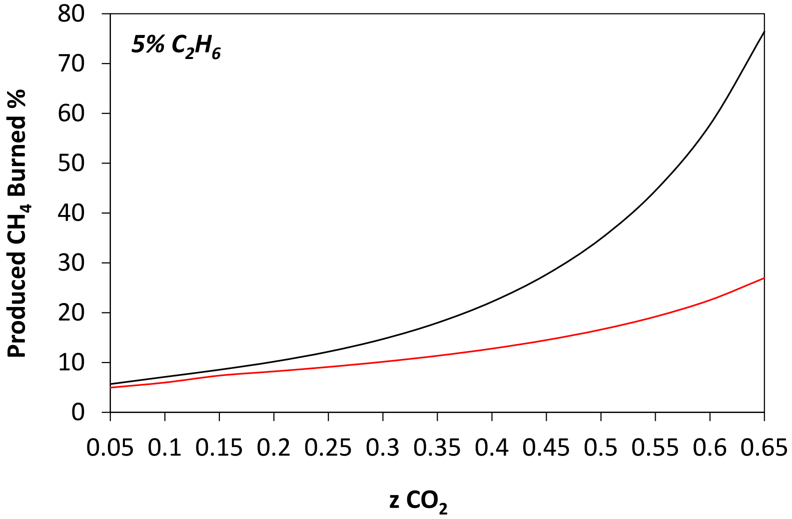

b)

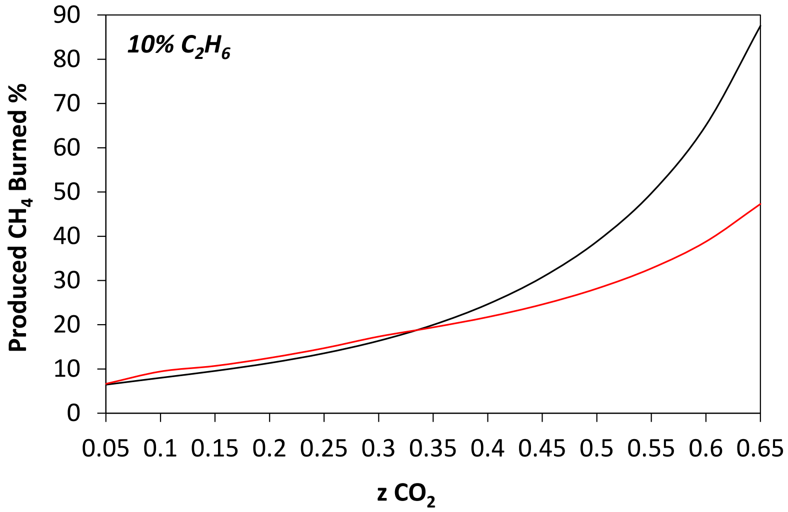
10% $C_2H_6$
Produced $CH_4$ Burned %
z $CO_2$
0
10
20
30
40
50
60
70
80
90
0.05
0.1
0.15
0.2
0.25
0.3
0.35
0.4
0.45
0.5
0.55
0.6
0.65

c)

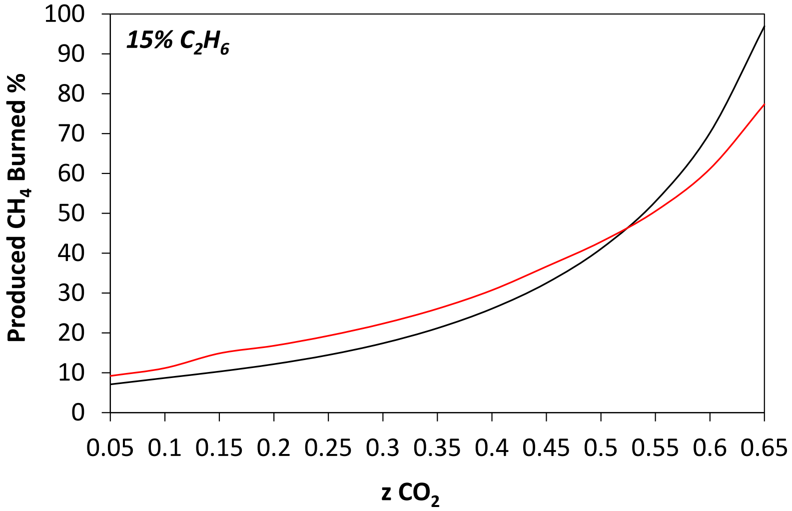
15% $C_2H_6$
Produced $CH_4$ Burned %
z $CO_2$
0
10
20
30
40
50
60
70
80
90
100
0.05
0.1
0.15
0.2
0.25
0.3
0.35
0.4
0.45
0.5
0.55
0.6
0.65

d)

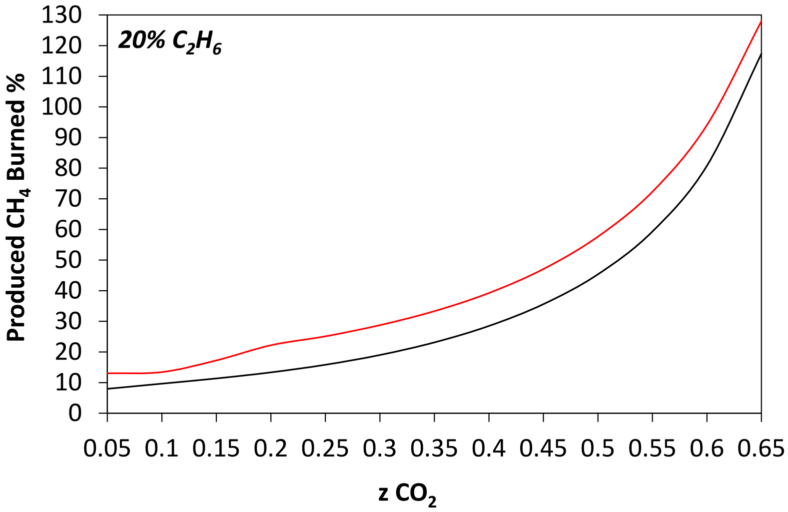

e)

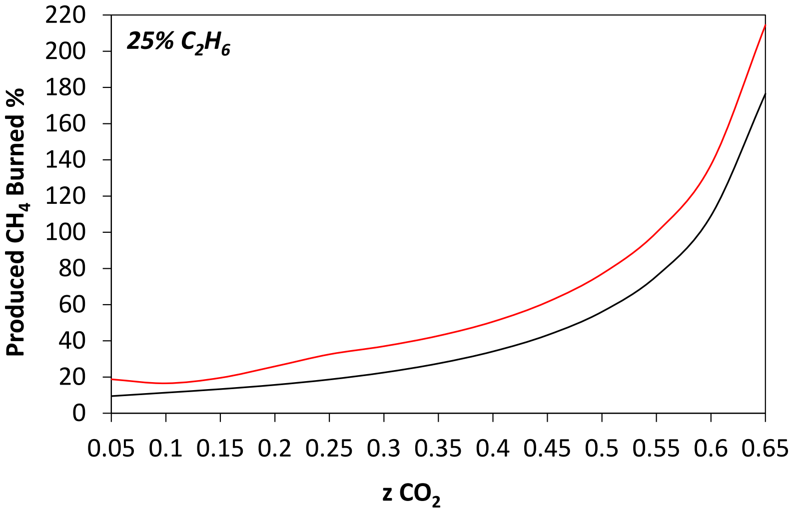

**Figure 24.** Energy comparison, in terms of % of produced methane that has to be burned to provide energy to the process, between (—) Dual Pressure Low-Temperature Distillation process and downstream $C_{2+}$ removal and (—) Dual Pressure Low-Temperature Distillation process and upstream $C_{2+}$ removal. a) 5 mol% of $C_2H_6$, b) 10 mol% of $C_2H_6$, c) 15 mol% of $C_2H_6$, d) 20 mol% of $C_2H_6$ and e) 25 mol% of $C_2H_6$ in the feed stream.

For an inlet feed stream having 5 mol% of ethane, the downstream removal of the $C_{2+}$ fraction is always less energy intensive than the upstream one. The difference is enhanced above 20 mol% of $CO_2$ in the inlet feed. When the ethane content is increased to 10 mol%, a trade-off between the two process solutions occurs for an inlet $CO_2$ content between 30 and 35 mol%. The downstream separation of $C_{2+}$ is favored, in this case, when the inlet content of $CO_2$ is higher than 35 mol%. For a feed stream containing 15 mol% of ethane, the trade-off is shifted up when $CO_2$ in the feed is about 50 mol%. For feed streams having 20 and 25 mol% of ethane, the upstream removal of the $C_{2+}$ fraction is always more profitable for any content of carbon dioxide in the feed gas.

Considering the downstream $CO_2$-$C_2H_6$ separation scheme, for 5 mol% of inlet ethane, the two-column extractive distillation process is less energy intensive for $CO_2$ contents from 5 mol% to 15 mol%, otherwise (CORRETTO, PRIMA DICEVO FINO A 15 MOL% DI CO2? RIGUARDATO ANCHE SUI RISULTATI IN EXCEL E TORNA) the three-column extractive distillation process is favored. At 10 mol% of ethane in the feed gas, the two-column process is more profitable for $CO_2$ contents of the feed stream between 10 and 30 mol%. Increasing the ethane content from 15 to 25 mol%, the two-column solution for the separation of $CO_2$ and $C_2H_6$ downstream of the low-temperature purification process is favored for $CO_2$ contents of the feed stream between 15 and 45, 20 and 60, 25 and 65 mol% respectively. Moreover, the purification of natural gas streams with high $CO_2$ and $C_{2+}$ contents results to be extremely energy intensive, with overall requirements higher than 100% of the produced methane.

### *4.3 Classic vs low-temperature purification plants without $CO_2$ recompression*

The energy analysis has been extended to the complete natural gas purification plant, neglecting the recompression of $CO_2$ in a preliminary phase. A classic scheme (Fig. 4) has been compared to a low-temperature scheme (Fig. 5) for the purification of natural gas and the recovery of the $C_{2+}$

fraction. Energy expenses have been accounted, after the net equivalent methane analysis, as percent of the produced gas that has to be burned to provide energy to the overall purification process. For the low-temperature purification scheme, both upstream and downstream $C_{2+}$ removal has been considered, according to the results obtained previously (see Section 4.2). The results of the comparison between the two complete purification plants, without $CO_2$ recompression, are shown in Figs. 25-28. As for the feed gas composition, the $H_2S$ content has been varied from 0 to 15 mol%, the $C_2H_6$ content from 0 to 25 mol% and the $CO_2$ content from 5 to 65 mol%.

a)

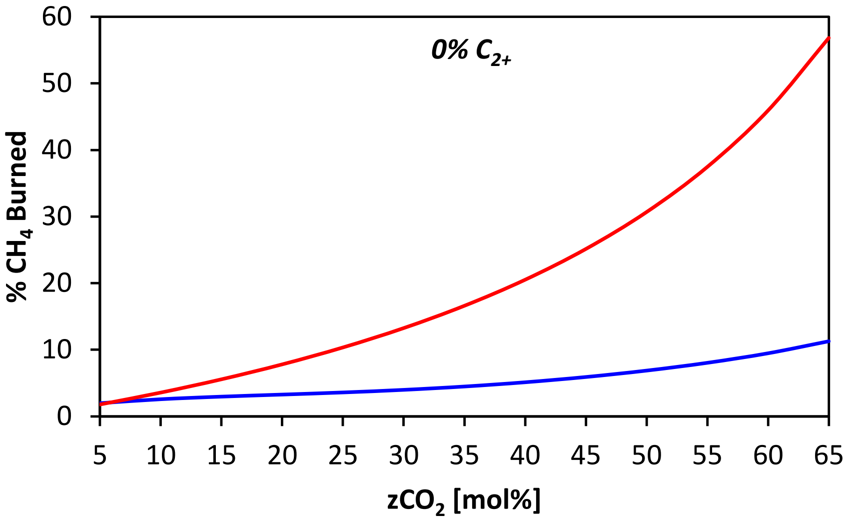

b)

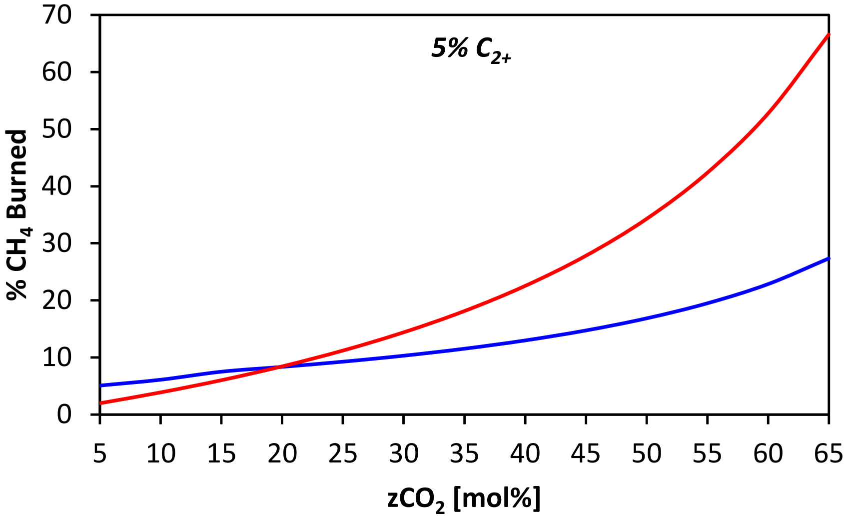
5% $C_{2+}$
% $CH_4$ Burned
0
10
20
30
40
50
60
70
5
10
15
20
25
30
35
40
45
50
55
60
65
$zCO_2$ [mol%]

c)

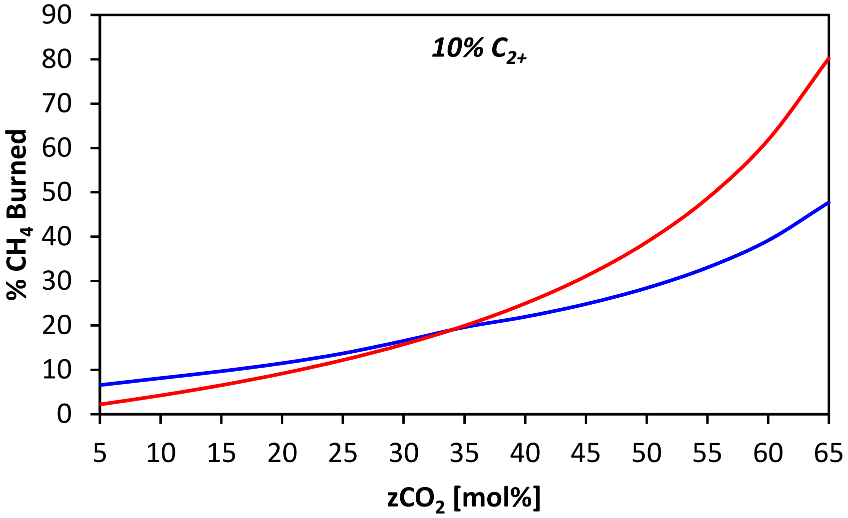
10% $C_{2+}$
% $CH_4$ Burned
0
10
20
30
40
50
60
70
80
90
5
10
15
20
25
30
35
40
45
50
55
60
65
$zCO_2$ [mol%]

d)

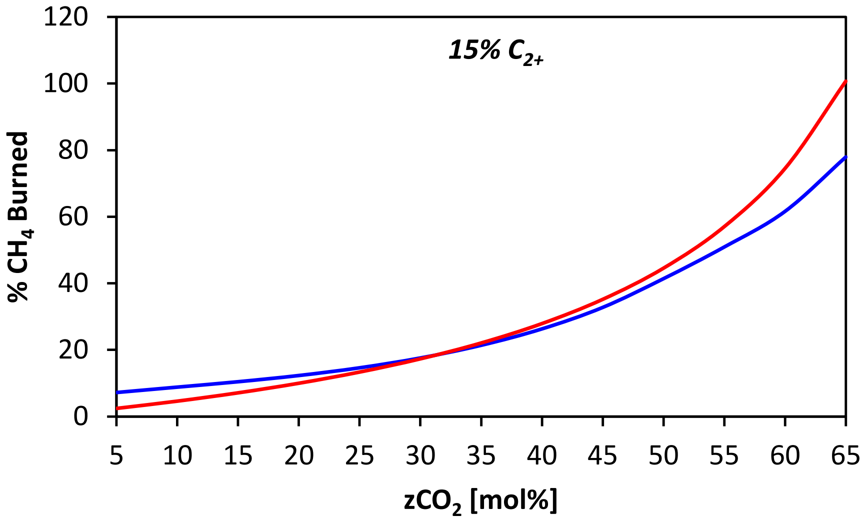
15% $C_{2+}$
% $CH_4$ Burned
120
100
80
60
40
20
0
5
10
15
20
25
30
35
40
45
50
55
60
65
$zCO_2$ [mol%]

e)

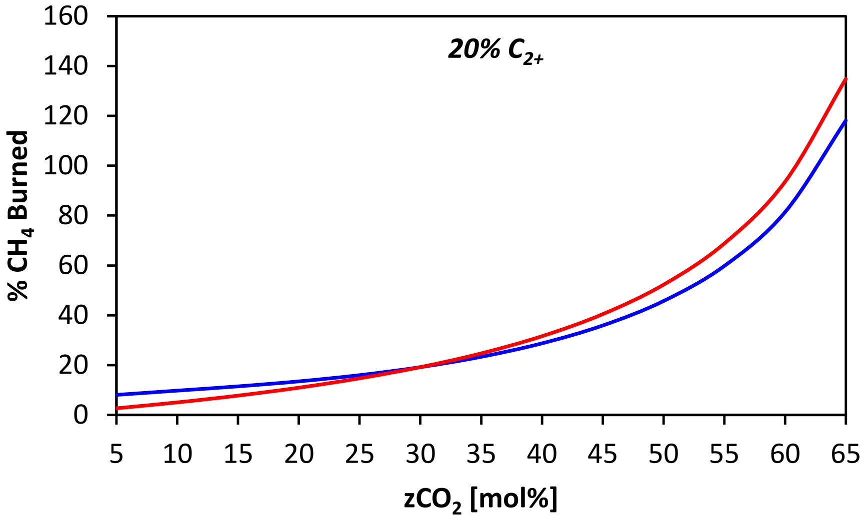
20% $C_{2+}$
% $CH_4$ Burned
160
140
120
100
80
60
40
20
0
5
10
15
20
25
30
35
40
45
50
55
60
65
$zCO_2$ [mol%]

f)

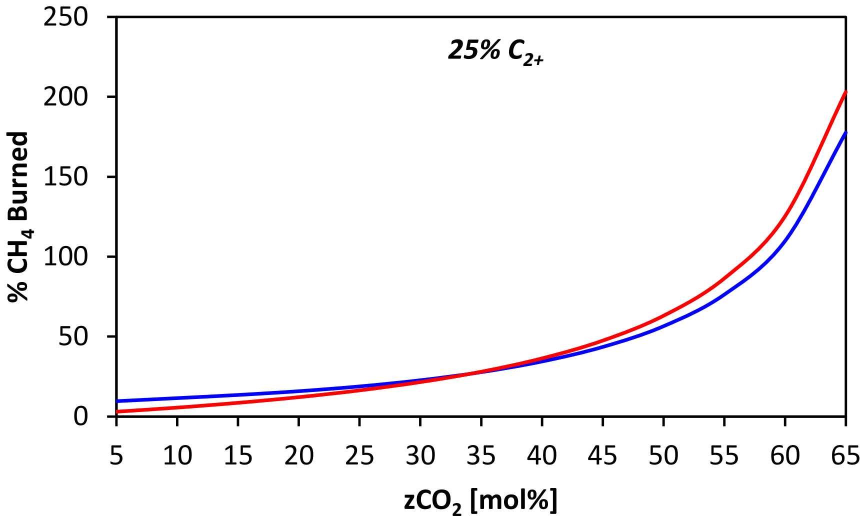

**Figure 25.** Energy comparison, in terms of % of produced methane that has to be burned to provide energy to the process, between (—) classic natural gas purification chain (Fig. 4) and (—) low-temperature purification chain (Fig. 5) for a gas feed stream having 0 mol% of $H_2S$ and a) 0 mol% of $C_2H_6$, b) 5 mol% of $C_2H_6$, c) 10 mol% of $C_2H_6$, d) 15 mol% of $C_2H_6$, e) 20 mol% of $C_2H_6$ and f) 25 mol% of $C_2H_6$.

When no $H_2S$ and no $C_{2+}$ are present in the feed stream, results are in agreement with the ones obtained in a previous work[14]: the breakeven point between the two technologies occurs for a $CO_2$ content of about 8 mol%. When the $C_{2+}$ content in the raw gas is increased from 5 to 25 mol%, the breakeven point occurs for a $CO_2$ content of the raw gas between 20 and 35 mol%. It is possible to notice that, the increasing content of the $C_{2+}$ fraction in the raw gas feed tends to reduce the difference between the energy expenses of the two processes and the overall energy expenses may become greater than 100% of the produced methane. The low-temperature purification plant is always favored than the classical one for high concentrations of $CO_2$ in the inlet gas.

a)

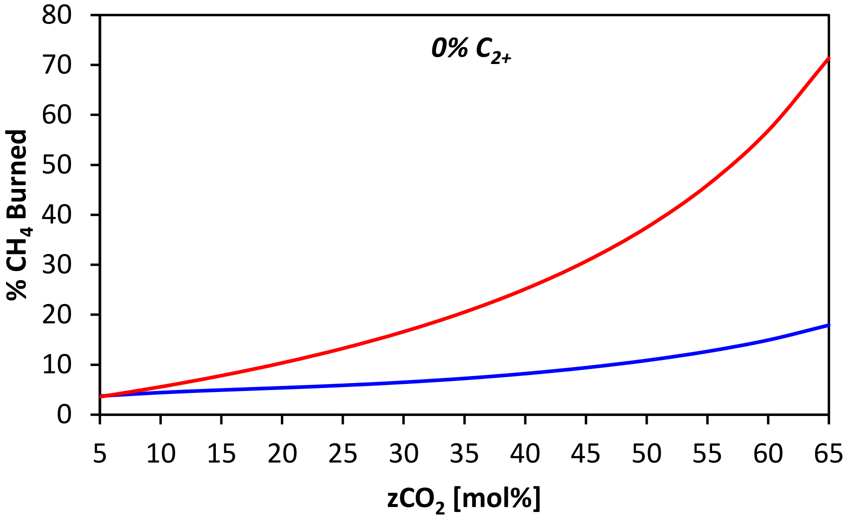
0% $C_{2+}$
% $CH_4$ Burned
0
10
20
30
40
50
60
70
80
5
10
15
20
25
30
35
40
45
50
55
60
65
$zCO_2$ [mol%]

b)

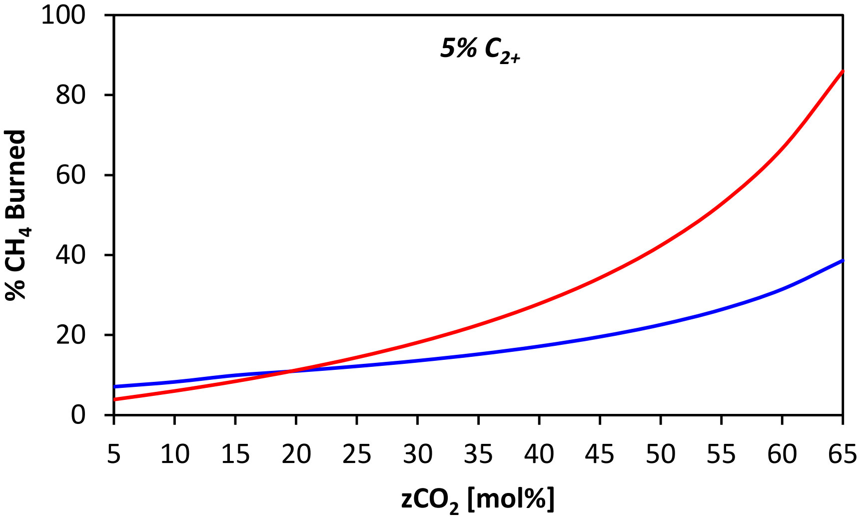
5% $C_{2+}$
% $CH_4$ Burned
0
20
40
60
80
100
5
10
15
20
25
30
35
40
45
50
55
60
65
$zCO_2$ [mol%]

c)

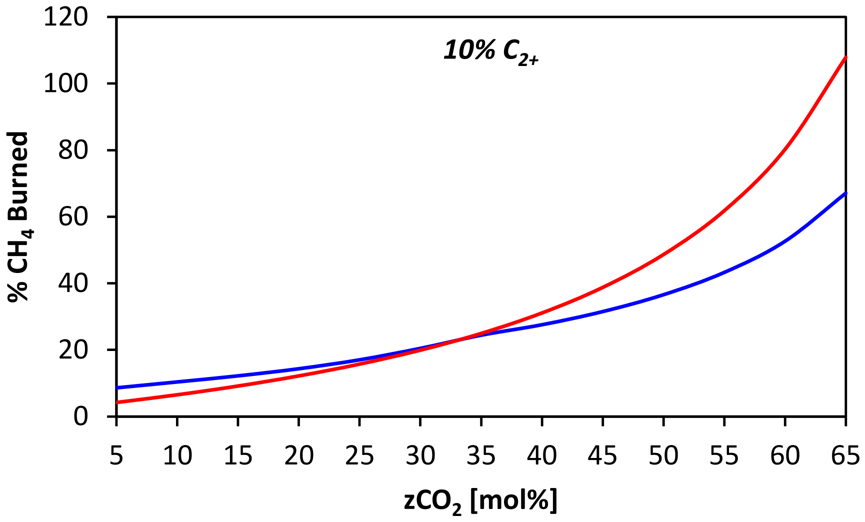

10% $C_{2+}$
120
100
80
60
40
20
0
% $CH_4$ Burned
5
10
15
20
25
30
35
40
45
50
55
60
65
$zCO_2$ [mol%]

d)

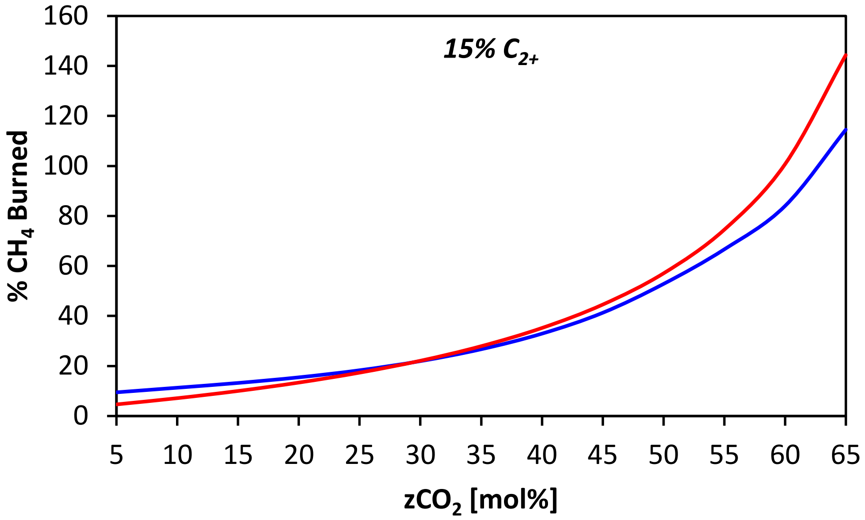

15% $C_{2+}$
160
140
120
100
80
60
40
20
0
% $CH_4$ Burned
5
10
15
20
25
30
35
40
45
50
55
60
65
$zCO_2$ [mol%]

e)

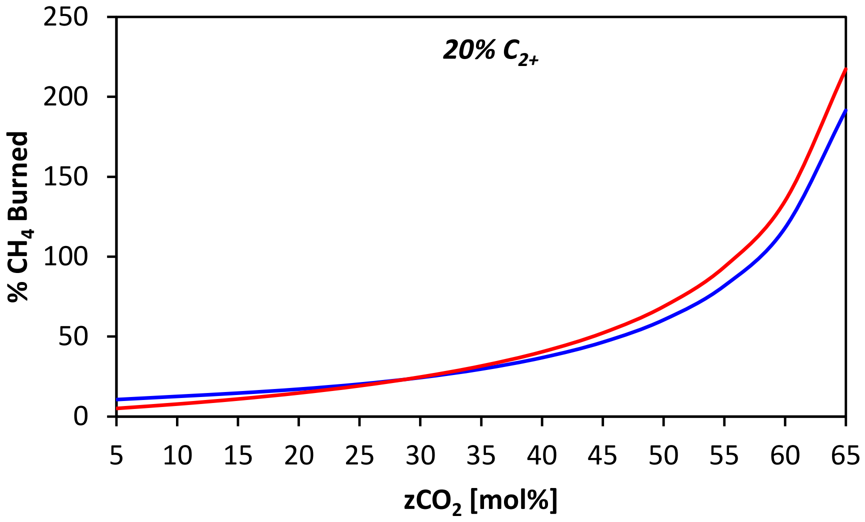

f)

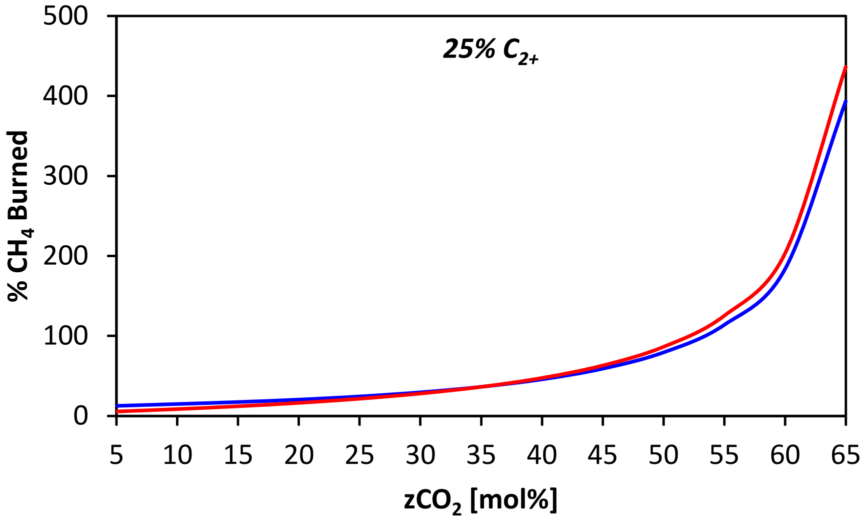

**Figure 26.** Energy comparison, in terms of % of produced methane that has to be burned to provide energy to the process, between (—) classic natural gas purification chain (Fig. 4) and (—) low-temperature purification chain (Fig. 5) for a gas feed stream having 5 mol% of $H_2S$ and a) 0 mol% of $C_2H_6$, b) 5 mol% of $C_2H_6$, c) 10 mol% of $C_2H_6$, d) 15 mol% of $C_2H_6$, e) 20 mol% of $C_2H_6$ and f) 25 mol% of $C_2H_6$.

The same considerations can be outsourced from results obtained for an inlet gas having 5 mol% of $H_2S$. The presence of hydrogen sulfide increases the overall energy expenses, but the obtained results in terms of breakeven points and trends are similar.

a)

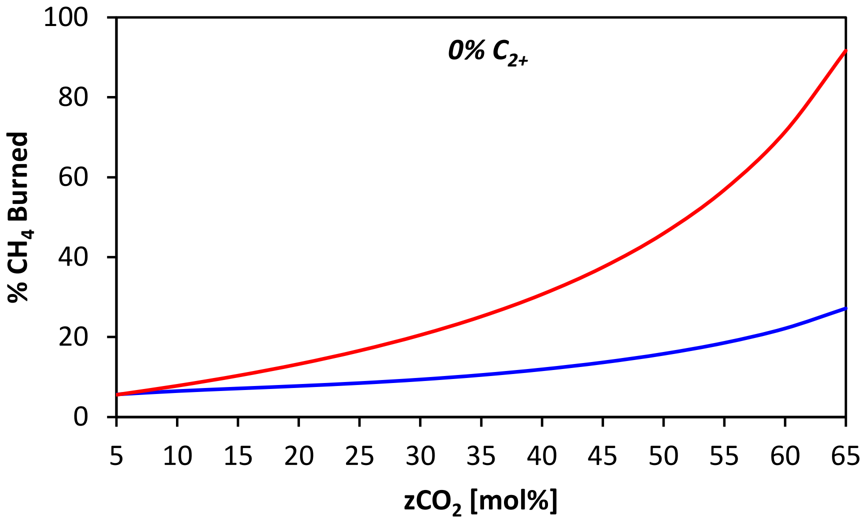

b)

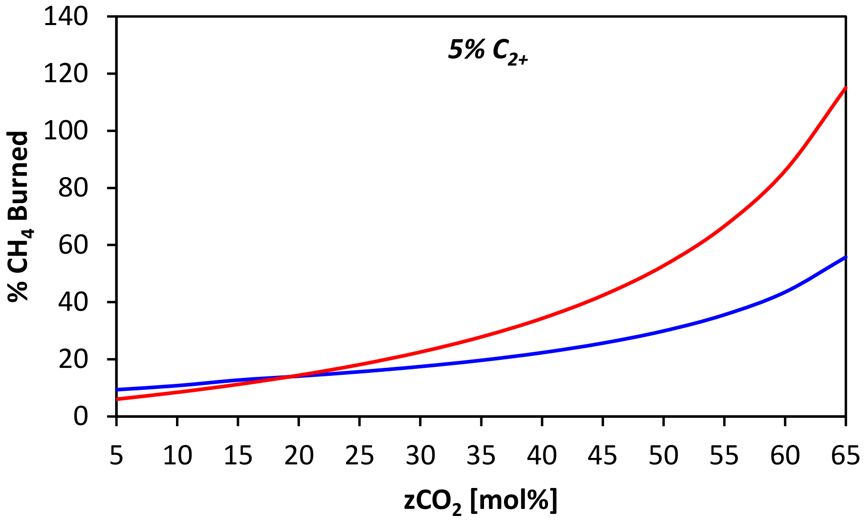

c)

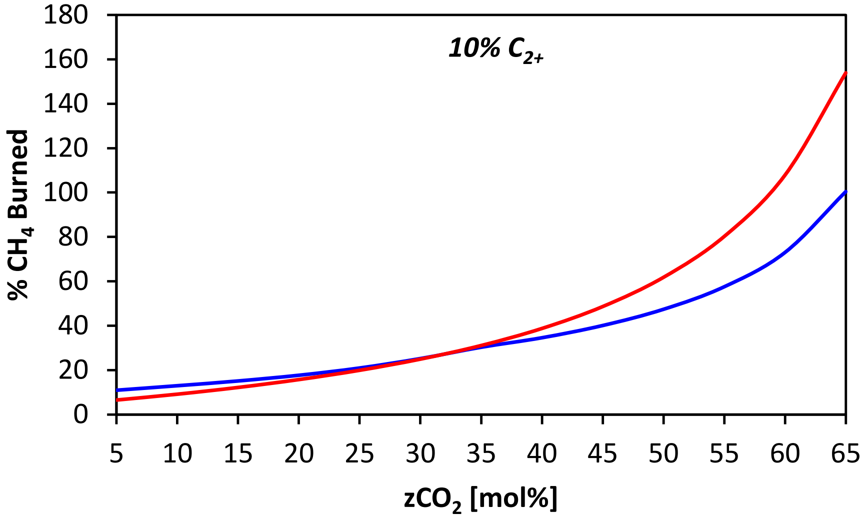
10% $C_{2+}$
% $CH_4$ Burned
zCO$_2$ [mol%]
0
20
40
60
80
100
120
140
160
180
5
10
15
20
25
30
35
40
45
50
55
60
65

d)

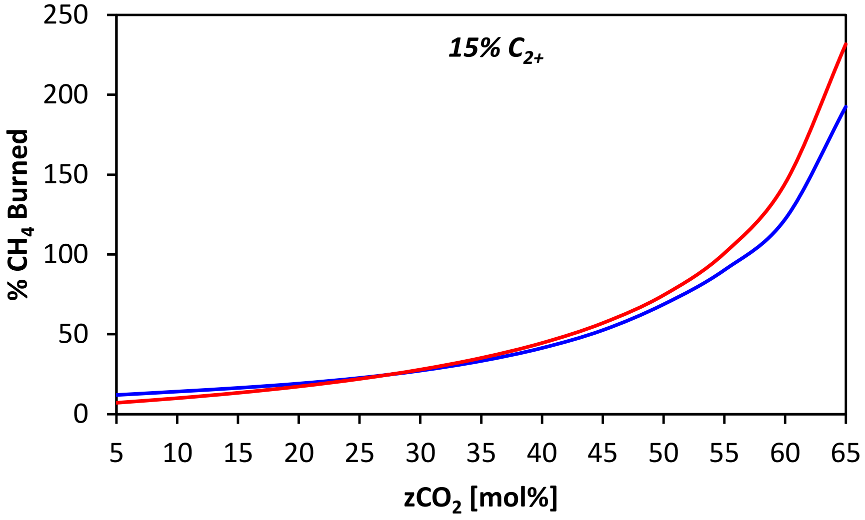
15% $C_{2+}$
% $CH_4$ Burned
zCO$_2$ [mol%]
0
50
100
150
200
250
5
10
15
20
25
30
35
40
45
50
55
60
65

e)

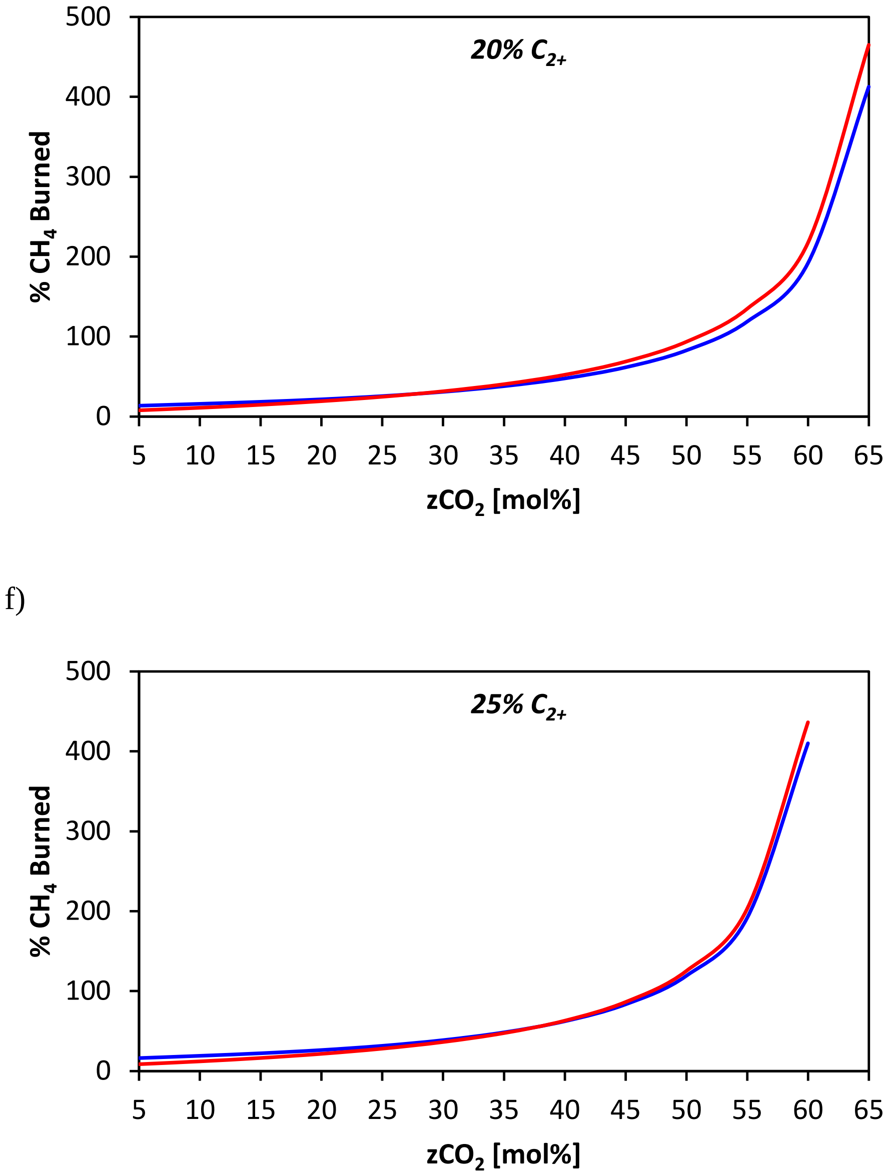

**Figure 27.** Energy comparison, in terms of % of produced methane that has to be burned to provide energy to the process, between (—) classic natural gas purification chain (Fig. 4) and (—) low-temperature purification chain (Fig. 5) for a gas feed stream having 10 mol% of $H_2S$ and a) 0 mol% of $C_2H_6$, b) 5 mol% of $C_2H_6$, c) 10 mol% of $C_2H_6$, d) 15 mol% of $C_2H_6$, e) 20 mol% of $C_2H_6$ and f) 25 mol% of $C_2H_6$.

For the case with 10 mol% of $H_2S$ the BEPs are shifted to higher $CO_2$ contents: for instance for 25 mol% of $C_{2+}$ in the raw gas feed the BEP is shifted from 35 mol% to 40 mol% of $CO_2$ in the feed stream.

a)

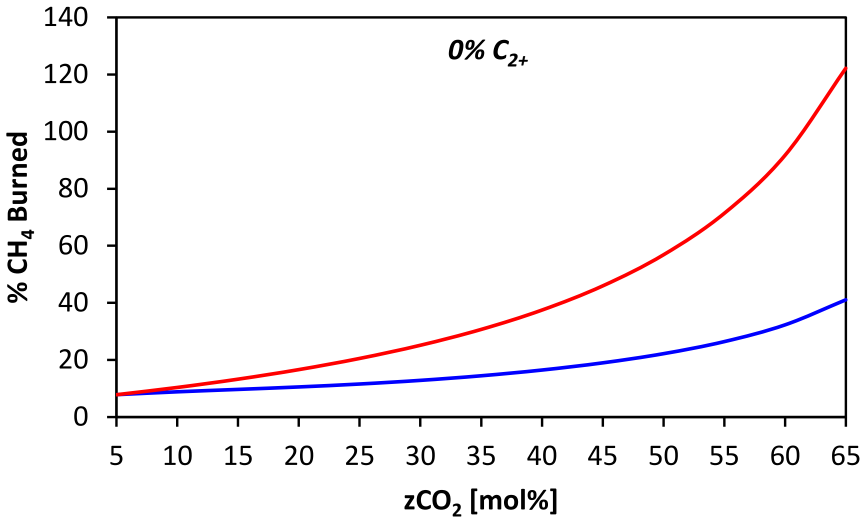

b)

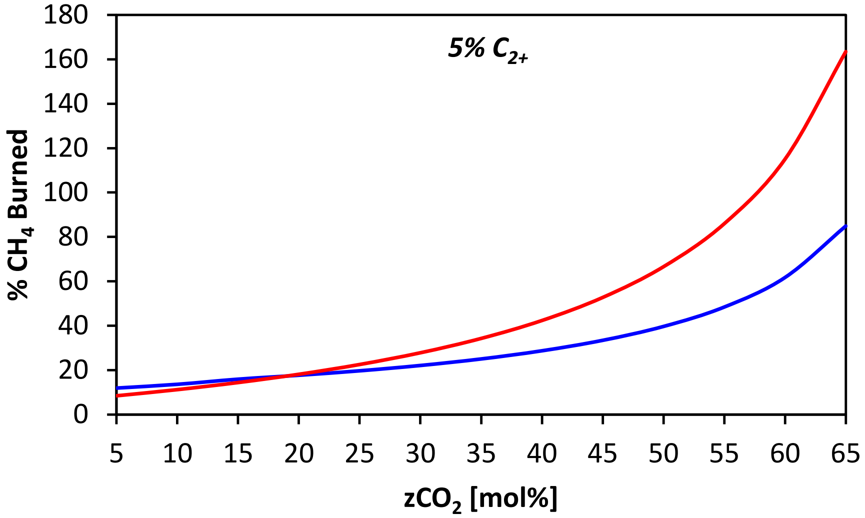

c)

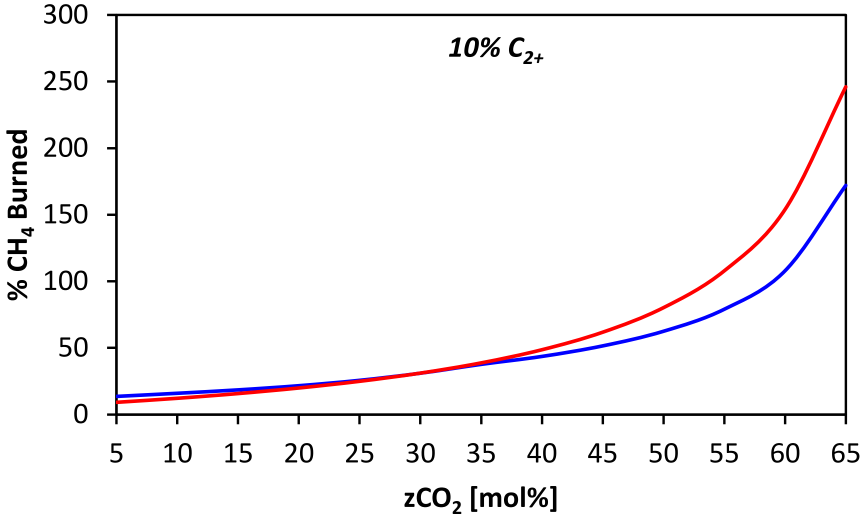
300
250
200
150
100
50
0
% $CH_4$ Burned
10% $C_{2+}$
5
10
15
20
25
30
35
40
45
50
55
60
65
$zCO_2$ [mol%]

d)

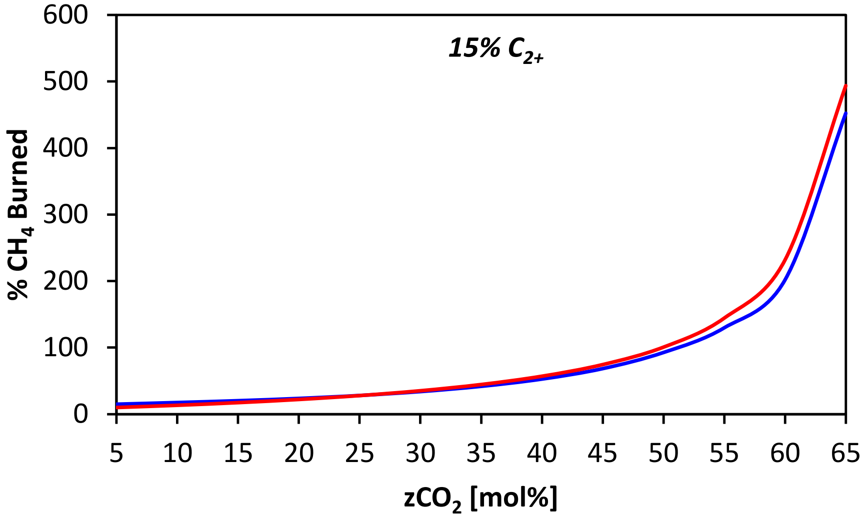
600
500
400
300
200
100
0
% $CH_4$ Burned
15% $C_{2+}$
5
10
15
20
25
30
35
40
45
50
55
60
65
$zCO_2$ [mol%]

e)

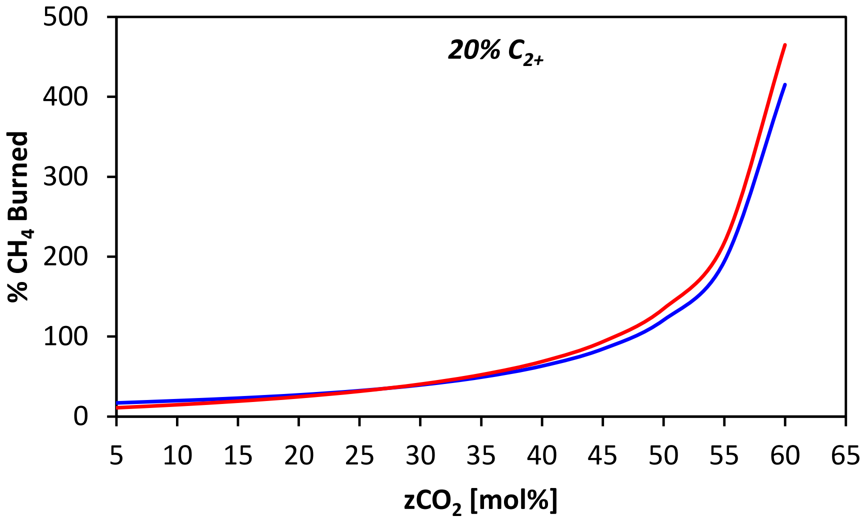

f)

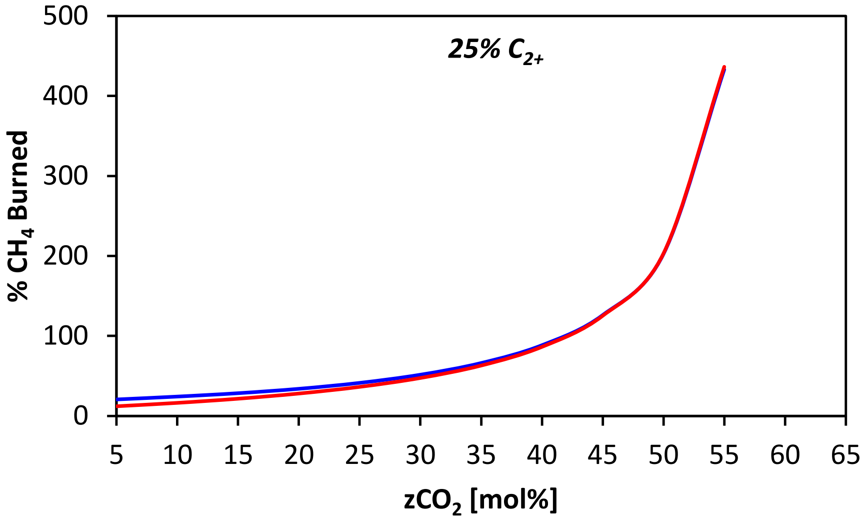

**Figure 28.** Energy comparison, in terms of % of produced methane that has to be burned to provide energy to the process, between (—) classic natural gas purification chain (Fig. 4) and (—) low-temperature purification chain (Fig. 5) for a gas feed stream having 15 mol% of $H_2S$ and a) 0 mol% of $C_2H_6$, b) 5 mol% of $C_2H_6$, c) 10 mol% of $C_2H_6$, d) 15 mol% of $C_2H_6$, e) 20 mol% of $C_2H_6$ and f) 25 mol% of $C_2H_6$.

For a gas feed with 15 mol% of $H_2S$, it is possible to notice that, for gases having also a high amount of $C_{2+}$, the classic process scheme is always less energy intensive than the low-temperature one up to 40 mol% of $CO_2$ in the feed gas.

The presence of $H_2S$ and $C_{2+}$ increases the overall energy expenses and reduces the differences between energy consumptions of the considered schemes, but it can be noticed that for $C_{2+}$ content $\leq$ 10 mol% the low-temperature process allows to significantly reduce the energy expenses below 100% of burned product even when the classical scheme requires more than 100% of the produced gas.

### *4.4 Classic vs low-temperature purification plants integrated with EOR or CCS*

The two process solutions have been finally compared when $CO_2$ recompression for EOR or CCS is required (Figs. 4-5). The results are shown here in Figs. 29-32.

a)

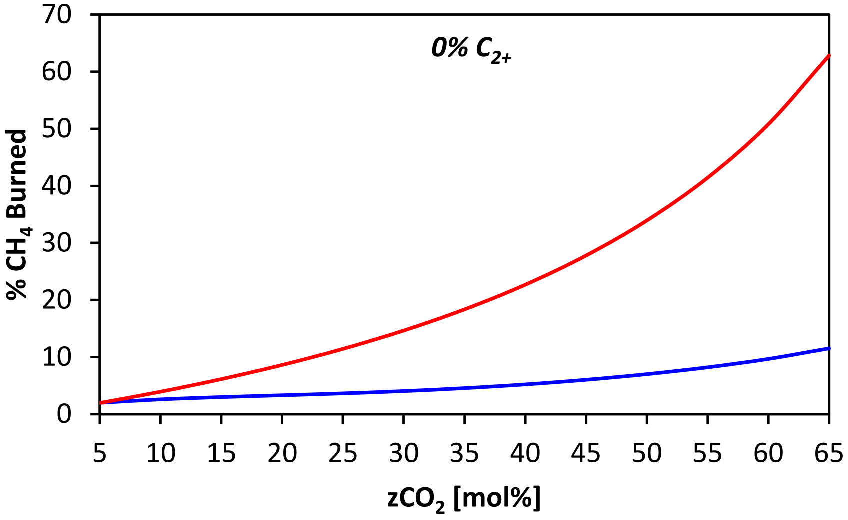

b)

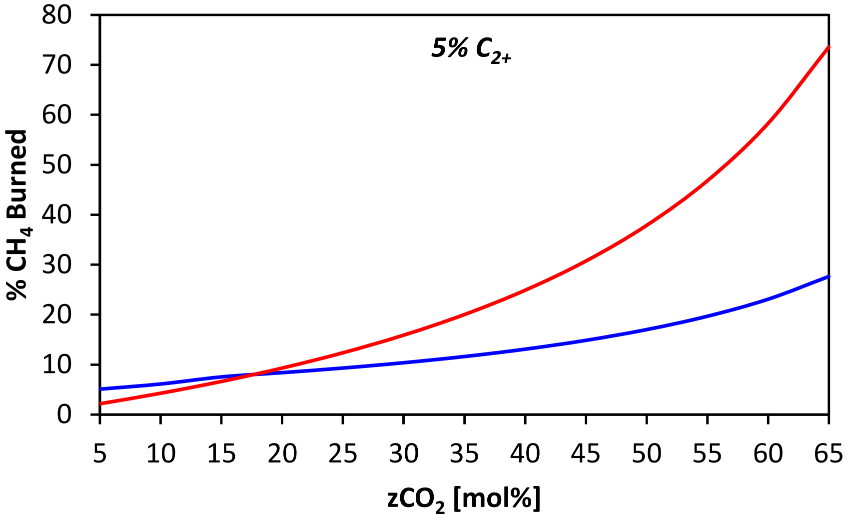
5% $C_{2+}$
% $CH_4$ Burned
0
10
20
30
40
50
60
70
80
5
10
15
20
25
30
35
40
45
50
55
60
65
$zCO_2$ [mol%]

c)

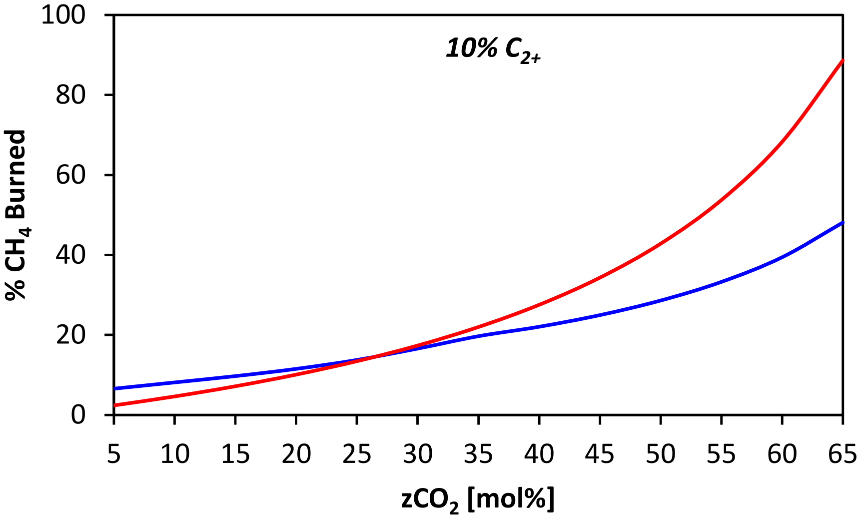
10% $C_{2+}$
% $CH_4$ Burned
0
20
40
60
80
100
5
10
15
20
25
30
35
40
45
50
55
60
65
$zCO_2$ [mol%]

d)

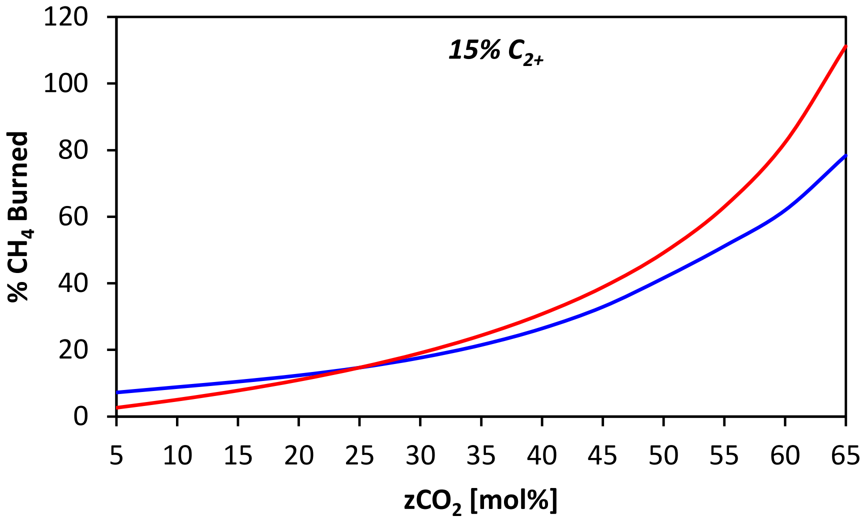
15% $C_{2+}$
% $CH_4$ Burned
120
100
80
60
40
20
0
5
10
15
20
25
30
35
40
45
50
55
60
65
$zCO_2$ [mol%]

e)

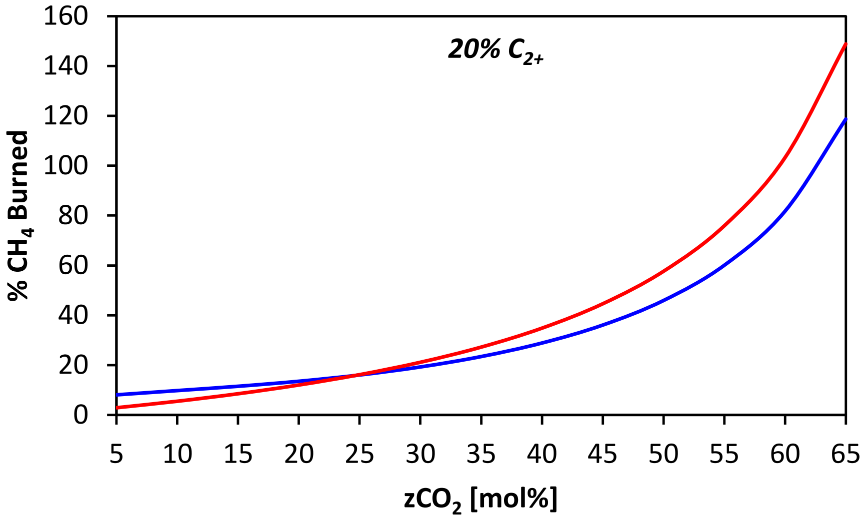
20% $C_{2+}$
% $CH_4$ Burned
160
140
120
100
80
60
40
20
0
5
10
15
20
25
30
35
40
45
50
55
60
65
$zCO_2$ [mol%]

f)

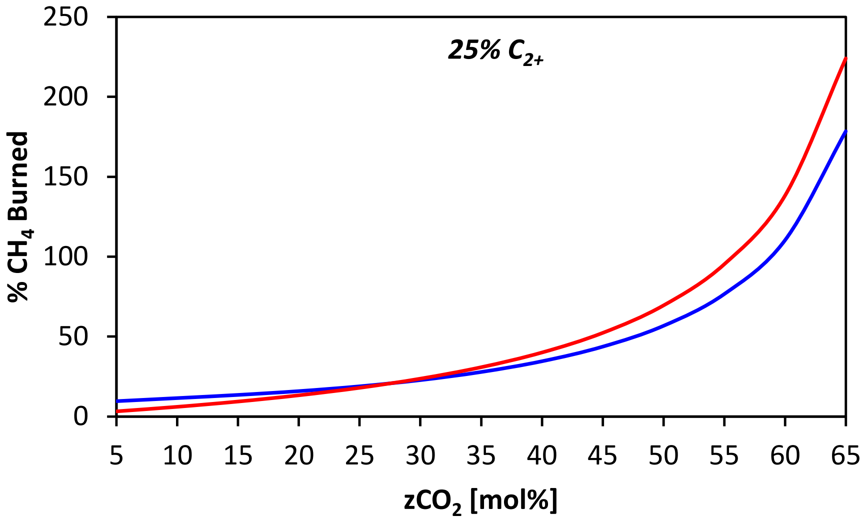

**Figure 29.** Energy comparison, in terms of % of produced methane that has to be burned to provide energy to the process, between (—) classic natural gas purification chain (Fig. 4) and (—) low-temperature purification chain (Fig. 5), with $CO_2$ recompression, for a gas feed stream having 0 mol% of $H_2S$ and a) 0 mol% of $C_2H_6$, b) 5 mol% of $C_2H_6$, c) 10 mol% of $C_2H_6$, d) 15 mol% of $C_2H_6$, e) 20 mol% of $C_2H_6$ and f) 25 mol% of $C_2H_6$.

a)

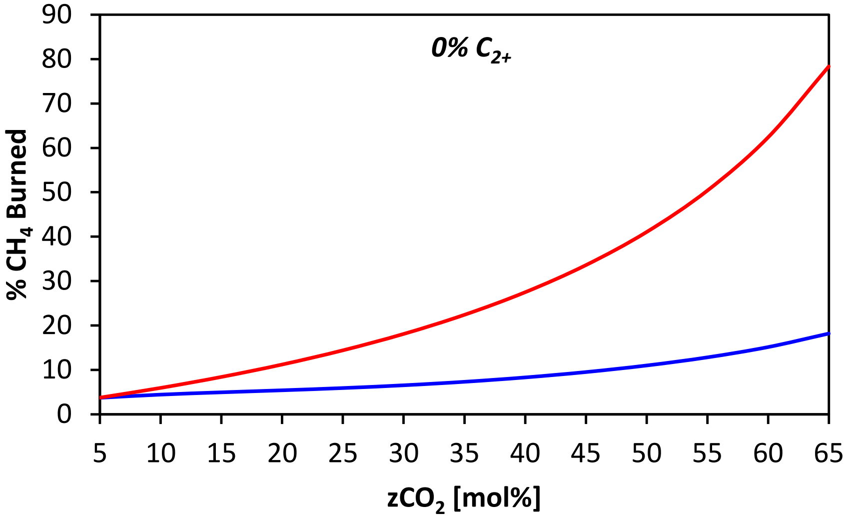

b)

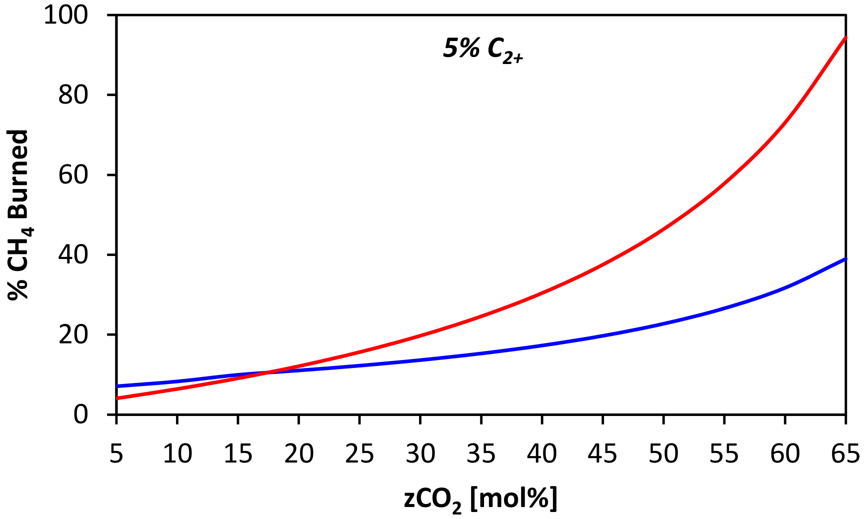
5% $C_{2+}$
% $CH_4$ Burned
0
20
40
60
80
100
5
10
15
20
25
30
35
40
45
50
55
60
65
$zCO_2$ [mol%]

c)

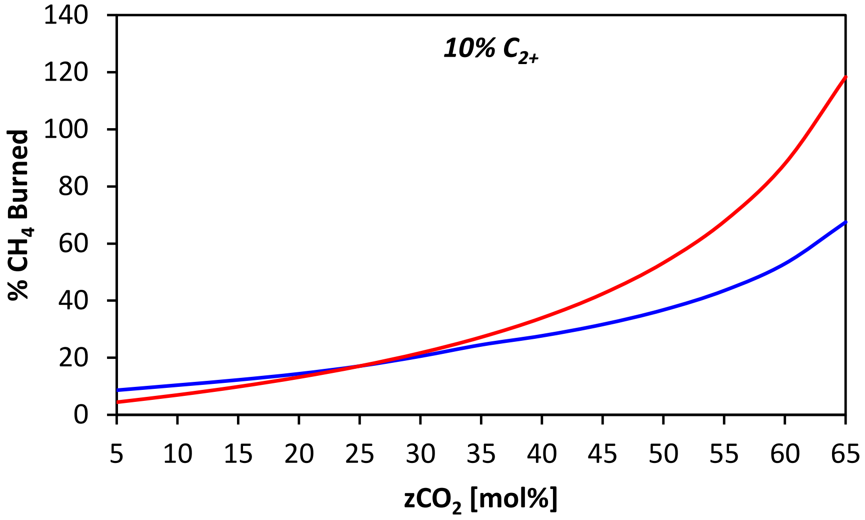
10% $C_{2+}$
% $CH_4$ Burned
0
20
40
60
80
100
120
140
5
10
15
20
25
30
35
40
45
50
55
60
65
$zCO_2$ [mol%]

d)

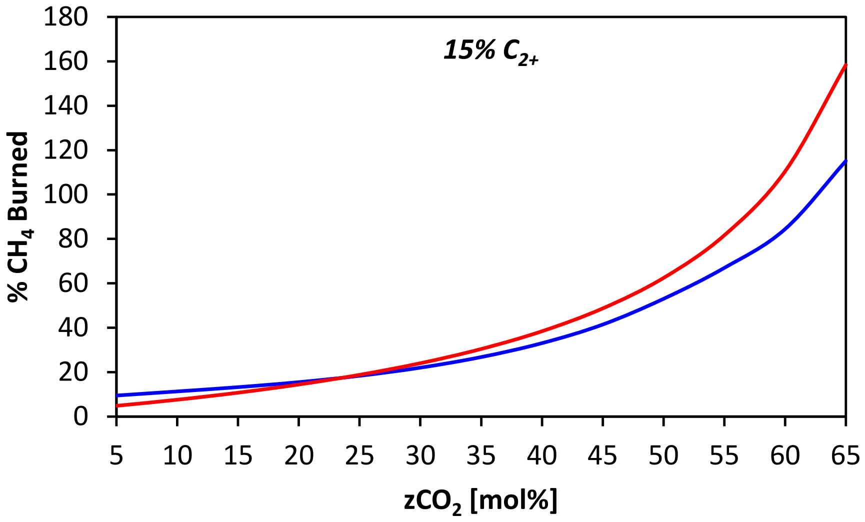

15% $C_{2+}$
% $CH_4$ Burned
0
20
40
60
80
100
120
140
160
180
5
10
15
20
25
30
35
40
45
50
55
60
65
z$CO_2$ [mol%]

e)

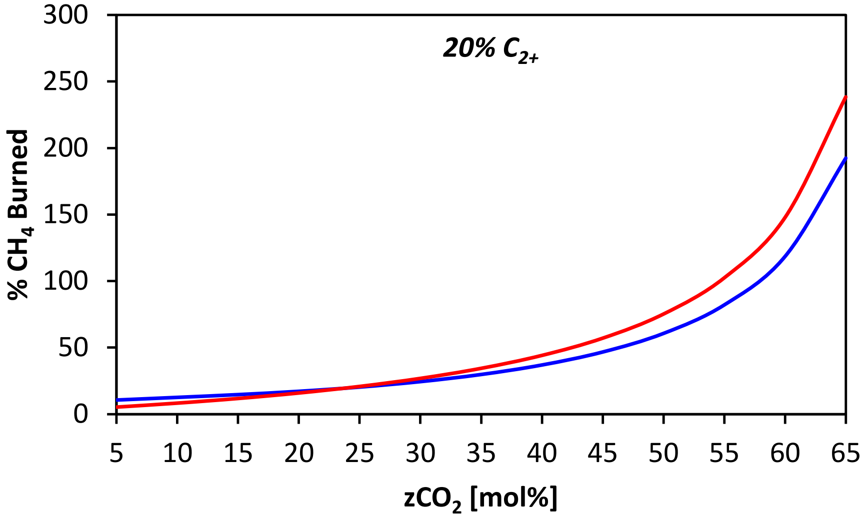

20% $C_{2+}$
% $CH_4$ Burned
0
50
100
150
200
250
300
5
10
15
20
25
30
35
40
45
50
55
60
65
z$CO_2$ [mol%]

f)

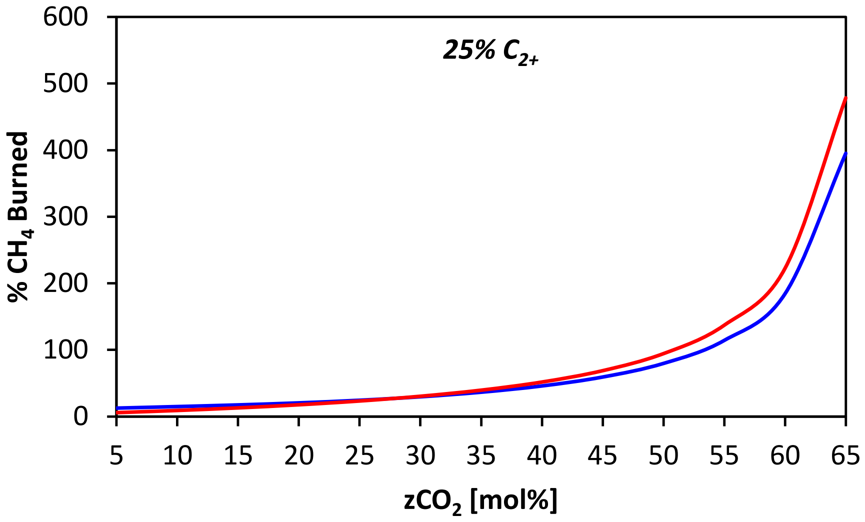

**Figure 30.** Energy comparison, in terms of % of produced methane that has to be burned to provide energy to the process, between (—) classic natural gas purification chain (Fig. 4) and (—) low-temperature purification chain (Fig. 5), with $CO_2$ recompression, for a gas feed stream having 5 mol% of $H_2S$ and a) 0 mol% of $C_2H_6$, b) 5 mol% of $C_2H_6$, c) 10 mol% of $C_2H_6$, d) 15 mol% of $C_2H_6$, e) 20 mol% of $C_2H_6$ and f) 25 mol% of $C_2H_6$.

a)

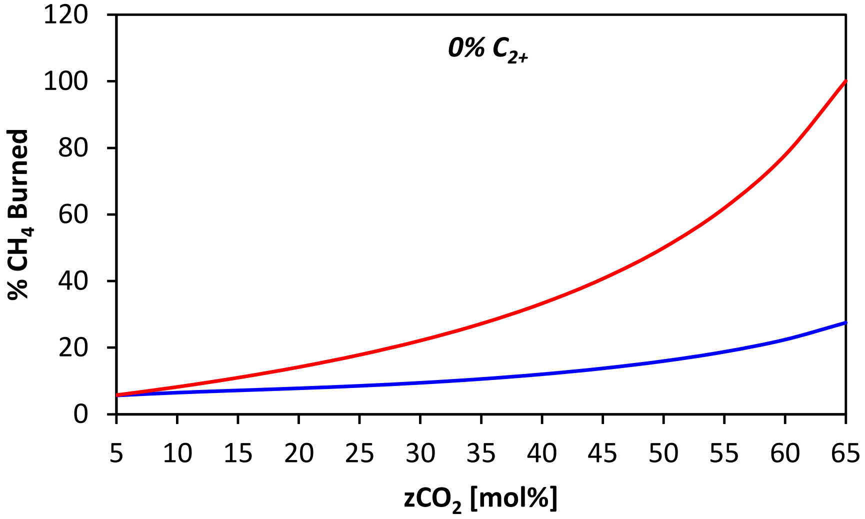

b)

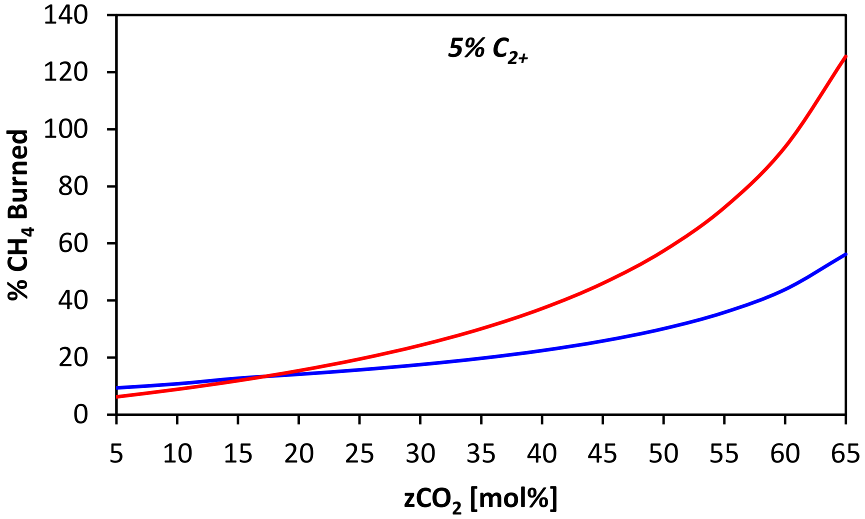

140
120
100
80
60
40
20
0
*5% $C_{2+}$*
% $CH_4$ Burned
5
10
15
20
25
30
35
40
45
50
55
60
65
z$CO_2$ [mol%]

c)

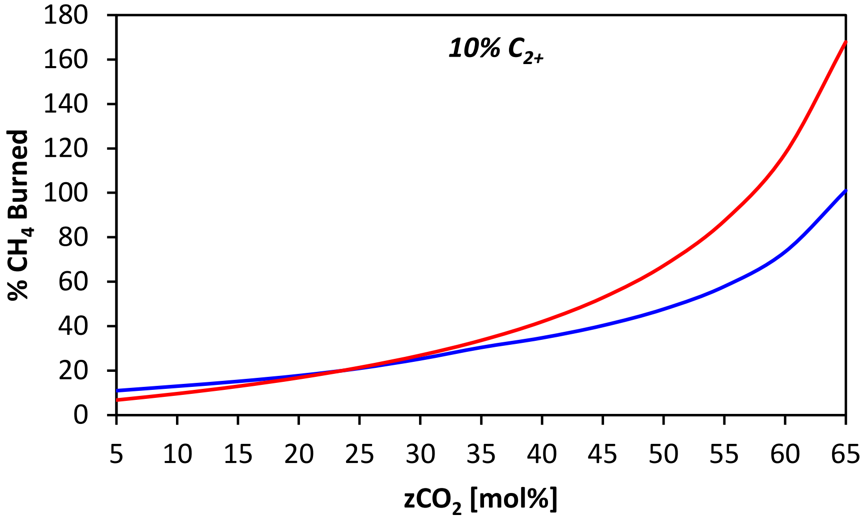

180
160
140
120
100
80
60
40
20
0
*10% $C_{2+}$*
% $CH_4$ Burned
5
10
15
20
25
30
35
40
45
50
55
60
65
z$CO_2$ [mol%]

d)

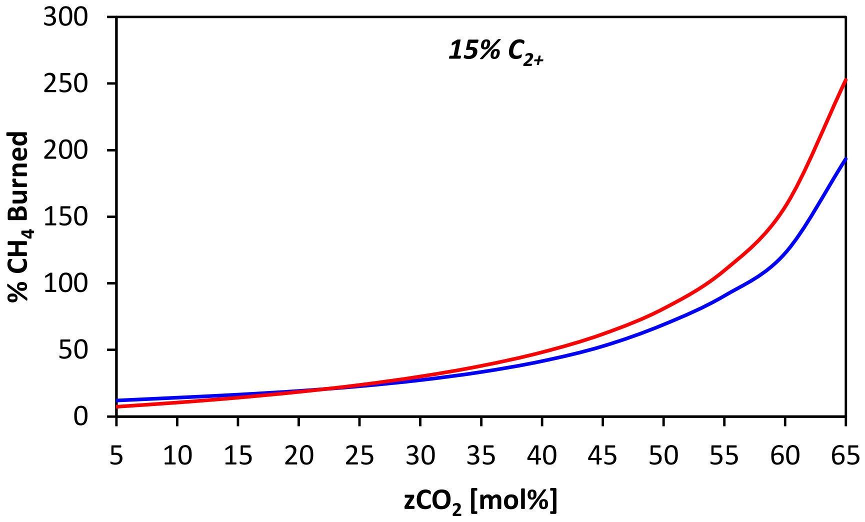
15% $C_{2+}$
% $CH_4$ Burned
zCO$_2$ [mol%]
0
50
100
150
200
250
300
5
10
15
20
25
30
35
40
45
50
55
60
65

e)

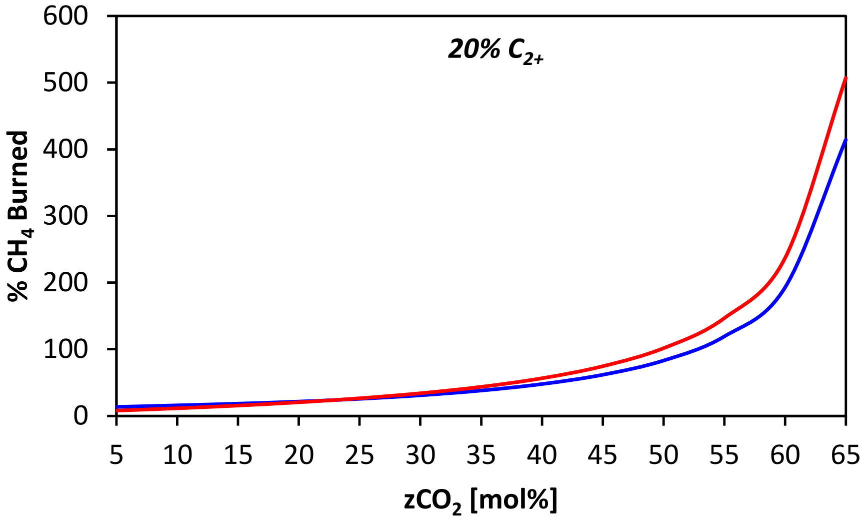
20% $C_{2+}$
% $CH_4$ Burned
zCO$_2$ [mol%]
0
100
200
300
400
500
600
5
10
15
20
25
30
35
40
45
50
55
60
65

f)

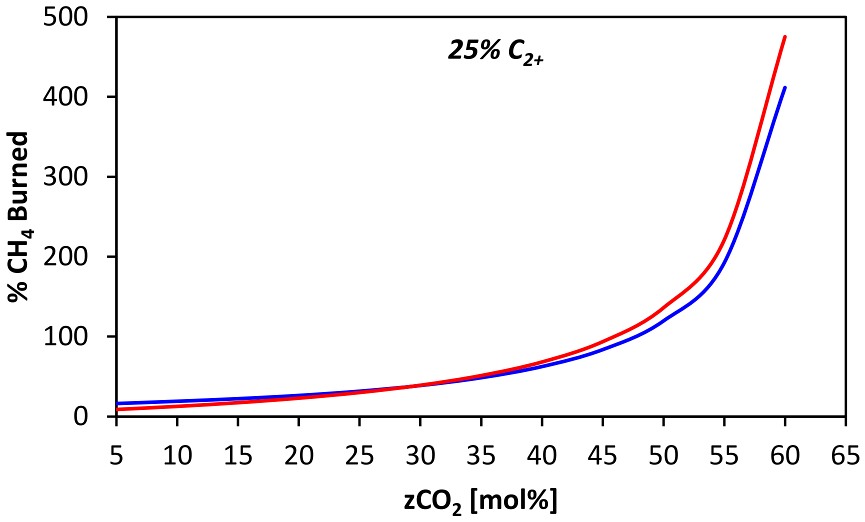

**Figure 31.** Energy comparison, in terms of % of produced methane that has to be burned to provide energy to the process, between (—) classic natural gas purification chain (Fig. 4) and (—) low-temperature purification chain (Fig. 5), with $CO_2$ recompression, for a gas feed stream having 10 mol% of $H_2S$ and a) 0 mol% of $C_2H_6$, b) 5 mol% of $C_2H_6$, c) 10 mol% of $C_2H_6$, d) 15 mol% of $C_2H_6$, e) 20 mol% of $C_2H_6$ and f) 25 mol% of $C_2H_6$.

a)

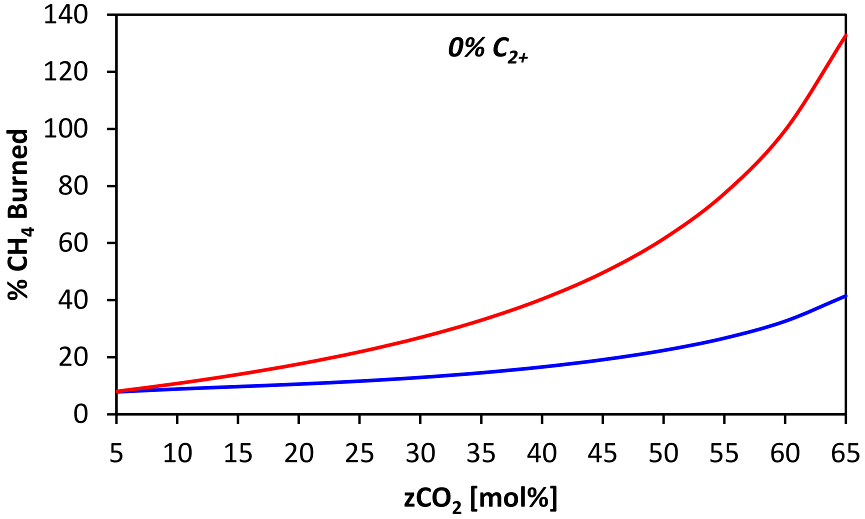

b)

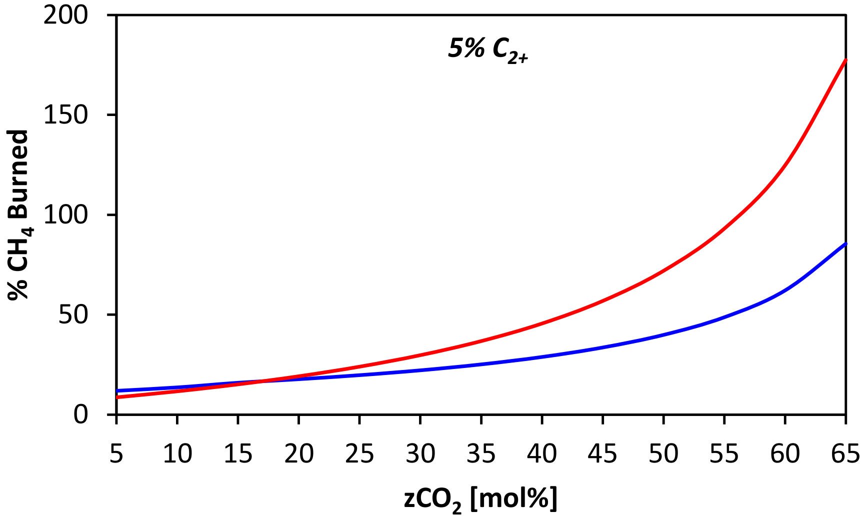
5% $C_{2+}$
% $CH_4$ Burned
200
150
100
50
0
5
10
15
20
25
30
35
40
45
50
55
60
65
$zCO_2$ [mol%]

c)

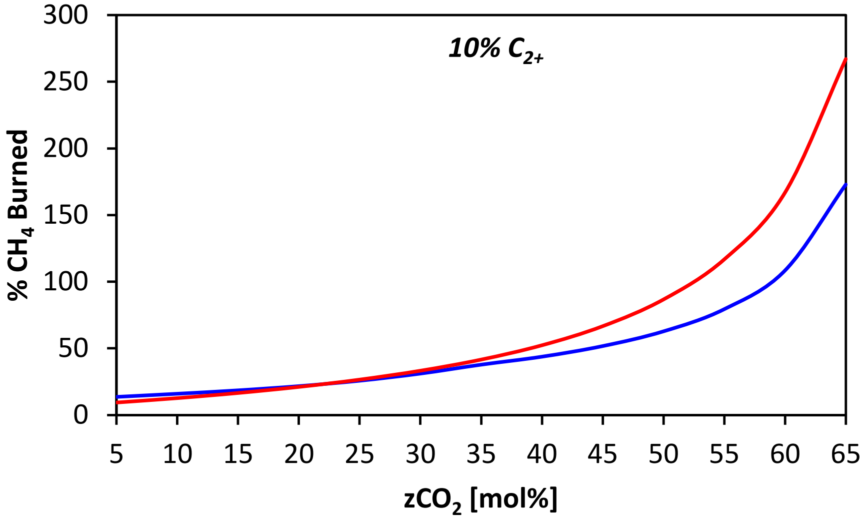
10% $C_{2+}$
% $CH_4$ Burned
300
250
200
150
100
50
0
5
10
15
20
25
30
35
40
45
50
55
60
65
$zCO_2$ [mol%]

d)

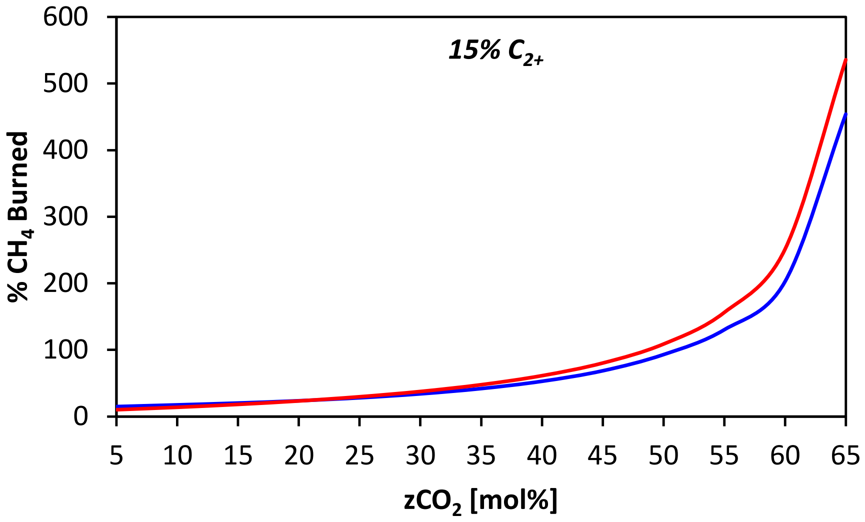
15% $C_{2+}$
% $CH_4$ Burned
zCO$_2$ [mol%]
0
100
200
300
400
500
600
5
10
15
20
25
30
35
40
45
50
55
60
65

e)

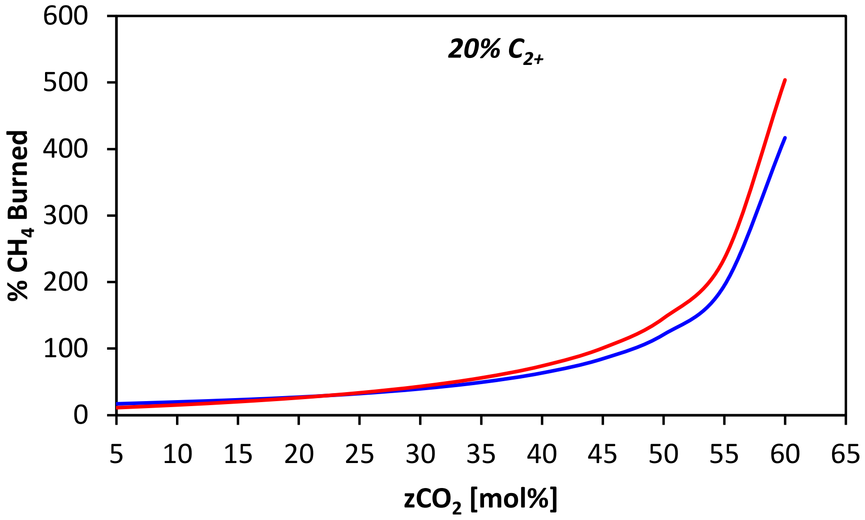
20% $C_{2+}$
% $CH_4$ Burned
zCO$_2$ [mol%]
0
100
200
300
400
500
600
5
10
15
20
25
30
35
40
45
50
55
60
65

f)

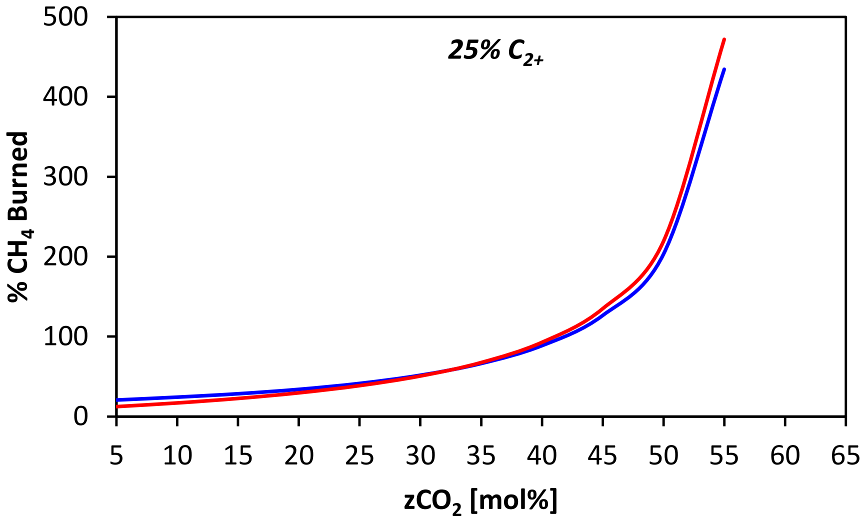

**Figure 32.** Energy comparison, in terms of % of produced methane that has to be burned to provide energy to the process, between (—) classic natural gas purification chain (Fig. 4) and (—) low-temperature purification chain (Fig. 5), with $CO_2$ recompression, for a gas feed stream having 15 mol% of $H_2S$ and a) 0 mol% of $C_2H_6$, b) 5 mol% of $C_2H_6$, c) 10 mol% of $C_2H_6$, d) 15 mol% of $C_2H_6$, e) 20 mol% of $C_2H_6$ and f) 25 mol% of $C_2H_6$.

The trend of the obtained results for the two considered natural gas production schemes with $CO_2$ recompression are qualitatively similar to the ones obtained previously. However, the $CO_2$ recompression affects the breakeven points, shifting them at lower values of the inlet $CO_2$ molar fraction. The highest penalty in terms of overall energy consumptions is paid for the recompression and dehydration of the wet $CO_2$ stream coming from the regeneration column of the acid gas removal unit, which operates a chemical absorption of acidic gases in aqueous MDEA. The $CO_2$ is rejected in gas phase at atmospheric pressure from traditional MDEA unit, while, from low-temperature natural gas distillation processes, it is rejected typically in liquid phase under pressure. Hence, the recompression work required by the classic purification plant is higher than the one required by the low-temperature plant. In this way, when $CO_2$ recompression is considered, the overall energy consumption of the classic scheme is significantly increased respect to the one of the low-temperature scheme. In this way, the breakeven points for any amount of $H_2S$ and $C_{2+}$ in the feed stream are moved to lower contents of $CO_2$ in the raw gas and the low-temperature purification scheme is favored.

In order to give a more general overview of the obtained results and the weight of $CO_2$ recompression on energy expenses for the two natural gas purification schemes, the main results of the study have been summarized in Table 6.

**Table 6.** Overall results of the energy analysis and comparison between the classic natural gas purification chain and the low-temperature purification chain with and without CO2 recompression.

| **Feed** | | **BEP without $CO_2$ recompression** | **BEP with $CO_2$ recompression** | **$C_{2+}$ removal upstream (U) or downstream (D) in LT scheme** | **$CO_2$-$C_2H_6$ separation process when the LT process is more profitable** | **$CO_2$ mol% in the feed at which 100% of the produced gas has to be burned to produce energy for the process** | |
|---|---|---|---|---|---|---|---|
| **$H_2S$** | **$C_{2+}$** | **$CO_2$ mol%** | **$CO_2$ mol%** | **U/D** | **2/3 columns** | **Classic Scheme** | **LT Scheme** |
| 0 | 0 | 8 | 8 | N/A | N/A | N/A | N/A |
| | 5 | 20 | 18 | D | 3 | N/A | N/A |
| | 10 | 35 | 30 | U at BEP, then D | 3 | N/A | N/A |
| | 15 | 35 | 25 | U from BEP to 55 mol% of $CO_2$, then D | 3 | 65 | N/A |
| | 20 | 30 | 25 | U | N/A | 60 | 65 |
| | 25 | 35 | 30 | U | N/A | 55 | 58 |
| 5 | 0 | 8 | 5 | N/A | N/A | N/A | N/A |
| | 5 | 20 | 18 | D | 3 | N/A | N/A |
| | 10 | 35 | 25 | U from BEP to 35 mol% of $CO_2$, then D | 3 | 63 | N/A |

| | | | | | | | |
|---|---|---|---|---|---|---|---|
| | 15 | 30 | 23 | U from BEP to 50 mol% of $CO_2$, then D | 3 | 58 | 63 |
| | 20 | 28 | 23 | U | N/A | 53 | 58 |
| | 25 | 38 | 28 | U | N/A | 51 | 53 |
| 10 | 0 | 8 | <5 | N/A | N/A | 65 | N/A |
| | 5 | 20 | 18 | D | 3 | 63 | N/A |
| | 10 | 33 | 23 | U from BEP to 35 mol% of $CO_2$, then D | 3 | 58 | 63 |
| | 15 | 28 | 23 | U from BEP to 55 mol% of $CO_2$, then D | 3 | 51 | 53 |
| | 20 | 28 | 23 | U | N/A | 48 | 53 |
| | 25 | 38 | 30 | U | N/A | 46 | 48 |
| 15 | 0 | 8 | <5 | N/A | N/A | 63 | N/A |
| | 5 | 18 | 18 | D | 3 | 58 | N/A |
| | 10 | 30 | 23 | U from BEP to 35 mol% of $CO_2$, then D | 3 | 53 | 58 |
| | 15 | 25 | 23 | U from BEP to 55 mol% of $CO_2$, then D | 3 | 48 | 53 |
| | 20 | 28 | 28 | U | N/A | 43 | 48 |
| | 25 | 45 | 33 | U | N/A | 42 | 43 |

Generally, the recompression of $CO_2$ favors the profitability of the low-temperature scheme, shifting the breakeven point typically to lower values of the inlet $CO_2$ mol%. When the downstream removal of $C_{2+}$ is considered, the three-columns extractive distillation process is the suggested solution. The low-temperature process allows to reduce significantly the energy consumptions for the processing of natural gases with low-contents of $C_{2+}$ and any amount of $H_2S$. When no $C_{2+}$ are present in the inlet raw gas stream, the presence of $H_2S$ shifts the breakeven point between the two processes below 5 mol% of $CO_2$ in the feed stream. For any value of $C_{2+}$ and high values of $H_2S$, this effect is reduced and the breakeven points do not vary significantly. Moreover the present analysis on an energy basis allows to find the limit values of the $CO_2$ mol% in the feed gas at which the produced gas is totally used to provide energy for the process.

## 5. Conclusion

The increase of the global energy demand, particularly the natural gas one, together with the availability of low-quality gas reserves with high $CO_2$ and/or $H_2S$ contents have driven the attention to the study and development of new purification process technologies, such as low-temperature distillation, for the commercialization of these kinds of highly acid and/or sour gases.

Associate gases may also have high $CO_2$ contents and NGLs recovery from these natural gases is of commercial interest, since heavier hydrocarbons (such as ethane, propane and n-butane) are used as raw materials for several petrochemical applications.

In this work, the complete natural gas purification process has been considered (acid gas removal, dehydration and NGLs recovery) with and without $CO_2$ recompression for EOR and CCS. A classic process scheme for natural gas purification and NGLs recovery and a low-temperature natural gas purification process scheme with NGLs recovery have been considered and compared on the basis of their energy requirements accounted as net equivalent methane and percentage of the produced gas that has to be burned in order to provide the energy for the entire process. The low-temperature process considered in this work is the recently-proposed dual pressure low-temperature distillation process. When dealing with the low-temperature process scheme, two different solutions for the split of the $CO_2$-$C_2H_6$ minimum azeotrope have been considered and compared. Moreover, the profitability of recovering the $C_{2+}$ fraction of the feed stream upstream or downstream of the dual pressure low-temperature distillation process has been investigated. Results have shown that, when considering the recovery of NGLs downstream of the dual pressure low-temperature distillation process, a three-columns extractive distillation process for the separation of $CO_2$ and $C_2H_6$ is more profitable than a two-columns extractive distillation process for values of $CO_2$ in the feed stream below 0.48 and above 0.75. Moreover, there is a trade-off between the NGLs recovery upstream and downstream of the dual pressure low-temperature distillation process: generally for high amounts of NGLs in the raw gas feed, it is preferable to remove them upstream, while for NGLs contents between 10-15 mol%, it exist a value of the $CO_2$ mol% in the feed stream (typically between 35 and 55 mol%) that establishes the trade-off between downstream and upstream recovery. This occurs for any value of $H_2S$ in the raw gas feed to be treated.

Comparisons between the classic scheme and the low-temperature scheme have shown that when no NGLs are present, the low-temperature process is more profitable, on an energy basis, starting from low contents of $CO_2$ in the feed stream; moreover, the presence of $H_2S$ enhances the profitability of the low-temperature solution. When the recovery of NGLs is considered, the low-temperature process allows energy savings at higher $CO_2$ contents in the natural gas feed stream. For any value of the $H_2S$ content in the feed, an increase of the $C_{2+}$ fraction in the raw natural gas stream leads to an increase of the $CO_2$ mol% of the gas feed at which the low-temperature scheme is more profitable than the classic scheme. The presence of $H_2S$ and $C_{2+}$ in the natural gas reduces the difference between the energy consumptions of the two considered global purification processes. When $CO_2$ recompression is needed, the breakeven points between the two technologies occur for lower values of $CO_2$ contents in the feed stream, because the classic scheme is significantly affected by the compression work required by the $CO_2$ compressor. On the contrary, in the low-temperature scheme, this effect is reduced because $CO_2$ is produced in liquid phase under pressure, hence a pump can be used to pressurize this stream instead of a compression train.

Generally, it can be established that low-temperature purification processes are more profitable than classic process schemes to handle natural gases with low NGLs content, while, when the

NGLs fraction is significant, low-temperature processes are more suitable for application when the $CO_2$ content in the feed stream is particularly high. The breakeven point shifts according to $H_2S$ and $C_{2+}$ contents.

Moreover, when low-temperature processes are more profitable than classic schemes to purify natural gas and recover NGLs, the energy savings can be significant.

**Abbreviations**

| | |
|---|---|
| BEP | BreakEven Point |
| BFD | Block Flow Diagram |
| BP | British Petroleum |
| CCS | Carbon Capture and Storage |
| COP | Coefficient of Performance |
| D | Downstream |
| EOR | Enhanced oil Recovery |
| EoS | Equation of State |
| GPSA | Gas Processors and Suppliers Association |
| H | Enthalpy |
| LHV | Lower Heating Value |
| LP | Low-Pressure |
| LT | Low-Temperature |
| $\dot{m}$ | Mass Flow |
| MDEA | Methyl Di Ethanol Amine |
| n | Number of Compression Stages |
| N/A | Not Applicable |
| NGLs | Natural Gas Liquids |

| | |
|---|---|
| P | Pressure |
| PFD | Process Flow Diagram |
| PR | Peng Robinson |
| $\dot{Q}$ | Thermal Flow |
| SLVE | Solid-Vapor-Liquid Equilibrium |
| SRK | Soave Redlich Kwong |
| SRU | Sulfur Recovery Unit |
| T | Temperature |
| TEG | Triethylene Glycol |
| U | Upstream |
| $\dot{V}$ | Volume Flow |
| VLE | Vapor-Liquid Equilibrium |
| $\dot{W}$ | Work Flow |
| z | Molar Fraction of the Feed Stream |

*Subscripts*

| | |
|---|---|
| B | Boiler |
| CC | Combined Cycle |
| COLD | Frigories |
| $CH_4$ | Methane |
| el | Electric |
| EQ | Equivalent |
| ev | Vaporization |

| | |
|---|---|
| f | Refrigeration |
| i | Process Unit |
| id | Ideal |
| n | Number of Compression Stage |
| 0 | Reference |
| II | Second Law of Thermodynamics |

*Superscripts*

| | |
|---|---|
| Demeth | Demethanizer |
| DPLTP | Dual Pressure Low-Temperature Distillation |
| EDU | Extractive Distillation Upstream |
| 2EDD | Two-Columns Extractive Distillation Downstream |
| 3EDD | Three-Columns Extractive Distillation Downstream |
| FEED | Feed Stream |
| Nproc | Number of Process Units |
| PROD | Produced |

*Greek Letters*

| | |
|---|---|
| $\eta$ | Efficiency |
| $\Delta$ | Difference |

## AUTHOR INFORMATION

### Corresponding Author

* To whom correspondence should be addressed. Tel.: +39 02 2399 4704. Fax: +39 02 7063 8173. E-mail: stefano.lange@polimi.it

**Author Contributions**

The manuscript was written through contributions of all authors. All authors have given approval to the final version of the manuscript. ‡These authors contributed equally. (match statement to author names with a symbol)

REFERENCES

(1) BP Energy Outlook 2035. www.bp.com (accessed September 2014).

(2) Carrol, J.; Foster, J. *New Challenges & Solutions in Designing Large Sour Gas Projects.* [Online] 2008, http://www.fwc.com (accessed September 2014).

(3) Bagirov, L. A.; Imaev, S. Z.; Borisov, V. E. R&D Technologies for Acid Gases Extraction from Natural Gases. In: *SPE/IATMI Asia Pacific Oil & Gas Conference and Exhibition* Proceedings of the Asia Pacific Oil and Gas Conference and Exhibition, Nusa Dua, Bali, Indonesia, Oct 20 – 22, 2015, Nusa Dua, Bali, Indonesia. Society of Petroleum Engineers.

(4) Burgers, W.J.F.; Northrop, P.S.; Khesghi, H.S.; Valencia, J.A. Worldwide Development Potential for Sour Gas. *Energy Proced.* **2011**, *4*, 2178.

(5) Rojey, A.; Jaffaret, C.; Cornot-Gandolphe, S.; Durand, B.; Jullian, S.; Valais, M. *Natural Gas Production Processing Transport*: ÉditionsTechnip, Paris, France, 1994.

(6) Parker, M. E.; Northrop, S.; Valencia, J.A.; Foglesong, R.E.; Duncan, W.T. $CO_2$ Management at ExxonMobil's La Barge Field, Wyoming, USA. *Energy Proced.* **2011**, *4*, 5455.

(7) Scherbinin A. Shell Experience in Sour Gas Fields. In: *Turkmenistan Gas Conference*, Proceedings of the Turkmenistan Gas Conference, Avaza, May 2012, Turkmenistan.

(8) Darman, N. H.; Arun, A. R. *Technical Challenges and Solutions on Natural Gas Development in Malaysia*. The petroleum Policy and Management (PPM) Project 4th Workshop of the China – Sichuan Basin Case Study. 30 May – 3 June 2006, Beijing, China. [Online] 2006. http://www.ccop.or.th/ppm/document/CHWS4/CHWS4DOC08_nasir.pdf (Accessed November 2015).

(9) Boschee, P. *Tackling the Challenges of Sour Gas Processing*. [Online] 2015. http://www.spe.org/news/article/tackling-the-challenges-of-sour-gas-processing (Accessed November 2015).

(10) Crotti, M. A.; Fernandez, G.; Terrado, M. Improving Reserves and Production Using a $CO_2$ Fluid Model in El Trapial Field, Argentina. In: *SPE Latin American and Caribbean Petroleum Engineering Conference*, Proceedings of the Latin American and Caribbean Petroleum Engineering Conference, Buenos Aires, Argentina, April 15 – 18, 2007. Society of Petroleum Engineers.

(11) Jukić, A. *Petroleum Refining and Petrochemical Processes. Natural Gas Composition, Classification, Processing.* [Online] 2013. https://www.fkit.unizg.hr/_download/repository/PRPP_2013_Natural_gas.pdf (Accessed November 2015).

(12) Pires, J.C.M.; Martins, F.G.; Alvim-Ferraz, M.C.M.; Simões, M. Recent Developments on Carbon Capture and Storage: an Overview. *Chem. Eng. Res. Des.* **2011,** *89*, 1446.

(13) Kelley, B. T.; Valencia, J. A.; Northrop, P. S.; Mart C. J. Controlled Freeze Zone$^{TM}$ for Developing Sour Gas Reserves. *Energy Proced.* **2011**, *4*, 824.

(14) Langé, S; Pellegrini, L. A.; Vergani, P.; Lo Savio, M. Energy and Economic Analysis of a New Low-Temperature Distillation Process for the Upgrading of High-$CO_2$ Content Natural Gas Streams. *Ind. Eng. Chem. Res.* **2015**, *54 (40)*, 9770.

(15) Haut, R.C.; Denton, R.D.; Thomas, E.R. Development and Application of the Controlled-Freeze-Zone Process. *SPE Prod. Eng.* **1989**, *August*, 265.

(16) Parker, M. E.; Northrop, S.; Valencia, J.A.; Foglesong, R.E.; Duncan, W.T. $CO_2$ Management at ExxonMobil's La Barge Field, Wyoming, USA. *Energy Proced.* **2011**, *4*, 5455.

(17) Northrop, P.S.; Valencia, J.A. The CFZ$^{TM}$ Process: a Cryogenic Method for Handling High-$CO_2$ and $H_2S$ Gas Reserves and Facilitating Geosequestration of $CO_2$ and Acid Gases. *Energy Proced.* **2009**, *1*, 171.

(18) Valencia, J.A.; Denton, R.D. Method and Apparatus for Separating Carbon Dioxide and Other Acid Gases from Methane by the Use of Distillation and a Controlled Freeze Zone. U.S. Patent 4533372, August 6, 1985.

(19) Valencia, J.A.; Victory, D.J. Method and Apparatus for Cryogenic Separation of Carbon Dioxide and Other Acid Gases from Methane. U.S. Patent 4923493, May 8, 1990.

(20) Valencia, J.A.; Victory, D.J. Bubble Cap Tray for Melting Solids and Method for Using Same. U.S. Patent 5265428, November 30, 1993.

(21) Amin, R.; Jackson, A. T.; Kennaird, T. The Cryocell: an advanced gas sweetening technology. In: *International Petroleum Technology Conference*, Proceedings of the International Petroleum Conference, Doha, Qatar, Nov 21 – 23, 2005. Society of Petroleum Engineers, 2005.

(22) Hart, A.; Gnanendran, N. Cryogenic $CO_2$ Capture in Natural Gas. *Energy Proced.* **2009**, *1*, 697.

(23) Crio Pur. http://www.cryopur.com/en/index.html (Accessed November 2015).

(24) Clodic, D.; Younes, M. A new Method for $CO_2$ Capture: Frosting $CO_2$ at Atmospheric Pressure. In: *Sixth International Conference on Greenhouse Gas Control Technologies GHGT6* Proceedings of the 6th International Conference on Greenhouse Gas Control Technologies, Kyoto, Japan, Oct 1 – 4, 2002, pp 155; Gale, J.; Kaya, Y., Eds.; Elsevier: Amsterdam, 2003.

(25) Xiong, X.; Lin, W.; Gu, A. Integration of $CO_2$ Cryogenic Removal with a Natural Gas Pressurized Liquefaction Process using Gas Expansion Refrigeration. *Energy* **2015**, *93*, 1.

(26) Holmes, A.S.; Ryan, J.M. Cryogenic Distillative Separation of Acid Gases from Methane. U.S. Patent 4318723, March 9, 1982a.

(27) Holmes, A.S.; Ryan, J.M. Distillative Separation of Carbon Dioxide from Light Hydrocarbons. U.S. Patent 4350511, September 21, 1982b.

(28) Holmes, A.S.; Price, B.C.; Ryan, J.M.; Styring, R.E. Pilot Tests Prove Out Cryogenic Acid–Gas/Hydrocarbon Separation Processes. *Oil Gas J.* **1983**, *27*, 85.

(29) Lallemand, F.; Lecomte, F.; Streicher, C.; 2005. Highly Sour Gas Processing: $H_2S$ Bulk Removal with the Sprex Process. In: *International Petroleum Technology Conference*, Proceedings of the International Petroleum Conference, Doha, Qatar, Nov 21 – 23, 2005. Society of Petroleum Engineers, 2005.

(30) Lallemand, F.; Perdu, G.; Normand, L.; Weiss, C.; Magne-Drisch, J.; Gonnard, S. *Extending the Treatment of Highly Sour Gases: Cryogenic Distillation*. [Online] 2014. www.digitalrefining.com/article/1000937 (accessed September 2014).

(31) Pellegrini, L.A. Process for the Removal of $CO_2$ from Acid Gas. W.O. Patent 2014/054945A2, April 10, 2014.

(32) IEA. *Natural gas Liquids Supply Outlook 2008-2015*. [Online] 2015. www.iea.org (Accessed November 2015).

(33) Finn, A.; O'Brien, J. Processing of Carbon Dioxide Rich Gas. In: *94th Annual GPA Convention*, Proceedings of the 94th Annual GPA Conference, San Antonio, TX, USA, April 12-15, 2015.

(34) Mak, J.; Devone, S.; Shih, J. New NGL Recovery Process for Unconventional Gas Applications. In: *GPA Europe Annual Conference*, Proceedings of the GPA Europe Annual Conference, Florence, Italy, Sept 16 – 18, 2015.

(35) GPSA (Gas Processors Suppliers Association). *Engineering Data Book*, Twelfth Edition: GPSA, Tulsa, OK, USA, 2004.

(36) Lastari, F.; Pareek, V.; Trebble, M.; Tade, M.O.; Chinn, D.; Tsai, N. C.; Chan, K.I. Extractive Distillation for $CO_2$–Ethane Azeotrope Separation. *Chem. Eng. Proc.* **2012**, *52*, 155.

(37) Torres-Ortega, C. E.; Segovia-Henández, J. G.; Gómez-Castra, F. I.; Henández, S.; Bonilla-Petriciolet, A.; Rong, B.-G.; Errico, M. Design, Optimization and Controllability of an Alternative Process Based on Extractive Distillation for an Ethane–Carbon Dioxide Mixture. *Chem. Eng. Proc.* **2013**, *74*, 55.

(38) Luyben, W. L. Control of an Extractive Distillation System for the Separation of $CO_2$ and Ethane in Enhanced Oil Recovery Processes. *Ind. Eng. Chem. Res.* **2013**, *52*, 10780.

(39) Tavan, Y.; Shahhosseini, S.; Hosseini, S. H. Feed-Splitting Technique in the Extractive Distillation of $CO_2$–Ethane Azeotropic Process. *Sep. Purif. Technol.* **2014**, *122*, 47.

(40) Pellegrini, L. A.; Langè, S.; Baccanelli, M.; De Guido, G. Techno-Economic Analysis of LNG Production using Cryogenic vs Conventional Techniques for Natural Gas Purification. In: *Offshore Mediterranean Conference & Exhibition OMC 2015*, Proceedings of the Offshore Mediterranean Conference and Exhibition, Ravenna, Italy, March 25 -27, 2015a. Society of Petroleum Engineers.

(41) Aspen Hysys® V7.3. Thermodynamics COM interface reference guide; unit operations guide. In: AspenONE V7.3 documentation. Burlington, MA: Aspen Technology, Inc.; 2011.

(42) Sobocinski, D. P.; Kurata, F. Heterogeneous Phase-Equilibria of the Hydrogen Sulfide-Carbon Dioxide System. *AIChE J.* **1959**, *5 (4)*, 545.

(43) Soave, G. Equilibrium Constants from a Modified Redlich-Kwong Equation of State. *Chem. Eng. Sci.* **1972**, *27*, 1197.

(44) De Guido, G.; Langè, S.; Moioli, S.; Pellegrini, L. A. Thermodynamic Method for the Prediction of Solid $CO_2$ Formation from Multicomponent Mixtures. *Process Saf. Environ. Prot.* **2014**, *92*, 70.

(45) Peng, D.-Y.; Robinson, D.B. A New Two-Constant Equation of State. *Ind. Eng. Chem. Fundam.* **1976**, 15, 59.

(46) Kurata, F. Solubility of Solid Carbon Dioxide in Pure Light Hydrocarbons and Mixtures of Light Hydrocarbons. GPA Research Report, RR - 10, Tulsa, Oklahoma, 1974.

(47) Aspen Plus® V7.3. NIST TDE in Aspen Properties Databank®: Burlington, 2010.

(48) Pellegrini, L. A., Langé, S.; De Guido, G.; Moioli, S.; Mikus, O.; Picutti, B.; Vergani, P.; Franzoni, G.; Lo Savio, M.; Brignoli, F. An Innovative Technology for Natural Gas Sweetening by means of Cryogenic Distillation. In: *GPA Europe Annual Conference*, Proceedings of the GPA Europe Annual Conference, Florence, Italy, Sept 16 – 18, 2015.

(49) Mokhatab, S.; Poe, W. A.; Speight, J. G. *Handbook of Natural Gas Transmission and Processing*. Gulf Professional Publishing: Burlington, MA, USA, 2006.

(50) Rufford, T. E.; Smart, S.; Watson, G. C. Y.; Graham, B. F.; Boxall, J.; Diniz da Costa, J. C.; May, E. F. The Removal of $CO_2$ and $N_2$ from Natural Gas: a Review of Conventional and Emerging Process Technologies. *J. Petrol. Sci. Eng.* **2012**, *94-95*, 123.

(51) de Visser, E.; Hendriks, C.; Barrio, M. DYNAMIS $CO_2$ Quality Recommendations. [Online] 2007. https://www.sintef.no/globalassets/project/dynamis-

hypogen/publications/d3-1-3-dynamis-co2-quality-recommendations1.pdf (Accessed November 2015).

(52) Turton, R., Bailie, R. C., Whiting, W. C., Shaeiwitz, J. A. *Analysis, Synthesis and Design of Chemical Processes*, Second Edition: Prentice Hall, Upper Saddle River, NJ, USA, 2003.

(53) Langè, S.; Pellegrini, L. A.; Stringari, P.; Coquelet, C. Experimental Determination of the Solid-Liquid-Vapor Locus for the $CH_4$-$CO_2$-$H_2S$ System and Application to the Design of a New Low-Temperature Distillation Process for the Purification of Natural Gas. In: *94th Annual GPA Convention*, Proceedings of the 94th Annual GPA Conference, San Antonio, TX, USA, April 12-15, 2015.

(54) Maddox, R. N.; Lilly, L.L. *Gas Conditioning and Processing*, Vol. 2: the Equipment Modules: Campbell Petroleum Series, Norman, OK, USA, 1984.

(55) Chakma, A., $CO_2$ Capture Processes-Opportunities for Improved Energy Efficiencies. *Energy Convers. Mgmt* **1997**, *38*, S51.

(56) Luyben, W. L. NGL Demethanizer Control. *Ind. Eng. Chem. Res.* **2013**, *52*, 11626.

(57) Chandel M. K.; Pratson, L. F.; Williams, E. Potential Economies of Scale in $CO_2$ Transport through use of a Trunk Pipeline. *Energy Conv. Manage.* **2010**, *51*, 2825.

(58) Reid, R. C.; Prausnitz, J. M.; Poling, B. E. *The Properties of Gases and Liquids*. Fourth Edition: Mc-Graw Hill, USA, 1987.